is found to be applicable using as little as 0.1 g of sample. The precision and accuracy of the α-correction method are generally better than that of the standard ratio technique.

The copper-base alloys analyzed in this study had been previously analyzed by XRF α-correction coefficients technique. The present results show higher accuracy due to the improved reliability of the coefficients determined and used in the present study.

ACKNOWLEDGEMENTS

The author would like to thank Professor J.G. Dick for his valuable guidance throughout the investigation.

The author is grateful to the Department of Chemistry for financial support of this study.

The author would also like to thank Mr. R. DiFruscia for the many helpful discussion.

TABLE OF CONTENTS

LIST OF TABLES

TABLE PAGE

LIST OF FIGURES

1. INTRODUCTION

1.1 Characteristic Radiation

A characteristic photon is generated by a two-step process. The first step is where a high-energy quantum, such as an electron, an x-ray photon or a proton, strikes an atom and knocks out an inner-shell electron. The second step is the readjustment within the atom almost immediately by the filling of the inner-shell vacancy by one of the outer-shell electrons and the simultaneous emission of an x-ray photon. The first step uses the energy of the incident quantum; in the second step energy is emitted as the characteristic x-ray photon. The incident quantum may have any energy greater than the binding energy of the inner-shell electron, with the excess energy used as kinetic energy for the electron being removed. But replacement of the inner-shell electron by one of the outer-shell electrons corresponds exactly to the difference in energy between the two levels, hence the emitted photon has the characteristic energy of the difference in energy for the levels. This photon energy can be expressed in wavelength using the Duane-Hunt[1] law:-

$$E = h \cdot \nu = h \cdot c/\lambda \qquad (1.1)$$

Where E is photon energy in ergs, h is Planck's constant (6.624×10^{-27} erg sec), c is the velocity of light (2.998×10^{10} cm sec^{-1}), ν is the frequency (Hz) and λ is the wavelength (cm) of the radiation. For more general applicability the x-ray photon energy can be expressed in volts (eV), therefore:

$$E_{eV} = h \cdot c / \lambda \cdot e \qquad (1.2)$$

Where e is electron charge in electrostatic unite (4.8×10^{-10} esu) and:

$$E_{eV} = 12396/\lambda \text{ or } \lambda = 12396/E_{eV} \qquad (1.3)$$

with λ in angstroms (Å)

The characteristic line spectrum is adequately explained in terms of Bohr atom concept. If an electron is removed from the K-shell and replaced by an electron from the L-shell, radiation known as K radiation may be generated. The emission of an L-line would follow for an electron from the M-shell filling the vacancy in the L-shell. Subsequent transitions and emission may continue until the energy transfer is equivalent to that associated with the outer orbital electron energy.

The x-ray spectrum emitted by any element is different from that for other elements, and consists of only a few characteristic lines. Hence, by measuring the wavelengths of each characteristic line, one can achieve a qualitative analysis picture.

In quantitative analysis, the intensities of the characteristic lines are measured. Intensities are almost always given as "counts" per unit time - that is, x-ray photons per unit area per unit time.

Theoretically, the more atoms that are impacted by primary x-ray beam, the more intense the characteristic radiation produced, and the higher the intensity of fluorescence generated by the specimen. A simple relationship may be set up, between the concentration and the intensity:

$$I_i = K \cdot C_i \quad \text{or} \quad I_i / I_i^o = C_i \qquad (1.4)$$

Where I_i and C_i are the intensity and concentration of analyte i respectively, I_i^o is the intensity of pure element i, and K is the proportionality constant.

Unfortunately, there is nearly always a nonlinear correlation between emitted radiation intensity and concentration of the emitting element. The useful emitted intensity is affected by:

1) The spectral distribution (both continuous and target-line spectra) of the primary x-ray beam.
2) The absorption of the analyte and the matrix for the primary x-rays.
3) The excitation probability and fluorescent yield of the analyte line.
4) The absorption of the analyte and matrix for the analyte line.
5) The geometry of the x-ray spectrometer.

1.2 Excitation of X-Ray - Continuous X-Ray

If an element is bombarded with high energy electrons, part of the kinetic energy of the electron stream, as the result of deceleration of the stream by successive collisions with the target atoms, is emitted as continuous or white radiation, covering a fairly broad wavelength range, which may include infrared, ultraviolet and x-radiation, the last being of immediate concern.

Any interaction will involve energy change within the atom and the atom will later return to its original (lowest) energy state by giving up any extra energy through the emission of radiation. Generally,

among the types of interaction which may occur are scattering of the bombarding electrons, increased perturbation of the electrons of the atom and, in the extreme case, removal of these electrons from their original atomic sites. The last effect may give rise to the production of characteristic radiation from the target atoms. Figure 1.1[2] shows the intensity distribution obtained from a tungsten target x-ray tube, and it consists of a broad band of continuous radiation, superimposed upon which are the characteristic wavelengths. The distribution of radiation of the continuum can be expressed in terms of Kramer's formula[3]:-

$$I(\lambda)d\lambda = K \cdot i \cdot Z \, (\lambda/\lambda_{min} - 1) \, 1/\lambda^2 \, d\lambda \quad (1.5)$$

It will been seen from this expression that the intensity distribution, $I(\lambda)d\lambda$, is a linear function of the x-ray tube current i and the atomic number Z of the x-ray tube anode material. λ_{min} represents the minimum wavelength of the continuum and this is found to correspond to the maximum energy of the electrons (i.e. the operating voltage V_o of the x-ray tube). This is given by the Duane-Hunt equation as:-

$$\lambda_{min} = h \cdot c/V_o = 12396/V_o \quad (1.6)$$

FIGURE 1.1 INTENSITY DISTRIBUTION - TUNGSTEN TARGET X-RAY TUBE

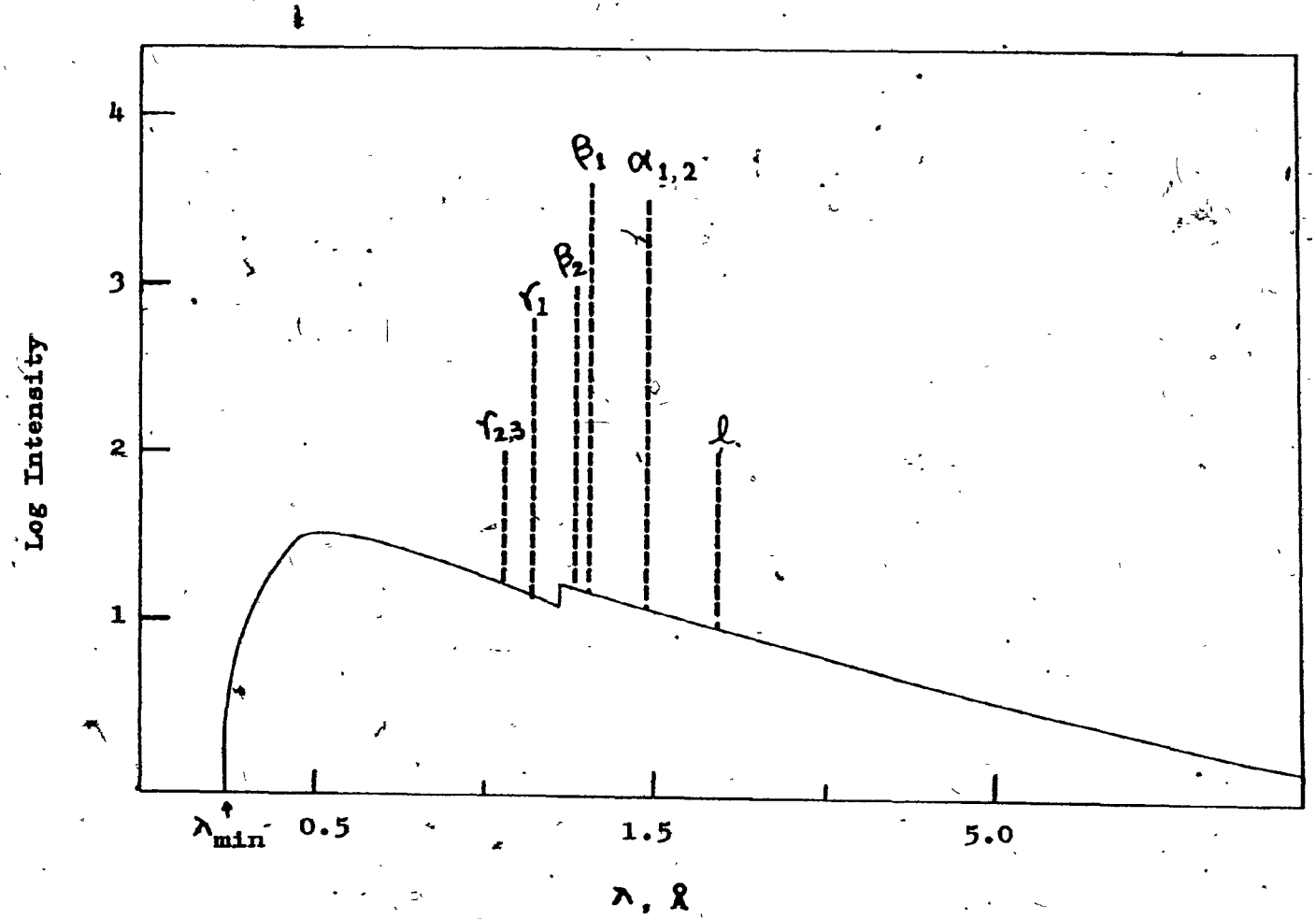

The intensity maximum of the continuum can be obtained by differentiating the Kramer formula, viz

$$I = K'.\left(\frac{1}{\lambda_{min}} - \frac{1}{\lambda^2}\right)$$

and:-

$$\frac{dI}{d\lambda} = -\left(\frac{K'}{\lambda^2.\lambda_{min}} - \frac{2K'}{\lambda^3}\right) = 0$$

or:- $$\frac{1}{\lambda_{min}} = \frac{2}{\lambda} \qquad (\text{i.e. } \lambda_{max} = 2\lambda_{min})$$

Hence the intensity maximum of the continuum always occurs at a wavelength twice the value of the minimum wavelength.

1.3 The Absorption of Primary X-Ray Radiation

When a beam of x-radiation falls onto an absorber, a number of different processes may occur. The fate of each individual incident x-ray photon is governed by the following three processes.

1.3.1 Absorption

A certain fraction (I/Io) of the radiation may pass through the absorber, and where this happens, the wavelength of the transmitted beam is unchanged and the intensity of this transmitted beam $I(\lambda)$ is given by[4]:-

$$I(\lambda) = I_o \exp\left(-(\mu_i \cdot \rho_i \cdot x_i)\right) \qquad (1.7)$$

where:-

μ_i = the mass absorption coefficient of absorber i for the wavelength λ.
I_o = the intensity of incident beam.
ρ_i = the density of the absorber.
x_i = the thickness of the absorber.

1.3.2 The photoelectric effect

From above it is apparent that an amount of intensity equal to $(I_o - I)$ has been lost, and the major portion of this is lost due to so-called photoelectric absorption. This will occur at each of the energy levels of the atom, and the total photoelectric absorption, τ_{total}, will be determined by the sum of each individual absorption. Thus:-

$$\tau_{total} = \tau_K + (\tau_{LI} + \tau_{LII} + \tau_{LIII}) + \ldots + \tau_n \qquad (1.8)$$

where τ_n represents the outermost electron level of the atom. All radiations produced as the result of electron transitions following ejection of orbital electrons will have wavelengths longer than λ (incident beam). In addition, not all of the radiation produced will be x-radiation, hence the photoelectric effect will give rise to x-radiation from the absorber, and to other photons.

1.3.3 Scatter

Scattering can occur when an x-ray photon interacts with one of the electrons of the absorbing elements, and can be coherent and/or incoherent[5]. Coherently-scattered radiation will suffer no energy change, and the wavelength will be the same as the incident beam. With incoherently-scattered radiation the x-ray photon loses part of its energy in the collision process and, in this case, the wavelength of the incoherently-scattered photons will be longer than the incident beam. The total scatter σ is made up of both the coherent and incoherent terms.

1.4 Primary Fluorescence - Absorption Effect

When a specimen is irradiated by primary radiation from an appropriate x-ray tube, the specimen will emit as secondary radiation the x-ray spectrum characteristic of its component atoms. For example, a certain element i, may have a wavelength λ_i excited by continuous radiation from a primary x-ray source, the effective range of the continuous radiation lying between the short wavelength limit of the continuum λ_{min} and the absorption edge λ_{edge} of the excited element i.

Jenkins[6] has suggested a convenient way to assess the efficiency of the primary continuum in exciting a specific analyte line, and this is by plotting the primary continuum spectral distribution and the analyte absorption curves superimposed on the same wavelength scale. An example of such plots is shown in Figure 1.2.

The excitation efficiency is given by the common area under the continuum and absorption curves on the short-wavelength side of the absorption edge (the shaded area in the figure).

The primary beam involves short-wavelength components ranging down to λ_{min}, which can penetrate deeper into the specimen than the depth from which secondary analyte-line radiation can emerge. Thus the most effective primary radiation is that lying at a wavelength just shorter than the absorption edge associated with the analyte line and, therefore, the intensity of the measured wavelength λ_i is then largely dependent upon absorption prior to emergence from the specimen, this being the so-called secondary absorption effect. However, it also depends on the absorption by the specimen of the exciting continuum, this effect being called primary absorption.

FIGURE 1.2

GRAPHICAL INTERPRETATION OF THE EXCITATION FUNCTION

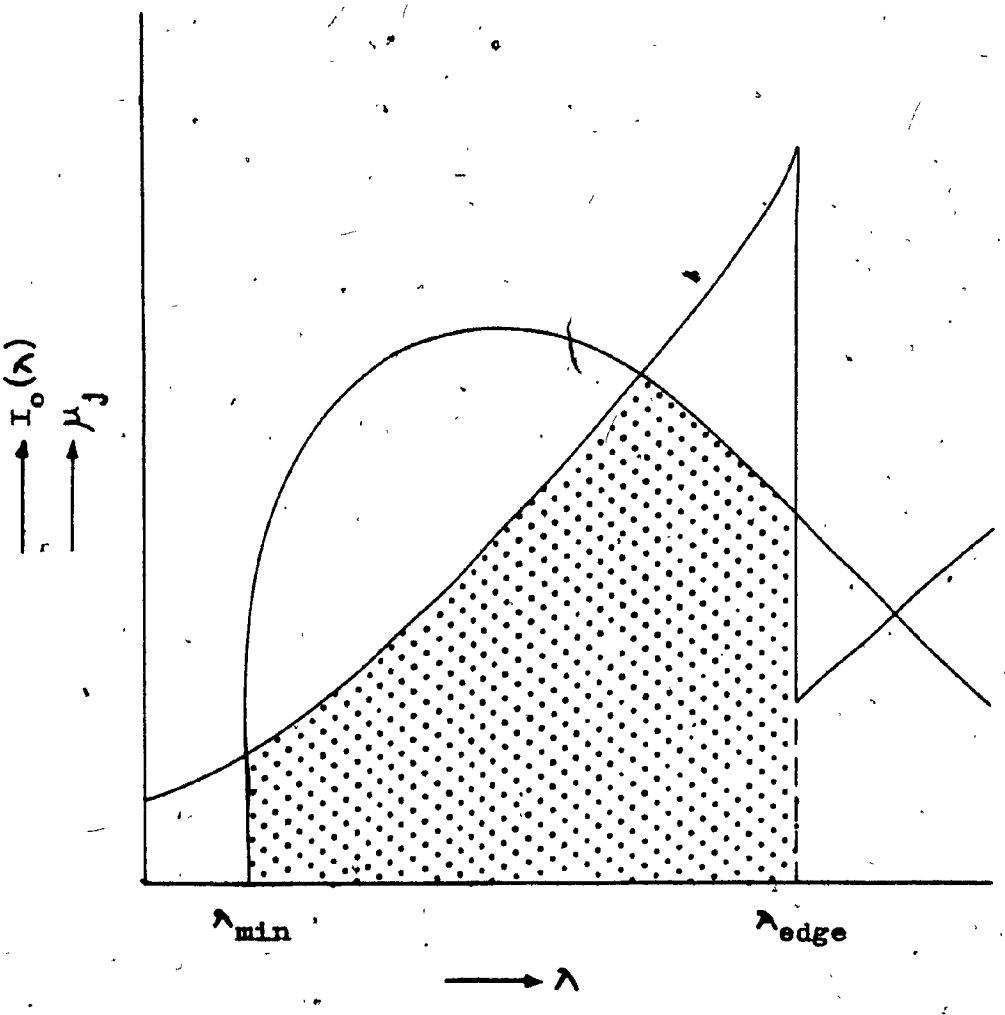

It is necessary that both primary and secondary absorption should be considered and the total specimen absorption can be given as:-

$$\text{Total absorption} = \sum \alpha_j \cdot C_j \qquad (1.9)$$

Where C_j is weight fraction of the elements j in the specimen, and α_j is defined as:-

$$\alpha_j = \left(\mu_j(\lambda) + A\, \mu_j(\lambda) \right) \qquad (1.10)$$

where:-

$\mu_j(\lambda)$ = the mass absorption coefficient of a matrix element for a wavelength λ in the primary beam.

$\mu_j(\lambda)$ = the mass absorption coefficient of the same matrix element j for the analyte line λ_i.

A = a constant equal to $\sin\phi_1/\sin\phi_2$, where ϕ_1, ϕ_2 are respectively the angles of incidence and emergence of primary x-rays at the specimen.

Therefore, the total excitation efficiency for a given element i, in a matrix made up of the elements j is given by:-

$$I_1(\lambda_i) = P_i \cdot C_i \int_{\lambda_{min}}^{\lambda_{edge}} I_o(\lambda) \frac{\mu_i(\lambda)}{\alpha_j \cdot C_j} d\lambda \qquad (1.11)$$

where:-

$I_1(\lambda_i)$ = the intensity of λ_i.

P_i = proportionality constant.

$I_o(\lambda)$ = the x-ray tube spectrum between its excitation limits.

Besides the excitation efficiency, there are some other effects having an influence on the fluorescent intensity, such as the absorption-edge jump ratio r and the fluorescent yield ω, etc.

1.4.1 Absorption-edge jump ratio (r)

This is a measure of that portion of the total absorbed x-ray that is absorbed by a specified atomic energy level. For example K jump ratio is defined by:-

$$r_K = \frac{\mu_K + \mu_{LI} + \mu_{LII} + \mu_{LIII} + \cdots\cdots}{\mu_{LI} + \mu_{LII} + \mu_{LIII} + \cdots\cdots} \qquad (1.12)$$

For the moment, the K spectrum alone is considered, only the number of photons which are absorbed by the K energy level is considered. This fraction $\bar{r}_K$ is equal to:-

$$\bar{r}_K = \frac{\mu_K}{\mu_K + \mu_{LI} + \mu_{LII} + \mu_{LIII} + \cdots\cdots} = \frac{r_K - 1}{r_K} \qquad (1.13)$$

1.4.2 Fluorescent yield, (w)

This is defined as the number, n, of x-ray protons emitted for a given series, divided by the total number N of vacancies formed in the associated level, each with the same time increment. For example, the fluorescent yield for the K series is given by:-

$$w_K = \frac{\sum (n)_K}{N_K} = \frac{n_{K\alpha_1} + n_{K\alpha_2} + n_{K\beta_1} + \ldots\ldots}{N_K} \qquad (1.14)$$

Actually, w varies with atomic number and the line series, and decreases markedly with decrease in atomic number.

Shiraiwa and Fujine[7,8,9] have presented, for the primary fluorescence, algorithms in more practical forms than the Equation (1.11). This is shown in Figure 1.3, Equation (1.15).

1.5 Higher Order Fluorescence - Enhancement Effect

Enhancement occurs when the characteristic radiation from an element has enough energy to excite the characteristic radiation of one or more other elements in the sample. This occurs when a element j in a specimen is first excited by the primary x-ray tube

FIGURE 1.3 INTENSITY FUNCTION - PRIMARY AND SECONDARY FLUORESCENCE

$$I_1(\lambda_i) = \frac{1}{\sin \phi_2} \int_{\lambda_{min}}^{\lambda_{i,edge}} \frac{\phi_i(\lambda) \cdot I_o(\lambda)}{(\mu_s(\lambda)/\sin \phi_1) + (\mu_s(\lambda_i)/\sin \phi_2)} d\lambda \quad (1.15)$$

$$I_2(\lambda_i) = \frac{1}{2\sin \phi_2} \sum_{j=1}^{n} \int_{\lambda_{min}}^{\lambda_{j,edge}} \frac{Q_j(\lambda) \, Q_i(\lambda_j) \, I_o(\lambda)}{(\mu_s(\lambda)/\sin \phi_1) + (\mu_s(\lambda_i)/\sin \phi_2)} \quad (1.16)$$

$$\times \left(\frac{\sin \phi_1}{\mu_s(\lambda)} \ln \left(1 + \frac{\mu_s(\lambda)/\sin \phi_1}{\mu_s(\lambda_j)} \right) + \frac{\sin \phi_2}{\mu_s(\lambda_i)} \ln \left(1 + \frac{\mu_s(\lambda_i)/\sin \phi_2}{\mu_s(\lambda_j)} \right) \right) d\lambda$$

where:-

$$Q_i(\lambda) = \mu_i(\lambda) \cdot c_i \cdot \bar{r}_i \cdot w_i \cdot g_i \qquad Q_j(\lambda) = \mu_j(\lambda) \cdot c_j \cdot \bar{r}_j \cdot w_j \cdot g_j$$

$$Q_i(\lambda_j) = \mu_i(\lambda_j) \cdot c_i \cdot \bar{r}_i \cdot w_i \cdot g_i$$

spectrum, and then where its radiation λ_j excites an analyte element i. This latter is called secondary fluorescence, and can increase the total intensity of the analyte line λ_i. There would be tertiary fluorescence, where another element k, besides the element j, is excited by primary tube spectrum, and where its radiation λ_K in turn excites the element j, which then as before excites the element i. However the element k may also cause secondary fluorescence for the analyte i directly. Figure 1.4 illustrates the first two of these excitation processes. It is an important condition for any enhancement effect, that the wavelength of the enhancing element (λ_j or λ_k) must be less than the absorption edge of the analyte element ($\lambda_{i,\,edge}$).

In fact, a very complex relationship exists between the intensity for an analyte and the concentrations of the matrix elements when enhancement effects are concerned. In secondary fluorescence, one must consider the excitation efficiency for the enhancing element(s) j which can excite the analyte i, the absorption effect for the characteristic line of the enhancing element (λ_j) and the secondary fluorescence (λ_i) due to the enhancement effect by j.

FIGURE 1.4 HIGHER-ORDER FLUORESCENCE - ENHANCEMENT

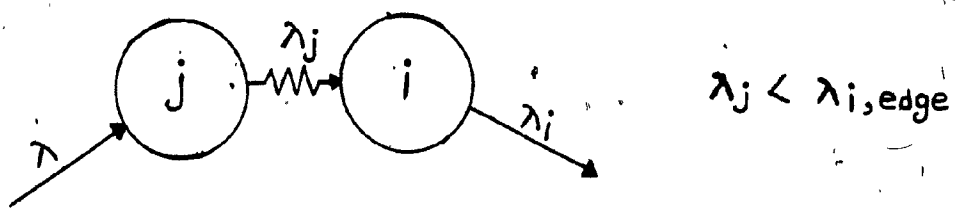

SECONDARY FLUORESCENCE

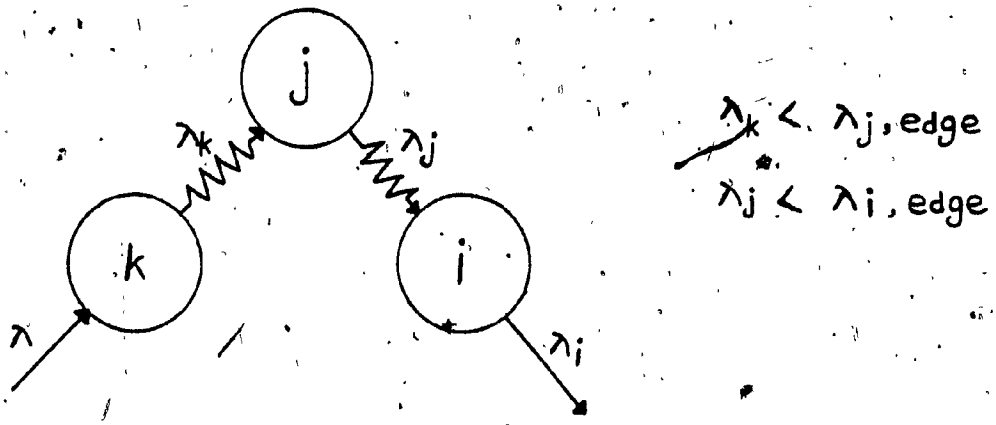

TERTIARY FLUORESCENCE

The expression for secondary fluorescence $I_2(\lambda_i)$ has been developed by many authors[7,10,11,12,13], and is shown by the Figure 1.3, Equation (1.16).

For the tertiary fluorescence or for any higher order of fluorescence, the situation is too complicated for definition. Due to their relative insignificance, with respect to the total fluorescent intensity of the analyte i, they may be ignored. The total measured intensity can therefore be taken as primary fluorescence plus secondary fluorescence:-

$$I(\lambda_i) = I_1(\lambda_i) + I_2(\lambda_i) \qquad (1.17)$$
$$= \text{Equation (1.15)} + \text{Equation (1.16)}$$

1.6 Matrix Effects And Their Corrections

It is apparent from the previous discussion that a complex relationship exists between the intensity $I(\lambda_i)$ of an analyte i in a matrix made up of the elements j. It was shown that the intensities of fluorescent x-rays produced within the specimen depend on the mass fractions of the elements in the specimen and the relationship of their mass absorption coefficients

for the primary radiation. Similarly, absorption of fluorescent radiation within the specimen depends on the various mass absorption coefficients for the fluorescent radiation. Figure (1.5)[14] illustrates the various types of effects in a binary system which contains analyte i and an interfering element j, where C_i is the weight fraction of i and R_i is the ratio of the intensity for analyte i and R_i for the pure element i, (i.e. $R_i = I_i/I_i^o$.)

Curve (a): A linear relationship exists when the absorption coefficients of the i and j are nearly the same, for the primary and fluorescent x-ray.

Curve (b): If absorption by the specimen of either the primary or the analyte line, or both, is greater than that of the analyte i, the relative intensity is below that given by the linear relationship. This effect is referred to as positive absorption.

Curve (c): If the specimen absorbs the primary or the fluorescent radiation, or both, less than does the analyte i, a negative absorption occurs.

Curve (d): Enhancement effect due to the further excitation of analyte line by the characteristic x-ray radiation of matrix element j.

FIGURE 1.5 INTERELEMENT EFFECTS - BINARY SYSTEM

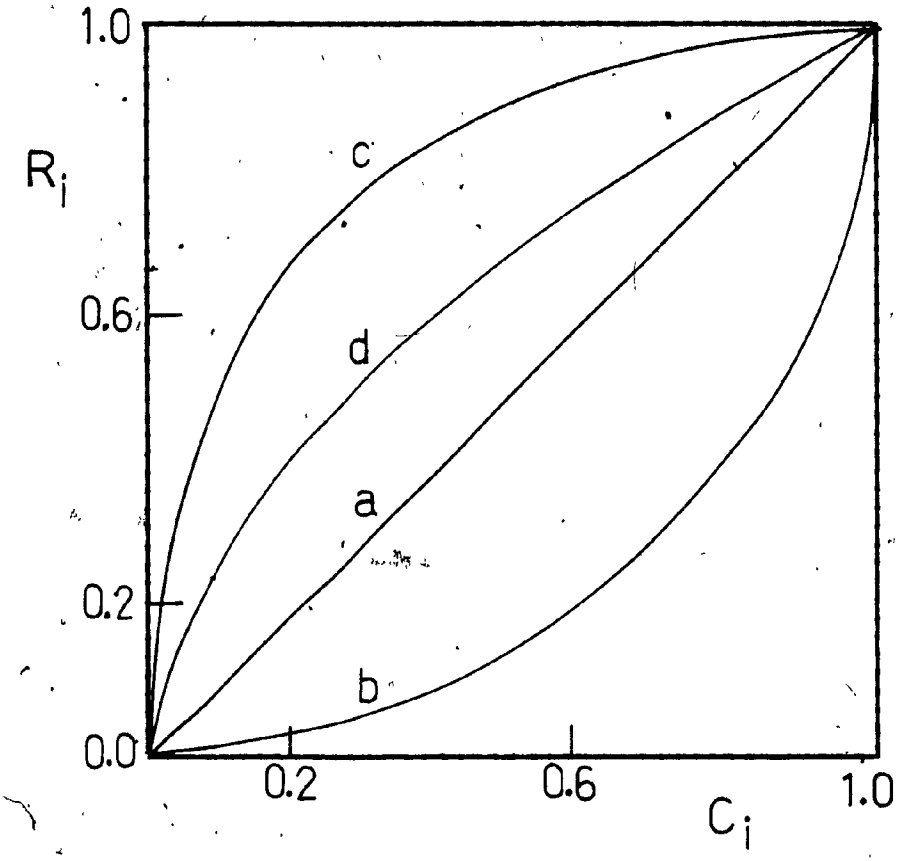

a) linear calibration curve
b) positive absorption curve
c) negative absorption curve
d) enhancement effect curve

In fact, it is very difficult to determine the absorption and enhancement effects separately from the experimental aspect, since both effects always coincide when one measures the intensities, except where only the absorption effect occurs within the specimen.

In general, two different mathematical correction procedures can be applied to the solution of the matrix-effects problem. The first is the fundamental parameters approach, and the second is the empirical correction approach.

1.6.1 Fundamental parameters approach

In this method, the basic assumptions used are that the specimen is homogeneous, with a flat surface and is infinitely thick with respect to penetration by the primary x-ray beam. The fundamental equations were derived by many authors.[9,15,16,17] Among them, Criss and Birks showed a most successful approach to the use of fundamental data for the evaluation of concentrations from measured intensities. In their method the basic algorithm is similar to the Equations (1.15) and (1.16). However, the applications were made on the basis shown in Figure 1.6 , Equation (1.18).

FIGURE 1.6 INTENSITY FUNCTION - FUNDAMENTAL PARAMETERS - CRISS AND BIRKS APPROACH

$$I(\lambda_i) = I_1(\lambda_i) + I_2(\lambda_i)$$

$$= \frac{C_i \cdot Q_i}{\sin\phi_2} \sum_i \frac{D_i(\lambda_i) \cdot I(\lambda) \Delta\lambda \cdot \mu_i(\lambda)}{\alpha_j C_j} + \frac{C_i \cdot Q_i}{2\sin\phi_2} \sum_i \frac{D_i(\lambda_i) \cdot I(\lambda) \Delta\lambda \cdot \mu_i(\lambda)}{\alpha_j C_j}$$

$$\times \left(C_j \cdot Q_j \sum_j D_j(\lambda_j) \cdot I(\lambda) \Delta\lambda \cdot \mu_j(\lambda) \times \frac{\sin\phi_1}{\mu(\lambda)} \ln \left(1 + \frac{\mu_i/\sin\phi_1}{\mu_j}\right) \right.$$

$$\left. + \frac{\sin\phi_2}{\mu(\lambda_i)} \ln \left(1 + \frac{\mu_i/\sin\phi_2}{\mu_j}\right) \right) \qquad (1.18)$$

The first parameter needed in this approach is the spectral distribution of the primary radiation from the x-ray tube. The authors tabulated the spectrum in the form of intensity $I(\lambda)$ per 0.02Å interval, $\Delta\lambda$, starting at λ_{min}. An extra term $D_i(\lambda_i)$ or $D_j(\lambda_j)$ was used in the summation term, and has the value 1 for $\lambda<\lambda_{edge}$, and 0 for $\lambda>\lambda_{edge}$, so that the integral form of $I_o(\lambda)d\lambda$ can be replaced by $\sum D_i(\lambda_i).I(\lambda)\Delta\lambda$ or $\sum D_j(\lambda_j).I(\lambda)\Delta\lambda$, and the integrated value, $I\Delta\lambda$, is the parameter for the primary intensity at each wavelength.

The other parameters, such as mass absorption coefficients (μ's), fluorescent yield (w's) and absorption-edge jump ratio (r's), are all derived by separate experiments or calculations.[16,18,19,20,21]

The summation over j indicates, it is noted, that the contributions of all such sufficiently-energetic ($\lambda_j<\lambda_{i,\ edge}$) lines must be added together.

A simplification of Equation (1.18) can be made, in which the relative x-ray intensity, R_i, is used, and the Q terms cancelled, leaving only terms in R and C. This is shown as:-

$$R_i = \frac{I_1(\lambda_i) + I_2(\lambda_i)}{I_1^s(\lambda_i) + I_2^s(\lambda_i)} \qquad (1.19)$$

Where s indicates a standard sample. If a pure element i is used for the standard, since no secondary fluorescence occurs with a pure element, Equation (1.19) may be written as:-

$$R_i = \frac{I_1(\lambda_i) + I_2(\lambda_i)}{I_1^o(\lambda_i)} \qquad (1.20)$$

Accordingly, with the iteration procedure as used by Criss and Birks, linear relationships between normalized R_i's and C_i's are assumed, and from these (incorrect) C_i's, a new set of R_i's is calculated. The differences between the measured and calculated R_i's are then used to correct the C_i's and the procedure is started all over again. The iteration equation[15] has been proposed:-

$$C_i^{corr.} = \frac{R_i^{meas.}\ C_i(1-R_i)}{R_i^{meas.}\ (C_i-R_i) + R_i(1-C_i)} \qquad (1.21)$$

Such interations are normally carried out until a desired precision of C_i is reached.

There is an additional concept which can further simplify the concentration-intensity equation. Many authors[22,23,24,25] have proposed the effective wavelength concept, in which it is considered that one single wavelength λ_e exists between λ_{min} and $\lambda_{i,edge}$, and that this λ_e has the same effectiveness in the excitation of λ_i as the whole continuum:-

$$\lambda_e = \int_{\lambda_{min}}^{\lambda_{edge}} I_o(\lambda)d\lambda \qquad (1.22)$$

so that the primary fluorescence Equation (1.18) can be simplified as:-

$$I_1(\lambda_i) = \frac{K_i \cdot C_i}{\sum_i C_j \cdot \alpha_j} \qquad (1.23)$$

where $K_i = Q_i/\sin\phi_2$

In practice, where the contribution from characteristic source lines is insignificant, this turns out to be equal roughly to 2/3 of $\lambda_{i,edge}$. The subject of the accuracy of the effective wavelength concept still invokes considerable discussion, but nevertheless it has been found extremely useful for simplification of the concentration-intensity algorithm. By using λ_e,

the handling of the calculation is similar to that of the Criss-Birks method. Stephenson[26] developed the program CORSET which makes use of both primary and secondary fluorescence corrections, but ignores the tertiary and higher-order fluorescence terms.

1.6.2 Empirical methods

The use of the fundamental method indicates that rather large computing facilities are required, which are not at the immediate disposal of every laboratory, and that the accuracies of the results will depend quite heavily on the accuracies of the fundamental parameters used.[15,27] These uncertainties impose limitations on the fundamental approach which has encouraged many authors[28,29,30] to develop empirical relationships between characteristic x-ray emission and chemical composition. The majority of the empirical methods involve determination of matrix-effect correction coefficients through simplified concentration-intensity equations and experimentation, followed by substitution into a set of equations, from which the composition of unknowns can then be evaluated.

In practice, two major classes of empirical procedures exist. The first, a semi-empirical approach in which the concentration-intensity algorithm is expressed in

such a form that the coefficients and correction terms have significance in terms of actual absorption coefficients. These constant terms can indeed be calculated from mass absorption coefficient data. Secondly, the truly empirical algorithms, in which the concentration-intensity relationship is expressed as a polynomial and then mathematical techniques are employed to solve for the correction terms. However, when one uses these methods, there are two important assumptions to be made:-

1) The primary x-ray beam is assumed to be monochromatic, and the integral form of $I_o(\lambda)$ in Equation (1.15) replaced by the effective wavelength λ_e.

2) Enhancement or secondary fluorescence is assumed to be treated acceptably as negative absorption[31,32] since the two effects behave in a similar manner. In this case, the absorption coefficient for the enhancing element is replaced by a hypothetical absorption coefficient which is lower than that for the analyte.

Therefore, the effect of each of the matrix elements j on the fluorescent intensity of a given analyte i is simply that of an absorption effect.

The intensity equation may thus be dramatically simplified, since only the primary fluorescent intensity is considered.

For Equation (1.23), consider a binary system i, j, where the following relationship holds:-[28,29,30]

$$I_i = \frac{K_i \cdot C_i}{C_i \cdot \alpha_i + C_j \cdot \alpha_j} \qquad (1.24)$$

Since $C_i + C_j = 1$, then $C_i = 1 - C_j$, and we obtain:-

$$I_i = \frac{K_i \cdot C_i}{(1-C_j)\alpha_i + C_j \cdot \alpha_j} = \frac{K_i \cdot C_i}{\alpha_i + C_j(\alpha_j - \alpha_i)} \qquad (1.25)$$

Let $\alpha_{ij} = \frac{\alpha_j - \alpha_i}{\alpha_i}$, so that $\alpha_j - \alpha_i = \alpha_{ij} \cdot \alpha_i$,

and let $K_i = \alpha_i / K_i'$

substitution Equation (1.25) yields:-

$$I_i = \frac{C_i / K_i'}{1 + \alpha_{ij} \cdot C_j}$$

Or

$$C_i = I_i \cdot K_i' (1 + \alpha_{ij} \cdot C_j) \qquad (1.26)$$

Since for a pure sample of element i, $C_i = 1$ and $C_j = 0$ then we have:-

$$K_i' = 1/I_i^o$$

If R_i is taken as the ratio of the sample intensity to the pure element intensity (i.e. I_i/I_i^o), substitution in Equation (1.26) gives:-

$$C_i = R_i(1 + \alpha_{ij} \cdot C_j) \qquad (1.27)$$

The constant α_{ij} is a factor, the so-called alpha coefficient, which represents the effect of element j on element i, and its value does have some theoretical significance in that it is related to the ratio of the total absorption for j to the total absorption for element i. The coefficient may be calculated from absorption coefficient data as:-

$$\alpha_{ij} \cong \frac{\alpha_j}{\alpha_i} - 1 = \frac{\mu_j(\lambda_e) + A \cdot \mu_j(\lambda_i)}{\mu_i(\lambda_e) + A \cdot \mu_i(\lambda_i)} - 1 \qquad (1.28)$$

In a multicomponent system, Equation (1.27) may then be easily applied as:-

$$C_i = R_i \left(1 + \sum_j^n \alpha_{ij} \cdot C_j \right) \qquad (1.29)$$

This is the well-known Lachance-Traill[28] model. In this model, the relative intensity R's for each element are measured experimentally, the alpha-correction coefficients are determined, also experimentally, from binary standards or, preferably, from multicomponent standards. The chemical compositions for unknown specimens can then be obtained from the measured intensities by solving a system of simultaneous linear equations.

Lachance and Traill[33] applied their correction equations quite successfully in the analysis of 9 components in steel alloys. The average relative errors were 8 percent at 0.5 percent concentration level, 3.7 percent at 5.5 percent concentration level, and 0.96 percent at the 55 percent level.

Sherman[34] had discussed the empirical method in 1954, the year before the publication of his theoretical equations, and his scheme involved the use of regression analysis to solve the equations. Equations (1.30) are typical of this approach, and are generally attributed to Beattie and Brissey,[35] although various refinements were employed by Marti.[36] The listed equations, refer to

a tertiary system of elements i, j and k.

$$C_i = R_i (C_i + K_i^j \cdot C_j + K_i^k \cdot C_k)$$

$$C_j = R_j (C_j + K_j^k \cdot C_k + K_j^i \cdot C_i) \qquad (1.30)$$

$$C_k = R_k (C_k + K_k^i \cdot C_i + K_k^j \cdot C_j)$$

This originated from the Equation (1.23), as the Lanchance and Traill equation, and the values of the K's are constants representing the effect of element j or i, etc., which have the same meaning for the alpha-correction coefficients as shown by:-

$$K_i^j = \alpha_{ij} + 1 = \frac{\alpha_j}{\alpha_i} = \frac{\mu_j(\lambda_e) + A \cdot \mu_j(\lambda_i)}{\mu_i(\lambda_e) + A \cdot \mu_i(\lambda_i)} \qquad (1.31)$$

1.7 The Validity Of The Correction Coefficient

In point of fact, all methods for interelement-effects correction are concerned with the proper evalution, or control of, the quantity "correction coefficient". Whether as the α-coefficient or the K-coefficient, they are derived from the same basic equations, and they suffer from the same areas of difficulty.

First, Equation (1.23) implicitly assumes that the primary radiation can be reduced to a single wavelength λ_e (effective wavelength) and that this representative wavelength is the same for all of the specimens to be analyzed, as well as for the pure element. However, Tertian[27] has shown that the effective mass absorption coefficients (given by him as α_i, α_j etc) cannot be considered as constant, even with a fixed excitation condiation, but as quantities varying with specimen compositions, as also does the effective wavelengths λ_e.

It should also be noted that both Tertian[27] and Lachance[37] have shown that, as a consequence of the polychromatic nature of the primary x-ray beam, the correction coefficients are not constants as assumed, but tend to vary over a wide range of concentrations. However, it is legitimate to suppose that if the compositional range narrows sufficiently then the λ_e is approximately fixed and the α or k coefficients can be considered as constants in a practical sense.

The Claisse-Quintin[23] relationship has taken the polychromatic nature of the primary beam into consideration. The authors modified the Lachance-Traill equations by including secondary terms. For example, for a ternary

system i, j, k, we have:-

$$C_i = R_i \left(1 + \alpha_{ij} C_j + \alpha_{ik} C_k + \alpha_{ijj} C_j^2 + \alpha_{ikk} C_k^2 + \alpha_{ijk} C_j C_k\right)$$

However, the evaluation of the various coefficients from such a relationship becomes highly complex, because of the large number of standards required.

The second problem that arises is how to deal with the enhancement effect. Starting with the basic Equation (1.23), if only the pure absorption effect (primary fluorescence) were present the situation would be simple. There may possibly be, however, enhancement effects (secondary or higher-order fluorescence), which are qualitatively similar to "negative absorption",[31,32] and which result in an increase in the fluorescent intensity. For this reason most investigators[27,28] have accounted for "negative absorption" by introducing negative coefficients relative to Equations (1.29) and (1.30). However, on a quantitative basis, enhancement obeys its own laws and, unlike pure absorption, does not follow the additivity law. Allowances for enhancement effects have been introduced by the Rasberry and Heinrich.[30] Their relationship is expressed by:-

$$C_i = R_i \left(1 + \sum_j A_{ij} \cdot C_j + \sum_j \frac{B_{ij}}{1 + C_i} \cdot C_j \right) \qquad (1.32)$$

When $B_{ij} = 0$, the net effect on the fluorescence of element i is absorption, and the equation has similar terms to the Lachance-Traill equation, with A_{ij} having same meaning as α_{ij}, but is always given a positive value. When $A_{ij} = 0$, the net effect on the fluorescence of element i is enhancement, and B_{ij} is always given a negative value. However, it is impossible to have pure enhancement effects occurring within the specimen which always coordinate with the absorption effect. Such relationship do not provide for a linear situation between concentration and intensity.

1.8 Modified Lachance-Traill Method

It was decided in the present investigation to evaluate binary systems using a modification of the original Lachance-Traill equation, with some improved experimental techniques for the determination of α-correction coefficients. Subsequently, a technique of applying these α-correction coefficients, in the general chemical analysis of multi-component specimen systems, was to be developed. This technique was expected

to provide high flexibility relative to the amount of the sample available for analysis.

From the theoretical calculations of Bachance,[37] three basic assumptions may be made:-

1) The absorption effects of lower atomic number elements such as oxygen, nitrogen, etc., on the higher atomic number elements such as iron, cadmium etc. can be considered as constants regardless of minor concentration variations for these lower atomic number elements.

2) The interelement-effect coefficients for the higher atomic number elements are approximately constant where the concentration levels are below 10 or 20 percent.

3) Higher-order correction coefficients are not significant where concentration levels are below 10 percent for the higher atomic number elements.

In addition, in order to minimize the interelement effects, and to eliminate such factors as particle size, compositional heterogeneity and surface finish, etc., the only one experimental technique that can be considered as generally suitable is the "dilution techniques", involving either dilution of solid samples by fusion, or dilution by water additions to aqueous solutions. The fusion technique at high concentration levels tends to be both difficult and time-consuming. Dilution of aqueous solutions[14,32,38] was therefore chosen as the basis of the technique.

In the original form the Lachance-Traill equation for multiple systems can be written as follow:-

$$C_i = R_i \left(1 + \sum_{\substack{j=1 \\ (j \neq i)}}^{n} \alpha_{ij} \cdot C_j \right) \qquad (1.33)$$

where:-

C_i = weight fraction of analyte i.

C_j = weight fraction of the interfering element j in the specimen.

R_i = relative intensity - measured intensity for i to intensity for pure i.

α_{ij} = correction coefficient for effect of element j on analyte i.

n = number of elements in the system.

In this investigation, since aqueous media are used, constituting the bulk($\sim$80%) of the solution, an additional term is introduced into Equation (1.33), which takes this into account, and the modified equation is shown as:-

$$C_i = R_i \left(1 + \alpha_{iM} \cdot C_M + \sum_{\substack{j=1 \\ (j \neq i)}}^{n} \alpha_{ij} \cdot C_j \right) \qquad (1.34)$$

where:-

C_M = weight fraction of the aqueous matrix (usually H_2O-HNO_3).

α_{iM} = correction coefficient for effect of aqueous matrix on analyte i.

The weight fraction of the aqueous matrix C_M can be obtained from:-

$$C_M = 1 - C_i - \sum_{\substack{j=1 \\ (j \neq i)}}^{n} C_j \qquad (1.35)$$

In this modification the major assumption is that the aqueous matrix effect is comprised of low absorbing elements such as hydrogen, oxygen, nitrogen, lithium and boron, which can be grouped into one correction coefficient representing the net effect.

In order to determine the interelement correction coefficients, the following experimental approaches were developed:-

1) determination of α_{iM}: Samples of differing concentration of analyte i and matrix(H_2O-HNO_3) are prepared.

2) determination of α_{ij}: Samples are prepared, which consist of differing concentrations of the interfering element j, matrix M and analyte i.

When all of the required α-correction coefficients have been determined for the elements of interest, a

single standard solution is needed to evaluate the $I^{o}_{i \to n}$ (intensity for $C_{i \to n} = 1$) and to calculate $R_{i \to n}$. Subsequent to this, the chemical composition of solutions involving materials of unknown composition may be evaluated by solving a system of linear equations of the following form:

$$\begin{aligned}
C_i &= R_i \left(1 + \alpha_{iM} C_M + \ldots + \alpha_{ij} C_j + \ldots + \alpha_{in} C_n \right) \\
&\ldots \quad \ldots \quad \ldots \quad \ldots \quad \ldots \\
C_j &= R_j \left(1 + \alpha_{jM} C_M + \ldots + \alpha_{ji} C_i + \ldots + \alpha_{jn} C_n \right) \qquad (1.36) \\
&\ldots \quad \ldots \quad \ldots \quad \ldots \quad \ldots \\
C_n &= R_n \left(1 + \alpha_{nM} C_M + \ldots + \alpha_{ni} C_i + \ldots + \alpha_{nj} C_j \right)
\end{aligned}$$

with

$$C_i + \ldots + C_j + \ldots + C_n = 1$$

The purpose of this investigation is to :- (1) Determine additional α-coefficients required in the analysis of copper-base and aluminum-base alloys; (2) to redetermine more reliably previous coefficients applicable in such analyses; (3) apply all such experimentally -determined and theoretically-calculated in the analysis of such alloys; (4) indicate the precision and accuracy of such analyses.

2. EXPERIMENTAL

2.1 Instrumentation

Throughout the study a Picker Nuclear Spectro-Diffractometer (45° incident and emergent angles), a radiation analyzer and an ultrastable two-tube generator were used.

2.1.1 X-ray tube

The useful source of excitation in fluorescent x-ray analysis is the primary spectrum from an x-ray tube. The spectral distribution in the primary spectrum is important because it determines how well the characteristic radiation will be excited in the specimen. The only effective part of the primary spectrum is that part which is of shorter wavelength than the absorption edge of the element to be excited in the specimen. If there are intense lines, characteristic of the x-ray tube target, close to the shorter wavelength side of absorption edge of the analyte, it would contribute a large part of the total radiation. Otherwise, the continuum would represent the primary source of excitation.

Target material and voltage determine the intensity in the effective part of the primary spectrum, and also control the efficiency and intensity of the fluorescent x-rays from the specimen. Figure 2.1 illustrates the effect of x-ray tube voltage and target meterial on the spectrum.

In the present studies, a chromium target x-ray tube with 0.25mm beryllium window thickness, operating at 50KV/36mA, was used in the intensity measuring process for the lower atomic number elements (ie Z=12 to 22). A tungsten tube with 1.5mm beryllium window thickness was used in the intensity measurements, operating at 50KV/20mA, associated with the characteristic radiation (K_α or L_α) for the higher atomic number elements such as chromium, manganese, iron, etc.

2.1.2 Spectrogoniometer

Spectrometer are designed with the specimen placed such that it is irradiated by the primary x-ray beam, and in which the angle of incidence of the primary radiation may be 60 degree, 55 degree or 45 degree. The 45 degree arrangement has the advantage of simplifying the calculations. As an example, consideration of the depth of

FIGURE 2.1

EFFECT OF X-RAY TUBE POTENTIAL AND TARGET ATOMIC NUMBER ON THE CONTINUOUS SPECTRUM

(A) TUBE POTENTIAL

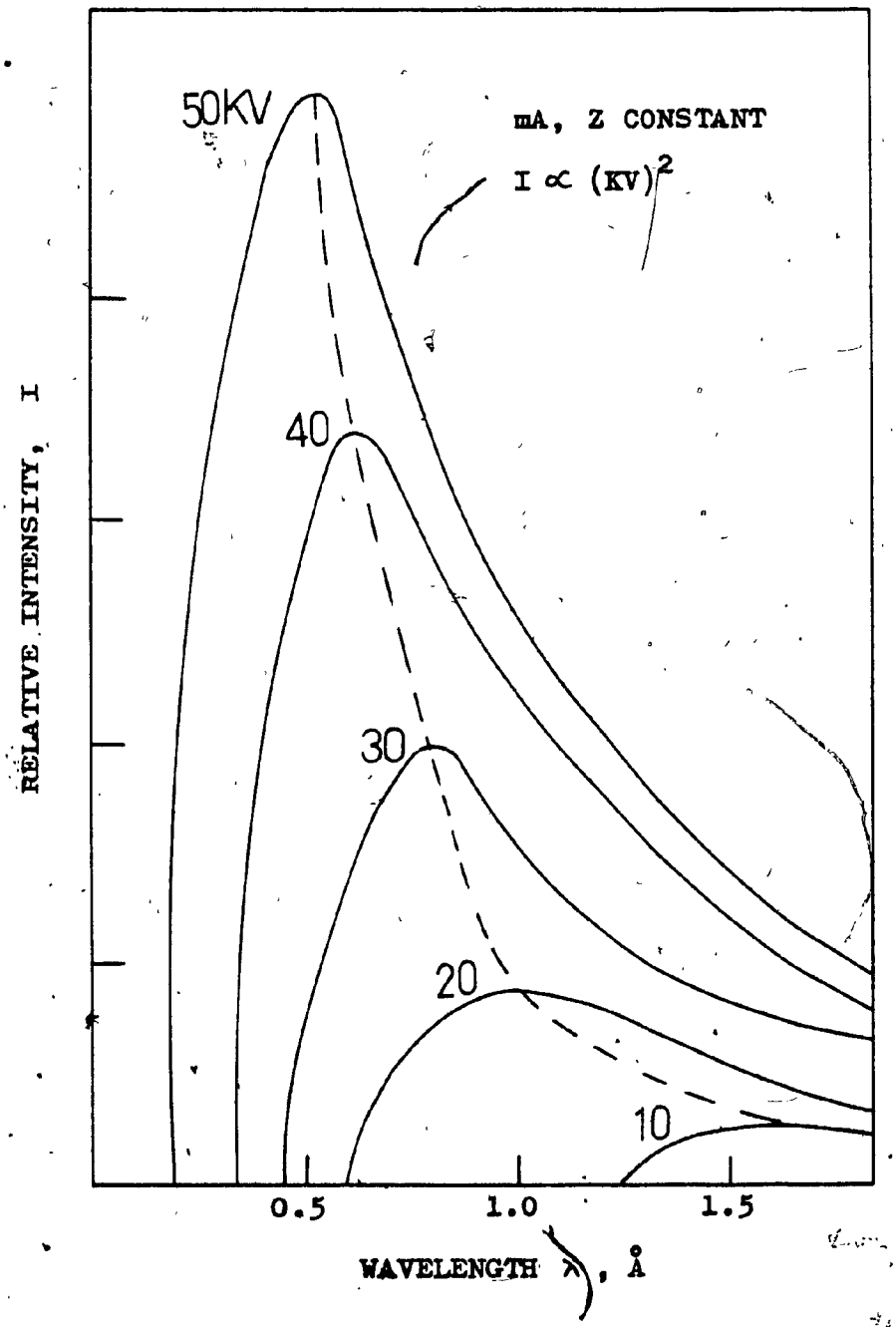

FIGURE 2.1
cont'd

(B) TARGET ATOMIC NUMBER

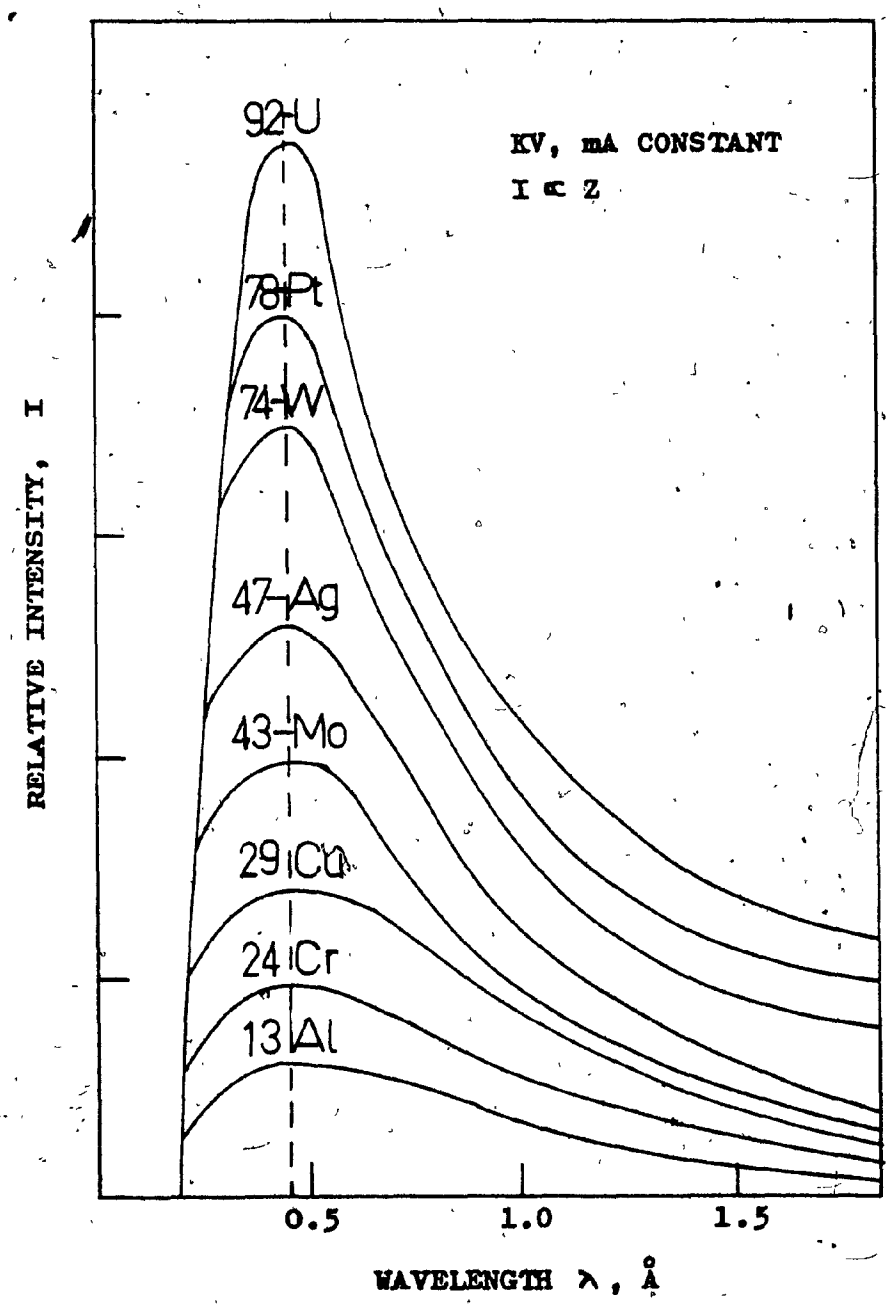

penetration requires inclusion of a spectrometer geometry factor which is the ratio of the sine of the incident angle to the sine of the take-off angle. For a $45^{o}/45^{o}$ geometry is 1, while for a $60^{o}/30^{o}$ and $55^{o}/35^{o}$ geometry, this factor are 1.732 and 1.428 respectively.

The goniometer is basically the analysing crystal and a system of slits or collimators. Figure 2.2 illustrates the general arrangement of the spectrogoniometer. The analyzing crystal is the basis of x-ray analysis, serving the purpose of separating the specimen radiation beam into its individual wavelength components. The flat, reflection crystal optical system is probably the most common of all the XRF techniques, and the crystal interplanar spacing d determines the angle θ at which the nth order of wavelength λ will be diffracted according to the Bragg[40] equation:-

$$n\lambda = 2d \cdot \sin\theta \qquad (2.1)$$

There is a wide selection of materials for the analyzing crystal. Table 2.1 lists common crystals used in x-ray spectrometers and the d spacings for these analyzing crystals. In practice one should generally use the smallest d-spacing crystal possible consistent

FIGURE 2.2

XRF SPECTROMETER GEOMETRIC ARRANGEMENT

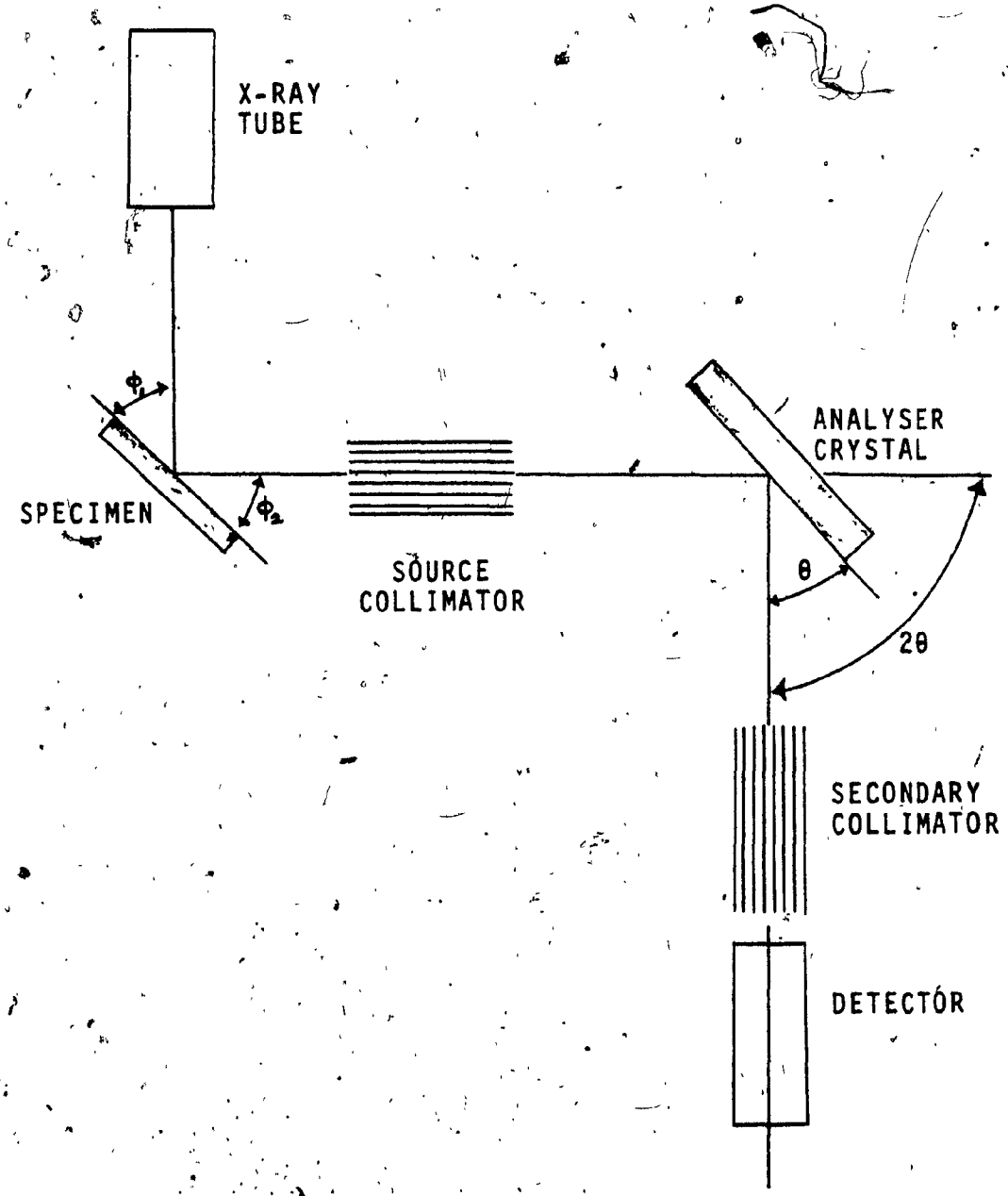

TABLE 2.1 COMMON ANALYZING CRYSTALS

CRYSTAL NAME	REFLECTION PLANE	2d, Å
TOPAZ (Al silicate)	(303)	2.712
LITHIUM FLUORIDE (LiF)	(200)	4.028
SODIUM CHLORIDE (NaCl)	(200)	5.640
PENTAERY-THRITOL (PET)	(002)	8.742
AMMONIUM DIHYDROGEN PHOSPHATE (ADP)	(011)	10.648
GYPSUM ($CaSO_4 \cdot 2H_2O$)	(020)	15.185
SORBITOL HEXA-ACETATE (SHA)	(110)	13.980

with the maximum wavelength to be measured. In this case, the ADP is the efficient crystal for the diffraction of MgK_α, the PET for AlK_α through ClK_α, and the LiF for CaK_α and upwards.

In x-ray analysis it is desirable to have a collinear radiation beam. However, sample excitation causes x-rays to be radiated in all directions. Slit or multiple slit collimators are normally used to restrict the divergence of the x-rays. The selection of the optimum secondary collimator for a given application must be made with the consideration being given to the dispersion of the analysing crystal employed.[41] A choice is frequently available between, on the one hand, a fine collimator and a crystal of poor dispersion but high reflectivity, and on the other hand, a coarse collimator and a crystal of high dispersion but poor reflectivity. Therefore, a coarse collimator can be used in the intensity(K_α) measurements for the elements from magnesium through vanadium, and a fine collimator for the elements from chromium upwards.

2.1.3 Detector

The basic principle of x-ray detection is that of converting the x-ray photon energy into a form of electric current pulses, which can be measured and integrated over

a finite period of time. There are three types, gas-filled, scintillation and lithium-drifted silicon detectors, which are normally used in XRF spectrometry. However, only the gas-filled and scintillation detector were used for the present studies.

a) Gas-Filled Counter: In this study, a proportional flow counter(PF) with P10 gas(argon 90% / methane 10%) flow was used. Figure 2.3 shows schematically the construction of this counter. In operation, a methane atom absorbs the x-rays and ejects a valence electron, which will be attracted toward the central wire and lose its energy by ionizing other methane atoms and generating a number of ion pairs (positive ions and electrons). One can measure the x-ray intensity, using this counter, because of the linear relation between ion-pairs and x-ray photon energy. Normally this counter is used to detect x-rays in the 2 - 10 Å range.

b) Scintillation Counter(Sc): This consists of a thallium activated NaI crystal, sealed to the window of a photomultiplier tube, to amplify the signal generated. Figure 2.4 illustrates this type of counter. When the crystal absorbs an x-ray photon it generates a number of visible-light photons which strike the light sensitive surface of the photomultipler and cause electrons to be

FIGURE 2.3

STRUCTURE OF GAS-FILLED COUNTER

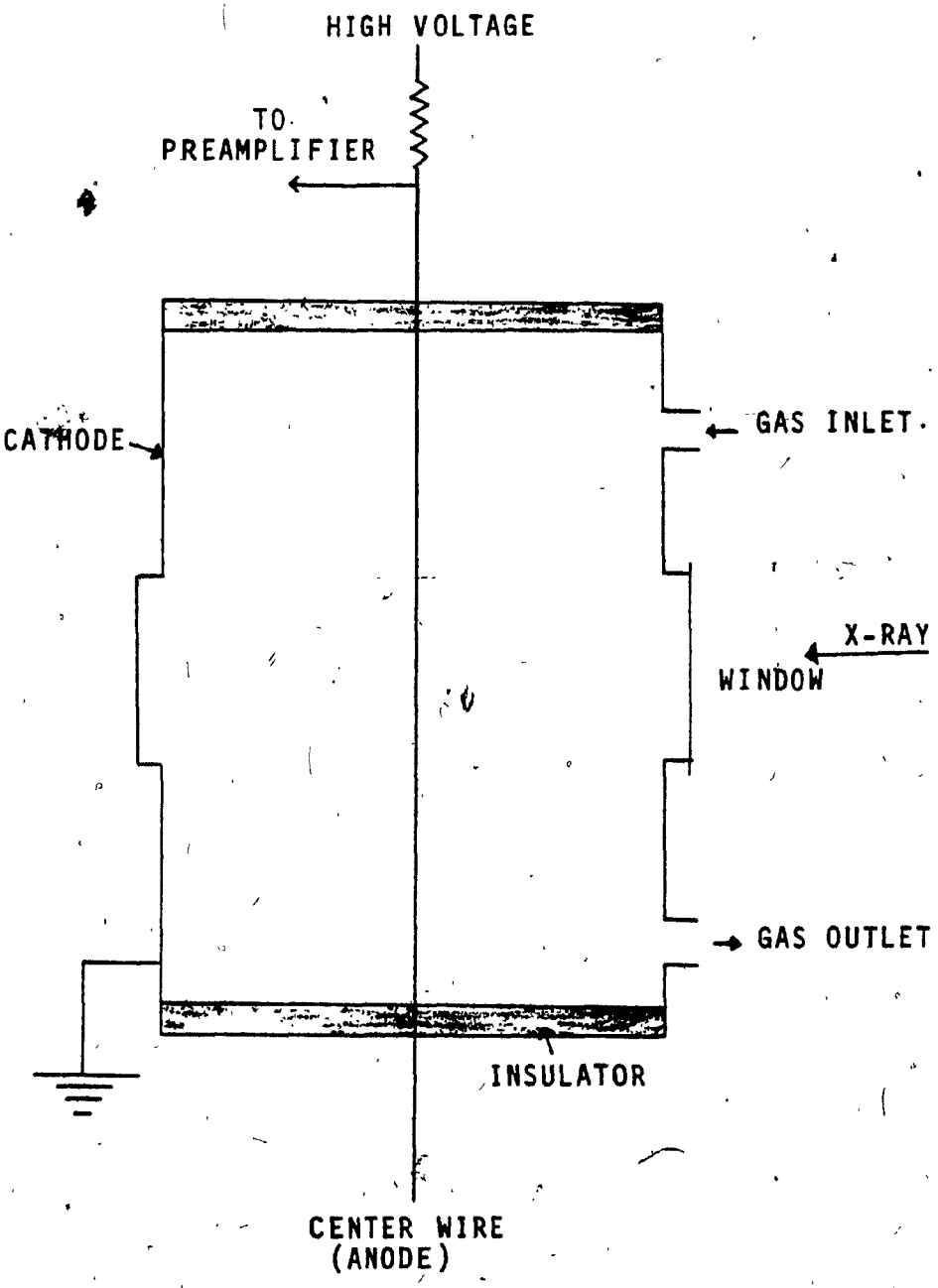

FIGURE 2.4

STRUCTURE OF SCINTILLATION COUNTER

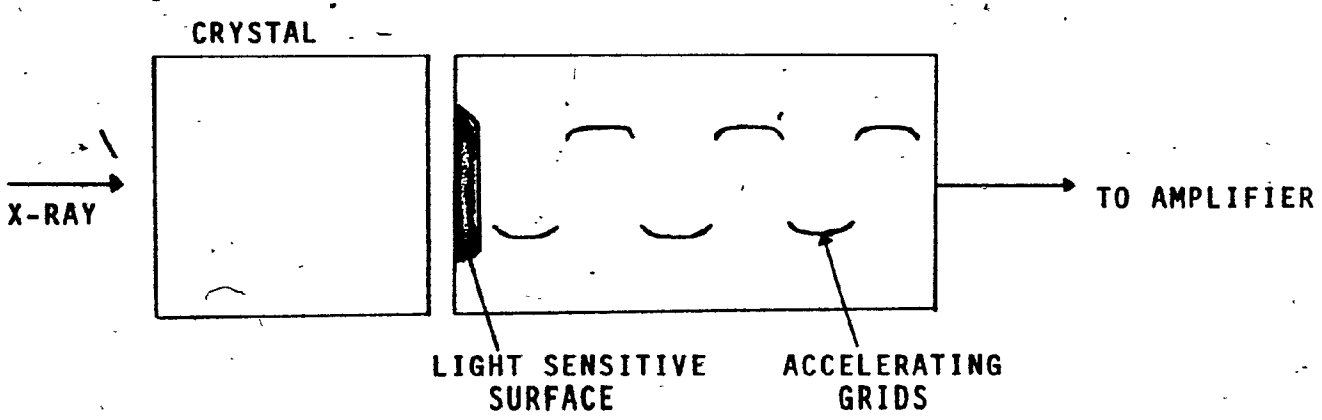

emitted. Thus, a multiplied electric-pulse appears at the output of the photomultiplier, and would be proportional to the x-ray photon energy. This detector was used for short-wavelength x-rays, where the range is 0.1 Å to 3.0 Å.

c) Lithium-Drifted Silicon Detector(Si(Li))[43]: Probably the most significant recent development in x-ray intensity measurement is this kind of counter. It consists of a silicon (or germanium) single-crystal semiconductor having a compensated intrinsic region sandwiched between positive and negative regions. Figure 2.5 shows schematically the construction of this detector. In operation,[44,45,46] an x-ray photon can be considered as entering the detector and passing through the active semiconductor volume - the lithium-drifted silicon region. Eventually, it undergoes photoelectric absorption by a silicon atom and imparts its energy to a photoelectron which produces electron-hole pairs along its path until its energy is expended - just as ion-electron pairs are produced in gas-filled detector and light photons in a scintillation counter. When in use, the detector must be maintained at liquid-nitrogen temperature (77 K) to reduce noise and ensure optimal resolution, and also to prevent a high diffusion rate for lithium.

FIGURE 2.5

SCHEMATIC OF LITHIUM-DRIFTED SILICON DETECTOR

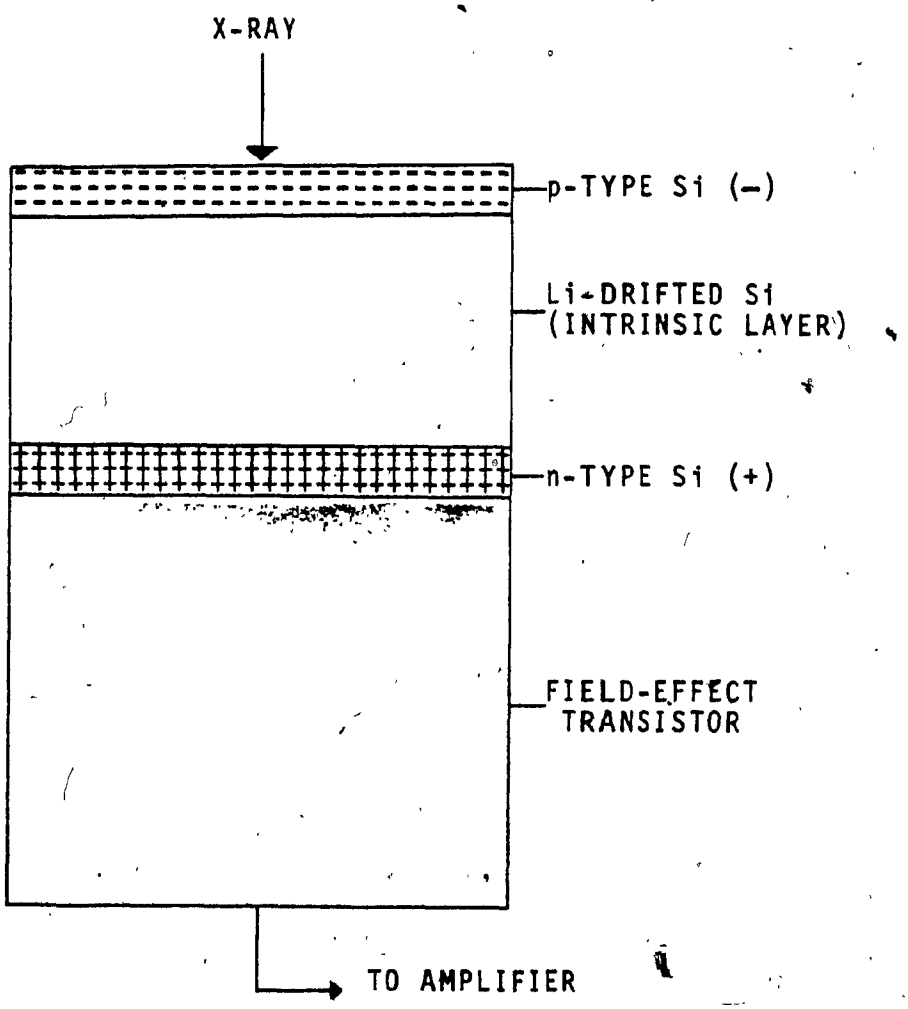

2.1.4 Dead-time correction

Under normal operating conditions the number of voltage pulses produced by the detector varies as the intensity of the incident x-rays. However, at high count rates the linear relationship does not hold, since the relatively slow dissipation of the positive ion sheath has a very significant effect upon the functioning of the counter in that, as long as the ions are in the immediate vicinity of the anode, the field is reduced, thus preventing further avalanches. This gives rise to the so-called dead-time of the counter, and a useful expression for the true counting rate was first proposed by Ruark and Brammer:[42]

$$I_t = \frac{I_m}{1 - I_m \cdot t} \qquad (2.2)$$

where:-

I_t = true counting rate
I_m = measured counting rate
t = dead-time of the counter

In this investigation, for the scintillation counter, when I_m was over 30,000 cps, a dead-time correction was made, and the empirical correction expression used throughout the present studies as :-

$$I_t = \frac{I_m}{1.024374 - 0.79681 \times 10^{-6} \cdot I_m} \qquad (2.3)$$

2.2 Sample Preparation

Solid standard samples supplied by Somar Ltd., were used to set up the instrumental parameters for XRF analyses. They were also used as references for the determination of I^o (intensity for a pure element).

A series of solutions for each element of interest were prepared from reagent-grade chemicals (i.e. pure elements or their nitrates). These solutions, in each case, showed considerable variation in the concentration range, generally from 0.005 to 0.1 weight fraction. Each series of solutions was prepared, from stock solutions by the dilution methods. The final weight of each prepared solution specimen was generally 100g, and the dilution water was boiled previously to prevent the formation of gas bubbles during the XRF analysis.

Using these stock solutions, the required amounts of the elements involved were made up in a minimum of acid mixture (H_2O-HNO_3), the concentration of the acid mixture not being considered critical. The solution were then boiled to expel dissolved gases, which might otherwise

form air bubbles upon irradiation. When an elemental mixture did not dissolve in this acid-water mixture, the use of another acid such as HCl or H_3PO_4 was resorted to . In such cases, however, the effects of the heavier elements Cl and P on the analyte had to be predetermined. The stock solutions of chlorine and phosphorus were prepared from concentrated hydrochloric acid and phosphoric acid, and the concentrations of chlorine and phosphorus were accurately determined by potentiometric titration.

The various commercial aluminum alloy samples used as standards and unknown in this investigation, were supplied by the Aluminum Company of Canada Limited. These alloy samples were examined in the form of discs obtained from standard chill-cast specimens, the final disc approximating $1\frac{1}{8}$" diameter and $\frac{1}{4}$" thickness. The surface exposed to the primary x-ray beam was prepared, in the order indicated, by:-

(a) Machining.

(b) Grinding with decreasing sizes of diamond grit.

(c) Polishing with 20 micron diamond dust.

The final polishing operation provided for a surface

roughness required for measuring the intensity of the secondary radiation emitted for the lowest atomic number analyte. In addition, the final polishing operation was carried out in a manner intended to minimize the surface smearing of the soft elements such as silicon or lead in the specimen. A good test for such superficial smearing is to measure, for a covered element, the $L\alpha_1/K\alpha$ intensity ratio for elements up to atomic number 60, and $M\alpha/L\alpha_1$ ratio for the heavier elements. This was done for any possibly smeared specimen and for another specimen of the same alloy known not to be smeared, or even from the pure element. The intensity of the longer-wavelength line($L\alpha_1$ or $M\alpha$)- and thereby the ratio - is decreased by any overlying smeared constituent.

A series of analyzed solid samples of various, commercial copper-base alloys, suitable for direct examination under XRF, were supplied by Professor J.G. Dick and made for this study. These samples were used also to prepare specimens in an aqueous solution form.

2.3 Measurement of Intensity

In principle, the integrated intensity under the entire analyte-line peak should be measured, however, in the present study, the peak intensity at the 2θ angle of maximum intensity was found to be representative

of the integrated intensity.

Table 2.2 shows the generation and detection parameters applied. These are not intended to represent optimum values, they are the applied values over the period of the investigation. In general, for each analyte, a scan of intensity versus 2θ angle was obtained at the parameters indicated (i.e. Table 2.2). These scans were then analyzed to determine the most suitable 2θ for peak and background counting.

As the general procedure for the measurement of intensity, the peak and background angles were counted five times, and the final values applied in subsequent treatments represented the averages of these measurements. Subsequently, these intensity values were corrected, where required, for counter dead time using Equation (2.3), and then for background intensity involving the use of Equation (2.4) as follows:-

$$I = I_{pk} - \left(I_{b1} + \frac{2\theta_{b1} - 2\theta_{pk}}{2_{b1} - 2_{b2}} (I_{b2} - I_{b1}) \right) \qquad (2.4)$$

where:-

I = the net corrected intensity;

I_{pk} = the intensity measured at the peak position;

TABLE 2.2 OPERATING CONDITIONS

ELEMENT	Mg	Al	Si	P	Cl	K	Ca	Ti	Cr	Mn	Fe	Co
TARGET	Cr	Cr	Cr	Cr	Cr	Cr	Cr	Cr	W	W	W	W
KV	50	50	50	50	50	50	44	50	50	50	50	50
COLLIMATOR	coarse	coarse	coarse	coarse	coarse	coarse	coarse	coarse	fine	fine	fine	fine
CRYSTAL	ADP	PET	PET	PET	PET	PET	LiF	LiF	LiF	LiF	LiF	LiF
COUNTER	PF	PF	PF	PF	PF	PF	Sc	Sc	Sc	Sc	Sc	Sc
TIME	50s	50s	50s	20s	20s	10s	10s	10s	10s	10s	10s	10s
RADIATION	Kα	Kα	Kα	Kα	Kα	Kα	Kα	Kα	Kα	Kα	Kα	Kα
PATH	He	He	He	He	He	He	He	He	air	air	air	air

TABLE 2.2 cont'd

ELEMENT	Ni	Cu	Zn	As	Br	Sr	Mo	Ag	Cd	Sn	Sb	I	Ba
TARGET	W	W	W	W	W	W	W	W	W	W	W	W	W
KV	50	50	50	50	50	50	50	50	50	50	50	50	50
COLLIMATOR	fine	fine	fine	fine	fine	fine	fine	fine	fine	fine	fine	fine	fine
CRYSTAL	LiF	LiF	LiF	LiF	LiF	LiF	LiF	LiF	LiF	LiF	LiF	LiF	LiF
COUNTER	Sc	Sc	Sc	Sc	Sc	Sc	Sc	Sc	Sc	Sc	Sc	Sc	Sc
TIME	10s	10s	10s	10s	10s	10s	10s	10s	10s	10s	10s	10s	10s
RADIATION	Kα	Kα	Kα	Kα	Kα	Kα	Kα	Kα	Kα	Kα	Kα	Kα	Kα
PATH	air	air	air	air	air	air	air	air	air	air	air	air	air

TABLE 2.2 cont'd

ELEMENT	La	Ce	Hg	Pb	Bi	Th	U
TARGET	W	W	W	W	W	W	W
KV	50	50	50	50	50	50	50
COLLIMATOR	fine	fine	fine	fine	fine	fine	fine
CRYSTAL	LiF	LiF	LiF	LiF	LiF	LiF	LiF
COUNTER	Sc	Sc	Sc	Sc	Sc	Sc	Sc
TIME	10s	10s	10s	10s	10s	10s	10s
RADIATION	Kα	Kα	Lα	Lα	Lα	Lα	Lα
PATH	air	air	air	air	air	air	air

I_{b1} = the intensity measured at lower background angle;

I_{b2} = the intensity measured at higher background angle;

$2\theta_{pk}$, $2\theta_{b1}$, $2\theta_{b2}$ = the 2θ angles for peak, lower background and higher background, respectively.

In addition to this, where a liquid specimen cell was used for solution samples, the absorption effect due to the mylar film cell covering required correction, especially in the analysis for lighter elements. To obtain the true intensity for the analyte, it has been found[33,47] that a correction for the absorbing effect of this mylar film can be applied:-

$$I^{my} = I_m \exp(k \cdot x) \quad \text{and} \quad k = 13.5 \cdot \lambda^{2.80} \qquad (2.5)$$

where:-

I^{my} = the corrected intensity;

I_m = the measured intensity;

k = the absorption coefficient for the film;

λ = the wavelength of the analyte line;

x = the thickness of the film (in inch).

2.4 Determination of α-Correction Coefficients

In the earlier discussion of empirical coefficients, it was suggested these coefficients be determined for each

pair of elements by preparing binary systems for those elements. In this investigation, solution specimens were used, and three situations arose:-

(a) Binary system - α_{iM}: A solution containing the analyte i, which is actually a binary mixture, with the aqueous matrix M as the second component.

(b) Ternary system - α_{ij}: The solution contains the analyte i, another element j and the residual aqueous matrix M, and is used to determine α_{ij} where α_{iM} is known.

(c) Quaternary system - α_{ij}: A solution, made up using HCl or H_3PO_4, contains analyte i, element j, the aqueous matrix M and a third element k (i.e. Cl or P), and is used to determine α_{ij}, where α_{iM} and α_{ik} are predetermined.

2.4.1 The calculation of α-correction coefficients

If the evaluation of the aqueous matrix effect is considered, two samples of differing concentration of the analyte are prepared. Using Equation (1.33), with $C_j = 0$, for each sample the following were obtained:-

$$C_{i(1)} = R_{i(1)} (1 + \alpha_{iM} \cdot C_{M(1)}) \qquad (2.6)$$

$$C_{i(2)} = R_{i(2)} \left(1 + \alpha_{iM} \cdot C_{M(2)} \right) \qquad (2.7)$$

where the subscripts (1) and (2) indicate the different samples. By taking the ratio of Equation (2.6) and (2.7) and rearranging them, one arrives at:-

$$\alpha_{iM} = \frac{I_{i(1)} \cdot C_{i(2)} - I_{i(2)} \cdot C_{i(1)}}{I_{i(2)} \cdot C_{i(1)} \cdot C_{M(2)} - I_{i(1)} \cdot C_{i(2)} \cdot C_{M(1)}} \qquad (2.8)$$

where I_i represents the net measured intensity for the analyte i.

Similarly, equations can be derived for the inter-element effects, α_{ij}, for the tertiary and quaternary systems, as Equations (2.9) and (2.10), with the introduction of the aqueous matrix coefficient previously determined.

$$\alpha_{ij} = \frac{I_{i(2)} \cdot C_{i(1)} \cdot \left(1 + \alpha_{iM} \cdot C_{M(2)} \right)}{I_{i(1)} \cdot C_{i(2)} \cdot C_{j(1)} - I_{i(2)} \cdot C_{i(1)} \cdot C_{j(2)}} - \frac{I_{i(1)} \cdot C_{i(2)} \left(1 + \alpha_{iM} \cdot C_{M(1)} \right)}{I_{i(1)} \cdot C_{i(2)} \cdot C_{j(1)} - I_{i(2)} \cdot C_{i(1)} \cdot C_{j(2)}} \qquad (2.9)$$

$$\alpha_{ij} = \frac{I_{i(2)} \cdot C_{i(1)} \cdot (1 + \alpha_{iM} \cdot C_{M(2)} + \alpha_{ik} \cdot C_{k(2)})}{I_{i(1)} \cdot C_{i(2)} \cdot C_{j(1)} - I_{i(2)} \cdot C_{i(1)} \cdot C_{j(2)}}$$

$$- \frac{I_{i(1)} \cdot C_{i(2)} \cdot (1 + \alpha_{iM} \cdot C_{M(1)} + \alpha_{ik} \cdot C_{k(1)})}{I_{i(1)} \cdot C_{i(2)} \cdot C_{j(1)} - I_{i(2)} \cdot C_{i(1)} \cdot C_{j(2)}} \qquad (2.10)$$

If, in the case of the interelement effect, α_{ij}, the weight fraction of the analyte C_i is kept constant, then this term can be eliminated from the Equations (2.9) and (2.10).

2.4.2 Experimental procedures

When considering the binary system, evaluation of α_{iM} was obtained through the use of a series of solutions (~ 8), of varying weight fraction of C_i and C_M. The intensity of the analyte radiation was then measured at the appropriate instrumental setting for optimum excitation, corrected for background and, where required, for dead-time. The ratios of all pairs of samples in the series were then treated by Equation (2.8) to obtain the coefficient.

In the cases of ternary and quaternary systems, a series of solutions was prepared and, in those instances, the weight fraction of the analyte C_i was kept constant, while the weight fractions of the interfering elements C_j and C_k (if any), and the aqueous matrix C_M are varied systematically. The measured intensities for all solution

pairs are corrected for background and dead-time as required, and then explored by Equation (2.9) or (2.10) to obtain the coefficient α_{ij}.

When the coefficients have been evaluated, the measured net intensities can then be corrected for aqueous matrix and interelement effects, and the net intensity for the pure analyte, I_i^o, can be calculated using the appropriate form of the following equations:-

$$I_{i(corr)} = I_i \cdot \left(1 + \alpha_{iM} \cdot C_M + \sum_{\substack{j=1 \\ (j \neq i)}}^{n} \alpha_{ij} \cdot C_j \right) \qquad (2.11)$$

$$I_i^o = \frac{I_{i(corr)}}{C_i} \qquad (2.12)$$

where:-

$I_{i(corr)}$ = corrected intensity of analyte i;

I_i^o = net intensity of pure element i.

The general processes of treating experimental data is now shown in Table 2.3 and Table 2.4, using as examples the determination of the effect of the aqueous matrix on potassium as a binary system for α_{iM}, and the effect of calcium on potassium as a tertiary system for α_{ij}.

Graphical depictions for these systems are shown in Figures 2.6 and 2.7, and these show the effects of the application of the determined coefficients. Even at a weight fraction below 10 percent significant effects exist, the intensity-weight fraction curves being far from linear. Utilization of the correction coefficients yielded linear relationships in each case.

2.4.3 Experimental results

It was anticipated that the correction coefficients would be obtained that would be as close as possible to the true values by using a large population for their evaluation. Accordingly, each system(for one α-correction coefficient) involved a triplicate series, each series involved a minimum of 28 pairs of data, all being treated were as discussed in Section (2.4.2.). The total coefficients from the series were examined by taking the average and standard deviation. The standard deviation was used to test the results. All values exceeding $\bar{x} \pm s$ were rejected. The acceptable values from each series were then averaged and the standard deviation determined. The same test criterion to determine rejectable data was applied.

TABLE 2.3 EFFECT OF AQUEOUS MATRIX ON POTASSIUM

Solution	C_K	C_M	I_K(cps)	I_K(corr) (cps)	I_K^o(cps)
1.	0.01000	0.99000	4279	1334	133399
2.	0.02000	0.98000	8465	2698	134899
3.	0.03000	0.97000	12238	3987	132899
4.	0.04000	0.96000	16141	5370	134249
5.	0.05000	0.95000	19643	6672	133439
6.	0.06000	0.94000	23373	8102	135033
7.	0.07000	0.93000	26700	9440	134857
8.	0.08000	0.92000	29179	10520	131499

Average value I_K^o = 134000

Std. devn. = ±1000

Combin. of Soln.	α_{KM}	Combin. of Soln.	α_{KM}	Combin. of Soln.	α_{KM}
1/2	-0.5263..*	2/5	-0.7311..	4/5	-0.7528..
1/3	-0.7150..	2/6	-0.6933..	4/6	-0.6590..
1/4	-0.6727..	2/7	-0.6964..	4/7	-0.6767..
1/5	-0.6952..	2/8	-0.7385..	4/8	-0.7484..
1/6	-0.6676..	3/4	-0.5304..*	5/6	-0.4702..*
1/7	-0.6746..	3/5	-0.6706..	5/7	-0.6183..
1/8	-0.7172..	3/6	-0.6228..	5/8	-0.7468..
2/3	-0.8024..*	3/7	-0.6470..	6/7	-0.7094..
2/4	-0.7199..	3/8	-0.7183..	6/8	-0.8104..*
				7/8	-0.8707..*

* rejects on first inspection

Acceptable data (22 data)

Average value α_{KM} = -0.695

Std. devn. = ±0.038

Series (1) $\alpha_{KM} = -0.69^5 \pm 0.03^8$

FIGURE 2.6 EFFECT OF AQUEOUS MATRIX ON POTASSIUM

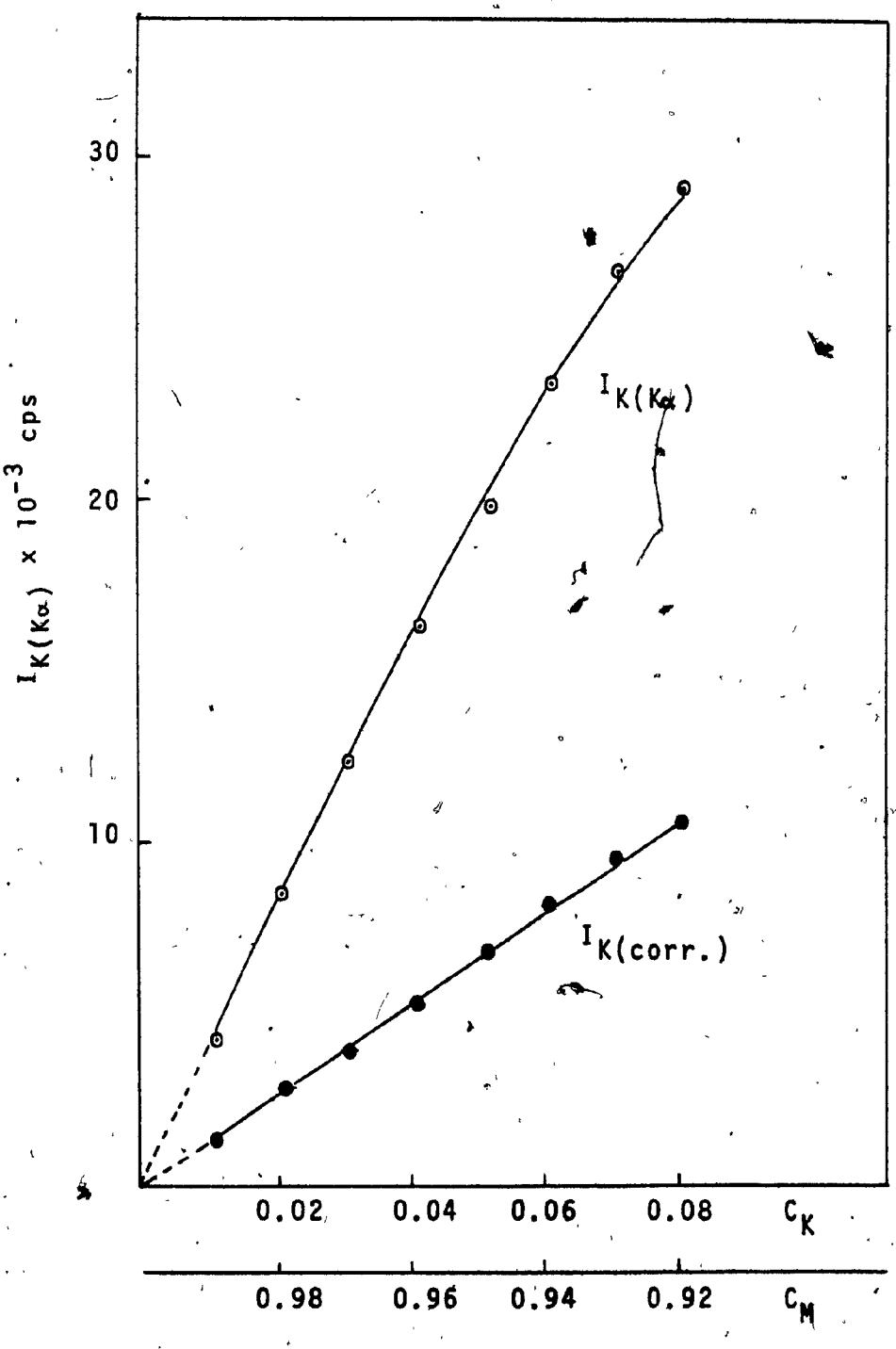

TABLE 2.4 EFFECT OF CALCIUM ON POTASSIUM

Solution	C_K	C_{Ca}	C_M	$I_{K(K\alpha)}$ (cps)
1.	0.02000	0.00000	0.98000	28537
2.	0.02000	0.01000	0.97000	27791
3.	0.02000	0.02000	0.96000	27640
4.	0.02000	0.03000	0.95000	27073
5.	0.02000	0.04000	0.94000	27016
6.	0.02000	0.05000	0.93000	26843
7.	0.02000	0.06000	0.92000	26548

Solution	I_K(corr for M) (cps)	I_K(corr. for M & Ca) (cps)	I_K^o (cps)
1.	8680	8680	433999
2.	8651	8546	427299
3.	8800	8591	429549
4.	8812	8504	425199
5.	8985	8576	428799
6.	9118	8610	430499
7.	9206	8604	430199

Average value I_K^o = 429000

Std. devn. = $\pm$3000

Combin. of Soln.	α_{KCa}	Combin. of Soln.	α_{KCa}	Combin. of Soln.	α_{KCa}
1/2	0.1066..*	2/4	-0.3012..	3/7	-0.3906..
1/3	-0.2164..	2/5	-0.4163..	4/5	-0.6454..*
1/4	-0.1617..*	2/6	-0.4390..	4/6	-0.5780..*
1/5	-0.2818..	2/7	-0.4224..	4/7	-0.5054..
1/6	-0.3261..	3/4	-0.0450..*	5/6	-0.5088..
1/7	-0.3302..	3/5	-0.3504..	5/7	-0.4321..
2/3	-0.5429..*	3/6	-0.4029..	6/7	-0.3521..

* rejects on first inspection

Acceptable data (15 data)

Average value α_{KCa} = -0.378

Std. devn. = $\pm$0.081

Series (1) α_{KCa} = $-0.37^8 \pm 0.08^1$

FIGURE 2.7 EFFECT OF CALCIUM ON POTASSIUM

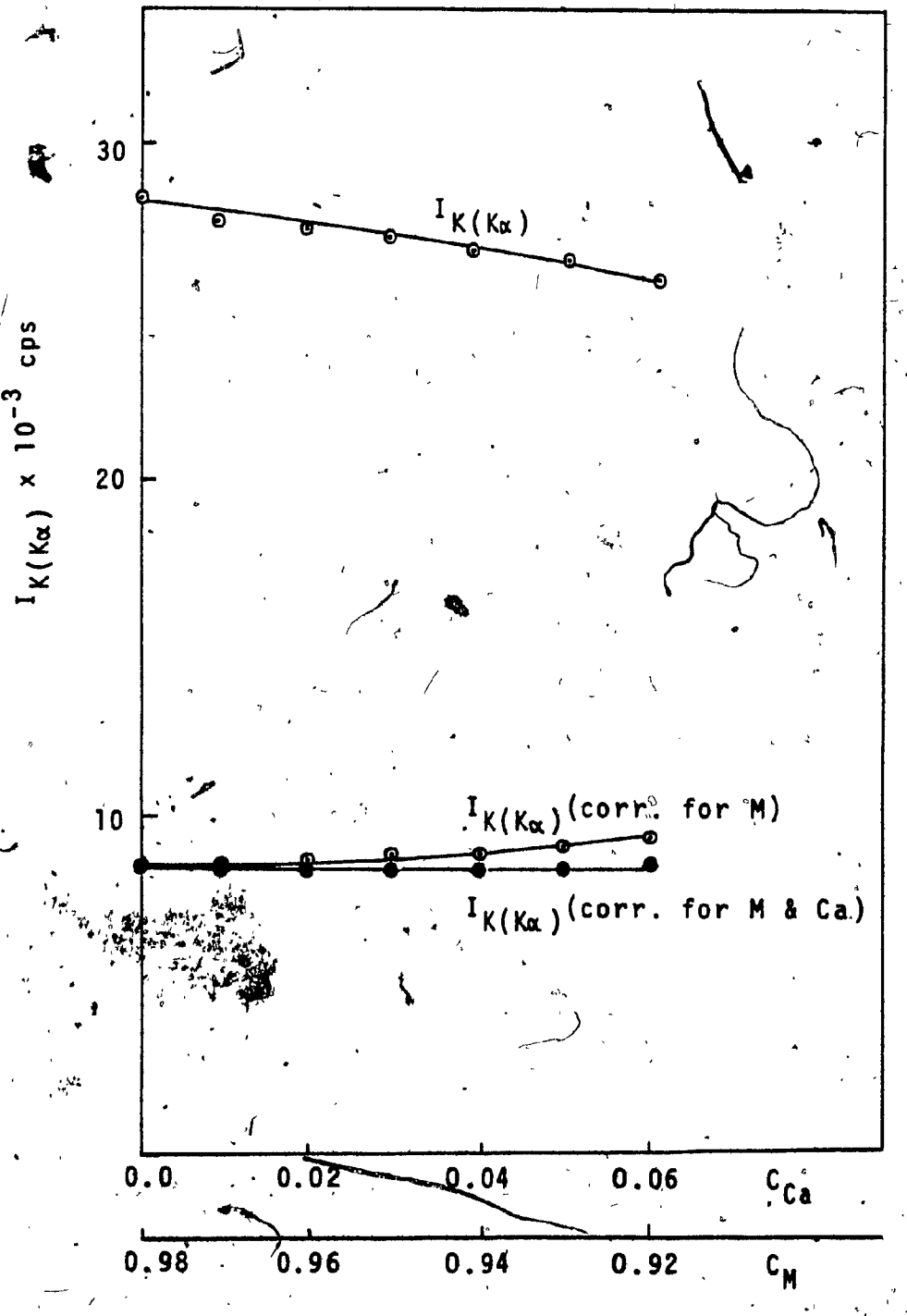

All of the final data for the α-correction coefficients may be found in the Section A.1. Some comparisons of the α-coefficient values found with literature values is shown in the Table 2.4(A). In which includes several coefficients previously determined by Dick and Nguyen,[32] but these were redetermined, together with addition coefficients, because of the improved experimental and data treatment approaches. Throughout this part of the experimental work, since a total of more than 300 coefficients were investigated, about 7,200 solutions prepared, and more than 20,000 calculations made, computer programs were developed to handle the mass of data, these programs being applied on a large CDC computer.[49]

2.5 Application of Determined α-Coefficients to Chemical Analysis for The Multicomponent Systems

2.5.1 General

From the previous studies, the effect of interfering element j on analyte i were discussed, and the coefficients, α_{ij}, were determined as representing the overall effects(absorption and enhancement) of one element on the other. In a binary system, when α_{ij} has a positive value, the measured intensity for the analyte line (I_i) will be lower than that predicted by the relationship of Equation (1.4) (i.e. $I_i = I_i^o \cdot C_i$), due to the positive absorption effect of element j. If α_{ij} has a negative

TABLE 2.4 (A)

SOME COMPARISONS OF AQUEOUS OR FUSION MEDIA α-COEFFICIENTS WITH LITERATURE VALUES

α	Experimental Aq. or Fusion	*Experimental* Multiple Standards
SiTi	1.35	-
SiFe	2.8	-
TiSi	-0.25	-
TiFe	-0.47	-
CrMn	-0.18	-
CrFe	-0.58	-0.46
CrCo	-0.60	-0.34
CrNi	-0.39	-0.23
CrCu	-0.39	-
MnFe	0.00	-
MnNi	-0.52	-
MnCu	-0.65	-
FeSi	-0.33	-
FeTi	1.27	1.20
FeCr	1.74	2.10
FeMn	-0.23	-
FeCo	-0.03	0.49
FeNi	-0.54	-0.49
FeCu	-0.58	-
CoCr	1.42	1.66
CoFe	-0.02	-0.05
CoNi	-0.05	0.05
NiCr	0.96	1.20
NiMn	1.12	-
NiFe	1.46	1.70
NiCo	-0.11	-0.15
NiCu	-0.34	-
CuCr	1.01	-
CuMn	1.16	-
CuFe	1.47	-
CuNi	-0.05	-

*K.F. Heinrich and S.D. Rasberry, Anal. Chem., 46, 81, (1974).

value, the effect of j will be either enhancement or negative-absorption, and the intensity I_i, of analyte i will be higher than that expected from Equation (1.4). However, where there is a physical significance, the α-coefficient values cannot be less than -1. A zero value is possible, when the effect of positive absorption is equal to the effect of enhancement for an interfering element j. With this situation, the measured intensity I_i shows an almost linear relationship with the analyte concentration.

In a multi-element system, the above situation was discussed in Section 1.8, wherein the total effect on an analyte-line (I_i) involves the summation of the effect of each interfering element in the specimen. Consider a ternary alloy, for instance, of nickel, iron, chromium, where the components vary from 0 to 100 weight percent. For nickel, the NiKα fluorescent radiation is simple fluorescence, and the effects of iron and chromium are absorption, their α-correction coefficients being respectively, 0.96 and 1.46. For iron, the fluorescent FeKα consists of simple fluorescence and enhancement or secondary fluorescences, wherein the enhancement effect is due to the additional excitation of FeKα by NiKα. The effect of chromium is absorption,

with the α-correction coefficient being 1.74. The effect of nickel is the enhancement noted and positive-absorption, with an over all α-correction coefficient of -0.54. For chromium, CrK_α this consists of simple, secondary and tertiary fluorescences, but the tertiary fluorescent intensity is too small to be considered relative to the total fluorescent intensity. Both iron and nickel cause enhancement and absorption effects on chromium with the α-correction coefficients being -0.58 for iron and -0.39 for nickel.

The compositions of this ternary alloy can then be determined by applying the Equation (1.36) as:-

$$C_{Ni} = \frac{I_{Ni}}{I^o_{Ni}} \left(1 + 1.46 \cdot C_{Cr} + 0.96 \cdot C_{Fe} \right)$$

$$C_{Fe} = \frac{I_{Fe}}{I^o_{Fe}} \left(1 + 1.74 \cdot C_{Cr} - 0.54 \cdot C_{Ni} \right) \qquad (2.13)$$

$$C_{Cr} = \frac{I_{Cr}}{I^o_{Cr}} \left(1 - 0.58 \cdot C_{Fe} - 0.39 \cdot C_{Ni} \right)$$

where, I^o_{Ni}, I^o_{Fe} and I^o_{Cr} are intensities for the pure elements nickel, iron and chromium, and are calculated from Equation (2.12) using a standard solution.

Tertian,[27] and Rasberry and Heinrich,[30] have pointed out that (1) a regular shift of the so-called effective wavelength(λ_e) of primary radiation occurs due to the variation of the analyte concentration C_i, and that (2) when a analyte fluoresence is strongly enhanced by an interfering element j, the secondary fluorescence increases more rapidly than the reinforcing element concentration C_j. In other words, α_{ij}, which is negative, rapidly increases (algebraically) with the fluorescent element concentration C_i. The above two facts are clearly shown in the Figure 2.8. The example is α_{FeNi} and α_{FeCr} versus C_{Fe}, in which the interelement coefficients α_{FeNi} and α_{FeCr} are no longer constant over a large concentration range, and Equation (2.13) is not valid for the solution of this type of ternary system. In practice,[14] however, it has been shown that the correction coefficients do not vary at concentration levels up to about 10 percent weight fraction. In such cases, a dilution method was used for the sample preparation, so that the analyte concentration was under the limit of 10 percent. Since aqueous media are used, an additional term M is introduced into this system, and the effect of M on elements has to be taken into

FIGURE 2.8

VARIATION OF α_{FeNi} AND α_{FeCr} CORRECTION COEFFICIENTS WITH IRON CONCENTRATION

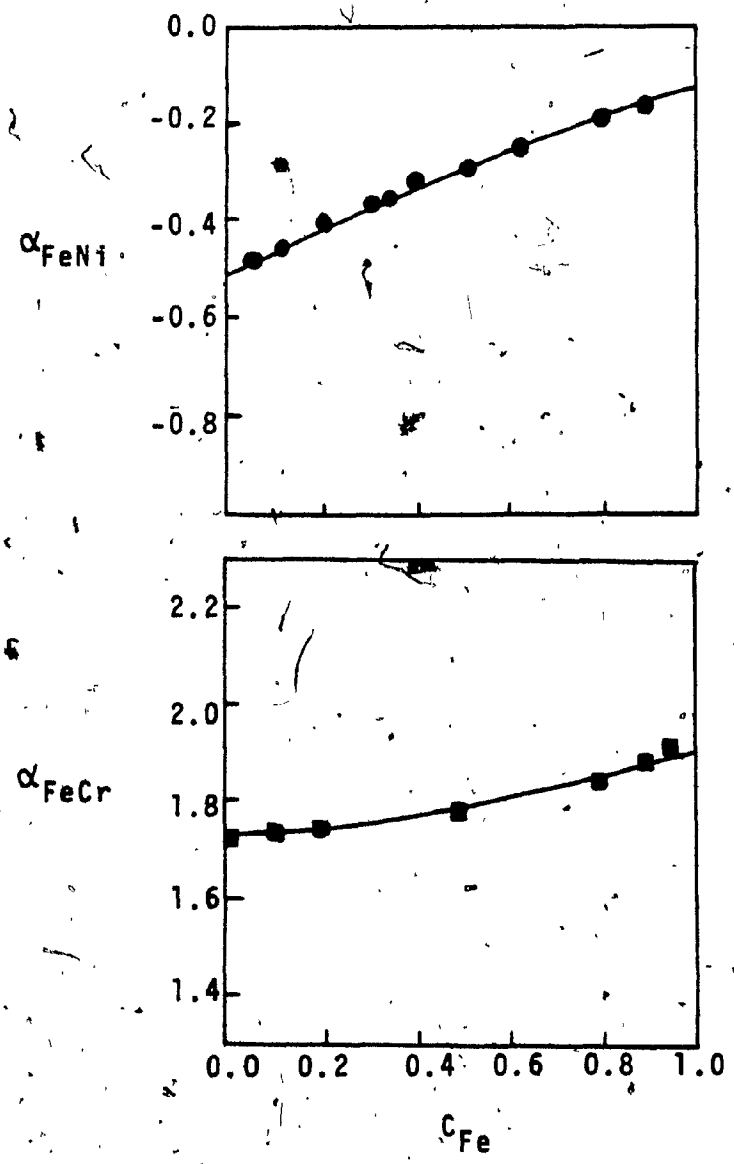

account. For nickel, the α_{NiM} is -0.923, for iron α_{FeM} it is -0.900, and for chromium α_{CrM} it is -0.850. Eventually, the system is a quaternary one, and Equation (2.13) may be rewritten as :-

$$
\begin{aligned}
C_{Ni} &= \frac{I_{Ni}}{I^{o}_{Ni}} \left(1 - 0.923 \cdot C_{M} + 1.46 \cdot C_{Cr} + 0.96 \cdot C_{Fe} \right) \\
C_{Fe} &= \frac{I_{Fe}}{I^{o}_{Fe}} \left(1 - 0.900 \cdot C_{M} + 1.74 \cdot C_{Cr} - 0.54 \cdot C_{Ni} \right) \\
C_{Cr} &= \frac{I_{Cr}}{I^{o}_{Cr}} \left(1 - 0.850 \cdot C_{M} - 0.58 \cdot C_{Fe} - 0.39 \cdot C_{Ni} \right) \\
C_{M} &= 1 - C_{Ni} - C_{Fe} - C_{Cr}
\end{aligned}
\qquad (2.14)
$$

By solving the above linear equations, the chemical composition of a unknown may be evaluated, while the characteristic intensities are measured and the I^{o} values are determined.

In this present study, a series of copper alloys and aluminum alloys were chosen to examine the use of the investigated α-correction coefficients in the analysis of multicomponent systems. This approach was carried out in two steps. First of all, synthetic solutions of known composition were prepared and analyzed by XRF to determine

the general applicability of the aqueous-media-determined correction coefficients. Secondly, samples of actual alloys of known composition were placed in solid and/or solution through XRF analysis. The results were then compared with the known composition values.

2.5.2 Analysis of copper-base alloys

2.5.2.1 Synthetic solutions

A series of mixtures of pure elements, each involving variable weights of the major elements in the available commercial alloys (copper, lead, iron and zinc), were prepared in a total weight of about 5 grams. These mixtures were then dissolved in nitric acid-water solutions and finally made up to 70 grams with boiled water. Table 2.5 shows the weights, weight fractions, and percentages of these synthetic solutions as prepared.

Each solution was eventually subjected to examination by XRF, this examination involving the measurement of the fluorescent intensities for each analyte element. In every case the average intensity was obtained, and this represented the average of five readings at each emission peak. For this series, the I^{o} values were determined from each solution for every analyte. Averaged values

TABLE 2.5 PREPARATION OF SERIES SC SYNTHETIC SOLUTIONS (COPPER-BASE)

SOLUTION	COPPER			LEAD			IRON			ZINC		
	A	B	C	A	B	C	A	B	C	A	B	C
SC-1	2.7500	0.03929	55.06	0.1805	0.00258	3.61	0.0200	0.00029	0.40	2.0440	0.02920	40.93
SC-2	2.9195	0.04171	58.98	0.0995	0.00142	2.01	0.0200	0.00029	0.40	1.9110	0.02730	38.61
SC-3	3.1000	0.04429	62.00	0.1500	0.00214	3.00	0.0280	0.00040	0.56	1.7220	0.02460	34.44
SC-4	2.9645	0.04235	59.23	0.0200	0.00029	0.40	0.0095	0.00014	0.19	2.0110	0.02873	40.18
SC-5	3.0595	0.04371	61.19	0.0500	0.00071	1.00	0.0075	0.00011	0.15	1.8830	0.02690	37.66
SC-6	3.1500	0.04500	63.00	0.1225	0.00175	2.45	0.0195	0.00028	0.39	1.7080	0.02440	34.16
SC-7	3.2490	0.04641	65.31	0.1000	0.00143	2.01	0.0100	0.00014	0.20	1.6160	0.02309	32.48
SC-8	3.3325	0.04761	66.65	0.0970	0.00139	1.94	0.0190	0.00027	0.38	1.5515	0.02216	31.03

A - weight(gm) of element

B - weight fraction of element in aqueous solution

C - percent weight (%) of element in the mixture

were used to calculate the chemical compositions in the solution. These I^o values, along with their standard deviation, are given in Table 2.6.

Finally, compositions were determined by the computer-programmed simultaneous solution of the linear equations as Equation (1.36) or Equation (2.14). Table 2.7 illustrates the final results of these analyses and comparisons with the original values. The pertinent data for this experimental program series SC, can be found in Section (A.2.1).

2.5.2.2 Commercial copper-base alloy samples

Two groups of standard alloys, Alloys 2 and Alloys 8, were examined by XRF under aqueous solution and solid specimen conditions.

In the solution approach, samples of these alloys of about 1 gram each were accurately weight out and dissolved in a mixture of hydrochloric and nitric acids. Subsequently, a dilution was carried out, to a total weight basis of about 50 grams, with boiled water. Chlorine was determined by potentiometric titration for every liquid sample. The intensities of the characteristic lines for each element, including chlorine, were measured

TABLE 2.6 I^{o} VALUES FOR ANALYSIS OF COPPER-BASE ALLOYS

Element	I^{o} ± Std. dev.
COPPER	214936 + 5471 = $(2.15 + 0.05) \times 10^{5}$ cps
LEAD	77823 + 1171 = $(7.7^{8} + 0.1^{2}) \times 10^{4}$ cps
IRON	559795 + 42062 = $(5.6 + 0.4) \times 10^{5}$ cps
ZINC	222015 + 1216 = $(2.22 + 0.01) \times 10^{5}$ cps

TABLE 2.7 RESULTS OF SERIES SC – α-CORRECTION COEFFICIENT METHOD

SOLUTION	COPPER			LEAD			IRON			ZINC		
	A	B	C	A	B	C	A	B	C	A	B	C
SC-1	55.05	55.06	0.01	3.02	3.61	0.59	0.46	0.40	0.06	41.27	40.93	0.34
SC-2	59.19	58.98	0.21	1.73	2.01	0.28	0.39	0.40	0.01	38.69	38.01	0.68
SC-3	62.46	62.00	0.46	2.61	3.00	0.39	0.55	0.56	0.01	34.39	34.44	0.05
SC-4	59.23	59.23	0.00	0.38	0.40	0.02	0.21	0.19	0.02	40.18	40.18	0.00
SC-5	61.13	61.19	0.06	0.86	1.00	0.14	0.15	0.15	0.00	37.87	37.66	0.21
SC-6	63.50	63.00	0.50	2.13	2.45	0.32	0.37	0.39	0.02	34.00	34.16	0.16
SC-7	65.41	65.31	0.10	1.77	2.01	0.24	0.20	0.20	0.00	32.62	32.48	0.14
SC-8	66.73	66.65	0.08	1.70	1.94	0.24	0.35	0.38	0.03	31.22	31.03	0.09
Av. abs. error			0.17			0.28			0.02			0.13

Column A values by α-correction coefficient technique
Column B values from synthetic solutions
Column C absolute error

All values expressed to two decimal places, regardless of indiyidual uncertainties

and I^o values were calculated as before.

For the solid specimen approach, the general procedures for the treatment of data were similar to that for the liquid specimens, but the intensity of the copper characteristic line was not measured, since copper was considered as a matrix element, (e.g. as "M" in the liquid specimen). In this case, the copper concentration can be represented as:-

$$C_{Cu} = 1 - C_{Sn} - C_{Fe} - C_{Pb} - C_{Zn} - C_{Ni}$$

Therefore, by obtaining and using only the measurements of the intensities for the rest of the elements in the alloy, the composition of these samples can be determined.

Table 2.8 indicates, in chart form, the determined α-correction coefficients from aqueous solution, which were required for the analysis of the solubilized copper-base alloys. The horizontal headings (i) list the elements affected. The vertical headings (j) list the elements providing the interfering effect. Among these latter headings, the heading M indicates the aqueous matrix.

Table 2.9 provides the results of the solid and solubilized specimen analyses for these copper-base alloys.

not used, since the fairly low solubility of these alloys in $HCl-HNO_3$ acid media, especially in the present of silicon and titanium, would require a lowering of the concentration of the analyte, and in turn a lowering of the counting rate and an increase in the counting error.

When a solid specimen was used, the surface to be exposed to the primary x-ray beam was prepared in the order previously indicated by (1) machining, (2) grinding with decreasing sizes of diamond grit, and (3) polishing with 20 micron diamond dust. A total of forty-two aluminum-base alloy standards were prepared for XRF examination. Table 2.13 shows their standard compositions.

Intensity measurements were carried out for each element magnesium, silicon, titanium, chromium, manganese, iron, nickel, copper, zinc, tin, lead and bismuth in the alloy. The exception was aluminum, which was considered as a matrix element in this system. The experimental data related to these surveys are presented in Section (A.3.2).

Table 2.14 shows all of the α-correction coefficients which were used in the calculatiin of the composition of these alloys.

Table 2.15 shows the final results on these alloys, using the α-correction techniques. The average-absolute -error for each element determined can be found in the Table 2.16.

TABLE 2.13

COMPOSITION OF ALUMINUM-BASE ALLOY STANDARD SAMPLES

SAMPLE	Magnesium	Silicon	Titanium	Chromium	Manganese	Iron	Nickel
117-AD	0.10	4.70	0.036	0.030	0.66	0.37	0.05
125-AI	0.47	5.55	0.12	0.034	0.023	0.32	0.029
225-AG	0.005	0.81	0.15	0.015	0.040	0.38	0.11
226-AC	0.06	0.17	0.15	0.035	0.09	0.19	0.05
125-AL	0.025	4.95	0.15	0.032	0.040	0.19	0.030
125-AN	0.57	5.12	0.17	0.042	0.042	0.20	0.042
B143-AA	0.86	9.24	0.11	0.050	0.27	0.39	0.05
143-AF	0.048	8.50	0.041	0.046	0.11	0.35	0.057
A143-AT	0.75	10.00	0.042	0.025	0.25	0.41	0.82
236-AC	0.28	2.05	0.15	0.023	0.11	1.21	0.031
6165-AA-D	1.06	18.00	0.025	0.020	0.040	0.44	1.07
24S-AT	1.43	0.17	0.016	0.028	0.72	0.28	0.032
218-AQ	1.56	0.20	0.15	0.025	0.035	0.48	2.05
162-AZ	1.09	12.10	0.034	0.027	0.037	0.41	2.50
38S-AI-D	1.13	11.43	0.06	0.034	0.055	0.37	0.84
135-AM	0.03	7.06	0.19	0.024	0.030	0.15	0.025
135-AN	0.41	7.31	0.18	0.032	0.042	0.19	0.026
A35-AJ	6.85	0.11	0.16	0.010	0.16	0.20	0.028
A56S-AB	4.78	0.16	0.053	0.038	0.63	0.29	0.028
M57S-AC	2.10	0.28	0.032	0.026	0.35	0.36	0.029
A135-AM	6.95	0.12	0.16	0.047	0.17	0.16	0.048

TABLE 2.13 cont'd

SAMPLE	Copper	Zinc	Tin	Lead	Bismuth	Aluminum
117-AD	2.92	0.060	0.034	0.038	0.030	90.97
125-AI	1.18	0.030	0.029	0.036	0.027	92.15
225-AG	4.20	0.033	0.026	0.030	0.027	94.17
226-AC	4.70	0.048	0.045	0.060	0.064	94.34
125-AL	1.20	0.030	0.029	0.031	0.029	93.26
125-AN	1.27	0.043	0.042	0.052	0.038	92.37
B143-AA	2.92	0.060	0.040	0.048	0.047	85.92
143-AF	3.46	0.060	0.041	0.060	0.050	87.18
A143-AT	2.97	0.035	0.024	0.028	0.030	84.62
236-AC	6.85	0.041	0.028	0.031	0.030	89.17
6165-AA-D	1.02	0.037	0.030	0.025	0.031	78.20
24S-AT	4.62	0.041	0.034	0.033	0.032	92.56
218-AQ	3.96	0.030	0.030	0.028	0.030	91.42
162-AZ	0.79	0.040	0.034	0.030	0.020	82.89
38S-AI-D	0.86	0.057	0.029	0.030	0.030	85.08
135-AM	0.034	0.043	0.033	0.032	0.031	92.32
135-AN	0.050	0.050	0.032	0.033	0.032	91.61
A35-AJ	0.028	0.040	0.031	0.030	0.028	90.05
A56S-AB	0.040	0.050	0.034	0.030	0.023	93.84
M57S-AC	0.042	0.033	0.031	0.030	0.028	96.66
A135-AM	0.050	0.053	0.056	0.050	0.040	92.10

TABLE 2.13 cont'd

SAMPLE	Magnesium	Silicon	Titanium	Chromium	Manganese	Iron	Nickel
340-AA-D	8.30	0.25	0.09	0.027	0.036	1.19	0.035
350-AQ	9.90	0.12	0.029	0.022	0.031	0.17	0.035
350-AS	9.97	0.15	0.11	0.035	0.035	0.19	0.036
123-AJ	0.022	5.00	0.11	0.025	0.023	0.28	0.020
161-AB	0.49	9.68	0.045	0.049	0.07	0.99	0.044
161-AE	0.55	11.70	0.042	0.033	0.51	0.40	0.048
B160-AA	0.048	12.27	0.041	0.030	0.043	0.83	0.037
160-DB	0.047	12.23	0.042	0.052	0.039	0.34	0.038
F40E-AG	0.65	0.15	0.20	0.42	0.036	0.34	0.036
6235-AA	0.040	0.10	0.040	0.030	0.036	0.16	0.010
6392-AA	1.12	0.15	0.08	0.10	0.16	0.16	0.040
79S-AD-D	3.19	0.15	0.07	0.16	0.20	0.29	0.035
79S-AE	3.34	0.18	0.06	0.20	0.22	0.29	0.043
6448-AA	2.84	0.07	0.040	0.21	0.038	0.31	0.031
LM24-AA	0.11	7.80	0.17	0.020	0.43	0.59	0.15
6195-AA-D	1.00	10.62	0.09	0.04	0.28	0.65	0.10
6195-AC	1.09	9.50	0.045	0.047	0.42	0.70	0.046
6252-AD	0.32	5.50	0.14	0.048	0.63	0.34	0.052
6363-AA	0.90	0.36	0.040	0.040	0.040	0.25	1.80
B51S-AF-D	0.63	1.00	0.045	0.042	0.54	0.25	0.036
6449-AA-D	0.89	0.65	0.08	0.09	0.15	0.25	0.037

TABLE 2.13 cont'd

SAMPLE	Copper	Zinc	Tin	Lead	Bismuth	Aluminum
340-AA-D	0.050	0.043	0.037	0.030	0.040	89.87
350-AQ	0.042	0.033	0.034	0.031	0.029	89.52
350-AS	0.10	0.038	0.036	0.030	0.027	89.24
123-AJ	0.035	0.034	0.027	0.034	0.032	94.36
161-AB	0.065	0.060	0.050	0.050	0.050	88.36
161-AE	0.052	0.050	0.040	0.040	0.033	86.50
B160-AA	0.060	0.043	0.031	0.028	0.043	86.50
160-DB	0.040	0.065	0.046	0.045	0.040	86.98
F40E-AG	0.037	5.45	0.031	0.028	0.035	92.59
6235-AA	0.030	5.50	0.030	0.030	0.030	93.96
6392-AA	0.10	4.34	0.040	0.020	0.040	93.65
79S-AD-D	0.62	4.51	0.030	0.020	0.030	90.70
79S-AE	0.65	4.70	0.042	0.041	0.042	90.19
6448-AA	2.05	7.19	0.060	0.060	0.021	87.04
LM24-AA	3.47	0.73	0.08	0.11	0.030	86.31
6195-AA-D	3.20	0.85	0.040	0.045	0.030	83.06
6195-AC	3.42	0.90	0.051	0.053	0.040	83.69
6252-AD	3.00	3.50	0.054	0.050	0.048	86.32
6363-AA	0.96	0.040	7.19	0.040	0.040	88.30
B51S-AF-D	0.045	0.042	0.042	0.040	0.042	97.25
6449-AA-D	0.32	0.050	0.044	0.46	0.46	96.52

TABLE 2.14

α-CORRECTION COEFFICIENTS TO BE USED IN THE ANALYSIS OF ALUMINUM ALLOYS

ELEMENT (i) / (j)	Mg	Si	Ti	Cr	Mn	Fe	Ni	Cu	Zn	Sn	Pb	Bi
Mg	----	4.03	-0.37	-0.35	-0.46	-0.57	-0.69	-0.71	-0.79	-0.949	-0.896	-0.903
Si	0.09	----	0.83	-0.20	-0.31	-0.38	-0.52	-0.54	-0.61	-0.923	-0.85	-0.861
Ti	2.52	0.83	----	1.62	1.30	1.11	0.69	0.61	0.41	-0.734	-0.45	-0.49
Cr	4.88	1.81	-0.57	----	-0.09	1.74	0.96	1.01	0.57	-0.58	-0.29	-0.34
Mn	5.94	2.29	-0.56	-0.18	----	-0.23	1.12	1.16	0.70	-0.54	-0.23	-0.28
Fe	7.67	3.06	-0.52	-0.58	0.00	----	1.46	1.47	1.04	-0.47	-0.14	-0.19
Ni	8.68	3.75	-0.40	-0.39	-0.52	-0.54	----	-0.05	1.51	-0.34	0.044	-0.014
Cu	9.39	4.10	-0.36	-0.39	-0.65	-0.58	-0.34	----	-0.17	-0.28	0.108	0.04
Zn	11.2	4.98	-0.25	-0.35	-0.42	-0.53	-0.59	-0.10	----	-0.17	0.29	0.21
Sn	12.0	3.35	2.67	2.11	1.74	1.51	1.00	0.88	0.65	----	-0.484	-0.48
Pb	12.83	3.33	2.34	1.96	1.66	1.09	0.67	0.71	0.40	0.522	----	-0.04
Bi	13.29	7.62	2.50	1.82	1.79	1.70	1.20	1.16	0.95	0.594	0.011	----
Al	-0.12	5.21	-0.21	-0.22	-0.33	-0.49	-0.63	-0.64	-0.70	-0.938	-0.87	-0.878

TABLE 2.15

RESULTS OF XRF EXAMINATION - ALUMINUM-BASE ALLOYS

SAMPLE	Magnesium	Silicon	Titanium	Chromium	Manganese	Iron	Nickel
117-AD	0.098	4.76	0.036	0.028	0.66	0.37	0.049
125-AI	0.43	5.59	0.12	0.035	0.023	0.32	0.029
225-AG	0.011	0.87	0.15	0.015	0.039	0.38	0.11
226-AC	0.057	0.15	0.15	0.037	0.091	0.19	0.050
125-AL	0.026	4.99	0.15	0.032	0.040	0.19	0.029
125-AN	0.57	5.10	0.17	0.042	0.042	0.21	0.042
B143-AA	0.83	9.35	0.11	0.051	0.27	0.41	0.051
143-AF	0.043	12.57	0.042	0.046	0.11	0.36	0.058
A143-AT	0.77	9.78	0.042	0.025	0.25	0.41	0.83
236-AC	0.27	2.02	0.15	0.022	0.11	1.22	0.031
6165-AA-D	0.96	18.10	0.025	0.021	0.038	0.44	1.08
24S-AT	1.41	0.17	0.016	0.028	0.72	0.28	0.032
218-AQ	1.61	0.20	0.11	0.024	0.034	0.48	2.06
162-AZ	1.07	12.29	0.035	0.027	0.036	0.41	2.53
38S-AI-D	1.17	11.66	0.061	0.034	0.057	0.37	0.85
135-AM	0.031	7.13	0.19	0.024	0.030	0.15	0.025
135-AN	0.39	7.37	0.18	0.032	0.042	0.19	0.026
A35-AJ	6.64	0.10	0.16	0.009	0.16	0.20	0.028
A56S-AB	4.84	0.16	0.053	0.040	0.64	0.29	0.028
M57S-AC	2.14	0.29	0.032	0.026	0.36	0.36	0.029
A135-AM	6.80	0.13	0.16	0.047	0.17	0.16	0.048

TABLE 2.15 cont'd

SAMPLE	Copper	Zinc	Tin	Lead	Bismuth	Aluminum
117-AD	2.91	0.059	0.033	0.038	0.028	90.93
125-AI	1.19	0.030	0.028	0.035	0.026	92.14
225-AG	4.22	0.032	0.025	0.029	0.027	94.09
226-AC	4.68	0.048	0.046	0.061	0.062	94.37
125-AL	1.20	0.030	0.029	0.030	0.028	93.22
125-AN	1.27	0.042	0.042	0.051	0.037	92.39
B143-AA	2.93	0.060	0.041	0.049	0.047	85.81
143-AF	3.50	0.061	0.041	0.059	0.050	83.06
A143-AT	2.97	0.035	0.024	0.029	0.028	84.82
236-AC	6.85	0.041	0.028	0.029	0.029	89.20
6165-AA-D	1.02	0.036	0.029	0.026	0.029	78.19
24S-AT	4.62	0.041	0.033	0.034	0.032	92.58
218-AQ	3.95	0.030	0.029	0.028	0.030	91.40
162-AZ	0.80	0.040	0.035	0.030	0.019	82.49
38S-AI-D	0.86	0.055	0.029	0.030	0.031	84.80
135-AM	0.034	0.043	0.033	0.031	0.031	92.25
135-AN	0.050	0.052	0.032	0.032	0.032	91.57
A35-AJ	0.027	0.039	0.029	0.029	0.026	92.56
A56S-AB	0.040	0.050	0.035	0.029	0.022	93.77
M57S-AC	0.042	0.033	0.031	0.027	0.028	98.60
A135-AM	0.050	0.053	0.055	0.050	0.042	92.24

TABLE 2.15 cont'd

SAMPLE	Magnesium	Silicon	Titanium	Chromium	Manganese	Iron	Nickel
340-AA-D	7.63	0.25	0.091	0.029	0.036	1.25	0.033
350-AQ	9.85	0.12	0.029	0.022	0.031	0.17	0.035
350-AS	9.88	0.15	0.11	0.035	0.037	0.19	0.036
123-AJ	0.023	5.10	0.11	0.024	0.024	0.28	0.021
161-AB	0.49	9.87	0.045	0.049	0.071	0.99	0.044
161-AE	0.54	11.94	0.042	0.032	0.51	0.40	0.048
B160-AA	0.049	12.49	0.041	0.029	0.043	0.84	0.037
160-DB	0.048	12.44	0.042	0.052	0.039	0.34	0.039
F40E-AG	0.68	0.16	0.20	0.42	0.036	0.34	0.036
6235-AA	0.038	0.10	0.040	0.030	0.035	0.16	0.009
6392-AA	1.10	0.15	0.079	0.099	0.16	0.16	0.039
79S-AD-D	3.23	0.15	0.069	0.16	0.20	0.29	0.035
79S-AE	3.34	0.19	0.059	0.20	0.22	0.29	0.043
6448-AA	2.83	0.076	0.042	0.21	0.038	0.31	0.031
LM24-AA	0.12	7.99	0.17	0.019	0.43	0.59	0.15
6195-AA-D	0.99	10.81	0.088	0.040	0.28	0.65	0.10
6195-AC	1.11	9.67	0.044	0.047	0.41	0.70	0.046
6252-AD	0.26	5.62	0.14	0.049	0.64	0.34	0.051
6363-AA	0.85	0.37	0.039	0.039	0.039	0.25	1.77
B51S-AF-D	0.64	1.01	0.045	0.042	0.54	0.25	0.036
6449-AA-D	0.89	0.65	0.080	0.090	0.15	0.25	0.037

TABLE 2.15 cont'd

SAMPLE	Copper	Zinc	Tin	Lead	Bismuth	Aluminum
340-AA-D	0.047	0.041	0.034	0.028	0.037	91.62
350-AQ	0.042	0.033	0.034	0.031	0.028	89.57
350-AS	0.10	0.038	0.036	0.030	0.026	89.33
123-AJ	0.036	0.034	0.027	0.034	0.032	94.25
161-AB	0.066	0.060	0.049	0.050	0.049	88.16
161-AE	0.052	0.049	0.040	0.040	0.032	86.28
B160-AA	0.061	0.043	0.031	0.028	0.043	86.28
160-DB	0.040	0.065	0.046	0.044	0.040	86.76
F40E-AG	0.037	5.44	0.031	0.027	0.035	92.56
6235-AA	0.031	5.51	0.030	0.029	0.028	93.96
6392-AA	0.10	4.33	0.039	0.019	0.038	93.69
79S-AD-D	0.62	4.50	0.030	0.020	0.030	90.66
79S-AE	0.65	4.68	0.042	0.039	0.044	90.20
6448-AA	2.04	7.17	0.059	0.060	0.021	87.11
LM24-AA	3.47	0.73	0.082	0.11	0.029	86.10
6195-AA-D	3.20	0.85	0.041	0.044	0.027	82.86
6195-AC	3.42	0.90	0.051	0.053	0.042	83.51
6252-AD	2.87	3.35	0.045	0.043	0.043	89.12
6363-AA	0.91	0.038	6.66	0.038	0.037	89.78
B51S-AF-D	0.045	0.042	0.042	0.040	0.043	97.22
6449-AA-D	0.32	0.050	0.044	0.46	0.46	96.53

TABLE 2.16

AVERAGE ABSOLUTE ERROR-ANALYSIS OF ALUMINUM-BASE ALLOYS

Magnesium	0.05
Silicon	0.17
Titanium	0.001
Chromium	0.001
Manganes	0.001
Iron	0.003
Nickel	0.003
Copper	0.008
Zinc	0.006
Tin	0.013
Lead	0.001
Bismuth	0.001
Aluminum	0.43

5. DISCUSSION

The purpose of this study, involving the determination of α-correction coefficients, was to obtain a mean value with as close a proximity as possible to the true value in each case. This could be relized only with an accurate measurement of intensity for coefficient evaluation. From the tables in Section (A.1), it is evident that the precision for the coefficients varies with the element, giving poor values for the lower atomic number elements. This can be anticipated, since the lighter elements yield significantly lower intensities so that, even by increasing the counting period to reduce the effect of the counting statistics, this influence on the evaluation of the coefficients remains significant.

DiFruscia[49] has carried out a method, where the fundamental Equation (1.18) was used to calculate the intensities for different compositions in binary systems. These intensities were then used in the Equation (2.8), (2.9) and (2.10) to evaluate the α-correction coefficients. Since the intensities were obtained by calculation (not by measurement), the counting error was limited and the coefficients were considered to be as close to the true

values as possible (if all the fundamental parameters are available). Table 3.1 illustrates the comparison of some coefficients (effect of magnesium on various elements) determined by DiFruscia with that in the present studies. This table shows better agreement for the values associated with those elements having higher atomic numbers, such as iron, cobalt, nickel, copper and zinc.

The XRF method of analysis is generally adopted on the basis of its inherent rapidity, this as compared to the more time-consuming and classical wet techniques. Errors in XRF analysis arise from several source areas. One of these, the reliability of the correction coefficients, was mentioned before. Table 3.2 (A.B) shows somewhat better results, due to improved reliability of the coefficients used in the present analysis of copper-base alloys. Also, Table 3.3 shows the accumulated relative errors for the chemical analysis portion of the investigation. The observation should be made that the high average percent relative error in some cases arose out of a few very poor results within the associated series. For the analysis of aluminum alloys, the ratio method was done and the relative error here is also presented in Table 3.3.

TABLE 3.1

COMPARISON OF α-CORRECTION COEFFICIENTS FOR EFFECT OF MAGNESIUM ON ELEMENTS

Element	A	B ± S
Phosphorus	2.42	1.5 ± 0.7
Chlorine	0.65	1.6 ± 0.3
Potassium	-0.12	0.11 ± 0.07
Calcium	-0.31	-0.10 ± 0.07
Chromium	-0.47	-0.35 ± 0.03
Manganese	-0.54	-0.46 ± 0.04
Iron	-0.57	-0.57 ± 0.05
Cobalt	-0.64	-0.64 ± 0.03
Nickel	-0.67	-0.69 ± 0.04
Copper	-0.69	-0.71 ± 0.02
Zinc	-0.73	-0.79 ± 0.02

A results from Reference (49)

B results from this study

TABLE 3.2 (A) COMPARISON OF THE RESULTS FOR COPPER-BASE ALLOYS WITH PREVIOUS STUDIES[48] - SOLID SPECIMEN

Alloy No.	COPPER					TIN					IRON		
	A	B	C	D	E	A	B	C	D	E	A	B	C
2-1	89.05	88.97	0.08	89.05	----	4.22	4.13	0.09	4.22	----	0.10	0.09	0.01
2-2	86.94	86.69	0.25	87.98	1.04	4.84	5.10	0.25	5.20	0.36	0.11	0.12	0.01
2-3	84.96	85.03	0.07	84.26	0.70	6.05	6.03	0.02	6.13	0.08	0.12	0.12	0.00
2-4	84.95	84.56	0.39	84.34	0.61	5.97	5.98	0.01	6.03	0.06	0.13	0.13	0.00
2-5	84.28	85.09	0.81	84.98	0.70	6.00	5.91	0.09	6.02	0.02	0.13	0.13	0.00
2-6	84.30	83.97	0.33	83.22	1.08	6.00	5.91	0.09	5.91	0.09	0.13	0.13	0.00
2-8	86.19	86.18	0.01	86.69	0.50	4.93	4.82	0.11	4.94	0.01	0.12	0.12	0.00
2-9	85.97	85.88	0.09	86.05	0.08	4.80	4.82	0.02	4.96	0.16	0.12	0.11	0.01
2-10	85.39	85.47	0.08	85.37	0.02	4.94	4.83	0.11	4.94	0.00	0.12	0.11	0.01
8-1	93.03	92.96	0.07	90.50	2.53	4.83	4.75	0.08	5.00	0.17	0.01	0.01	0.00
8-8	90.19	90.46	0.27	88.19	2.00	5.63	5.40	0.23	5.80	0.17	0.02	0.02	0.00
8-13	87.59	88.37	0.78	85.05	2.54	6.61	6.21	0.40	6.72	0.11	0.03	0.01	0.02
Av, Abs. Error			0.27		1.07			0.13		0.11			0.01

Column A standard values
Column B values from present studies
Column C absolute error - present studies
Column D values from Reference 48
Column E absolute error - Reference 48

All values expressed to two decimal places, regardless of individual uncertainties

TABLE 3.2 (A) cont'd

Alloy No.	Lead					Zinc					Nickel		
	A	B	C	D	E	A	B	C	D	E	A	B	C
2-1	4.01	3.97	0.04	4.01	----	2.40	2.57	0.17	2.40	----	0.22	0.27	0.05
2-2	3.95	3.87	0.08	3.94	0.01	3.92	3.96	0.04	3.70	0.22	0.24	0.26	0.02
2-3	3.96	3.88	0.08	3.94	0.02	4.65	4.70	0.05	4.40	0.25	0.26	0.25	0.01
2-4	4.37	4.42	0.05	4.40	0.05	4.30	4.65	0.35	4.45	0.15	0.29	0.25	0.04
2-5	4.87	4.17	0.70	4.28	0.57	4.34	4.44	0.10	4.21	0.13	0.27	0.25	0.02
2-6	5.46	5.40	0.06	5.40	0.02	3.84	4.54	0.30	4.19	0.35	0.28	0.25	0.03
2-8	5.57	5.51	0.06	5.53	0.02	2.82	3.01	0.19	2.88	0.06	0.34	0.36	0.02
2-9	6.16	5.86	0.30	6.01	0.11	2.58	2.93	0.35	2.79	0.21	0.38	0.40	0.02
2-10	6.25	6.33	0.08	6.36	0.16	2.86	2.86	0.00	2.68	0.18	0.40	0.41	0.01
8-1	0.60	0.60	0.00	0.59	0.01	1.49	1.68	0.19	1.73	0.24	0.01	0.00	0.01
8-8	1.81	1.85	0.04	1.77	0.04	2.27	2.21	0.06	2.30	0.03	0.07	0.07	0.00
8-13	2.78	2.33	0.45	2.22	0.53	2.88	2.94	0.06	3.01	0.13	0.11	0.14	0.03
Av. Abs. Error			0.15		0.15			0.16		0.18			0.03

TABLE 3.2 (B) COMPARISON OF THE RESULTS FOR COPPER-BASE ALLOYS WITH PREVIOUS STUDIES[48] - LIQUID SPECIMEN

Alloy No.	Copper					Tin					Iron		
	A	B	C	D	E	A	B	C	D	E	A	B	C
2-1	89.05	88.77	0.28	89.05	----	4.22	4.15	0.07	4.22	----	0.10	0.11	0.01
2-2	86.94	86.55	0.39	87.42	0.48	4.84	4.94	0.10	5.68	0.84	0.11	0.13	0.02
2-3	84.96	85.12	0.16	85.46	0.50	6.05	5.74	0.31	6.90	0.85	0.12	0.13	0.01
2-4	84.95	84.81	0.14	87.90	2.95	5.97	6.02	0.05	7.56	1.59	0.13	0.13	0.00
2-5	84.28	84.50	0.22	84.27	0.01	6.00	5.89	0.11	7.50	1.50	0.13	0.13	0.00
2-6	84.30	84.47	0.17	86.43	2.13	6.00	5.95	0.05	8.22	2.22	0.13	0.13	0.00
2-7	83.77	83.60	0.17	86.63	0.24	6.03	6.04	0.01	6.75	0.72	0.13	0.12	0.01
2-8	86.19	86.26	0.07	87.65	1.46	4.93	4.80	0.13	5.34	0.41	0.12	0.13	0.01
2-9	85.97	85.21	0.76	88.89	2.92	4.80	5.01	0.21	5.41	0.61	0.12	0.12	0.00
2-10	85.39	84.99	0.40	87.31	1.92	4.94	4.93	0.01	5.10	0.16	0.12	0.11	0.01
8-1	93.03	92.90	0.13	92.98	0.05	4.83	4.73	0.10	5.71	0.88	0.01	0.02	0.01
8-8	90.19	90.60	0.39	92.51	2.32	5.63	5.45	0.18	6.54	0.91	0.02	0.02	0.00
8-13	87.59	87.80	0.21	90.57	2.98	6.61	6.34	0.27	7.80	1.19	0.03	0.02	0.01
Ave. Abs. Error			0.27		1.50			0.12		0.99			0.01

Column A standard values
Column B values from present studies
Column C absolute error - present studies
Column D values from Reference 48
Column E absolute error - Reference 48

All values expressed to two decimal places, regardless of individual uncertainties

TABLE 3.2 (B) cont'd

Alloy No.	Lead					Zinc					Nickel		
	A	B	C	D	E	A	B	C	D	E	A	B	C
2-1	4.01	4.13	0.12	4.01	----	2.40	2.60	0.20	2.40	----	0.22	0.26	0.04
2-2	3.95	4.09	0.14	4.08	0.13	3.92	4.04	0.12	3.67	0.25	0.24	0.26	0.02
2-3	3.96	3.91	0.05	3.95	0.01	4.65	4.86	0.21	4.29	0.36	0.26	0.26	0.00
2-4	4.37	3.99	0.38	4.59	0.22	4.30	4.81	0.51	4.37	0.07	0.29	0.26	0.03
2-5	4.87	4.69	0.18	5.14	0.27	4.34	4.54	0.20	4.09	0.25	0.27	0.25	0.02
2-6	5.46	4.79	0.67	6.27	0.81	3.84	4.41	0.43	4.20	0.36	0.28	0.26	0.02
2-7	5.90	5.84	0.06	6.40	0.50	3.76	4.15	0.39	3.88	0.12	0.21	0.25	0.04
2-8	5.57	5.50	0.07	5.56	0.01	2.82	2.96	0.14	2.79	0.03	0.34	0.36	0.02
2-9	6.16	6.40	0.24	6.35	0.19	2.58	2.88	0.30	2.85	0.27	0.38	0.39	0.01
2-10	6.25	6.75	0.50	6.54	0.29	2.86	2.83	0.03	2.79	0.07	0.40	0.40	0.00
8-1	0.60	0.58	0.02	0.62	0.02	1.49	1.75	0.26	1.72	0.23	0.01	0.02	0.01
8-8	1.81	1.74	0.07	1.83	0.02	2.27	2.33	0.06	2.19	0.18	0.07	0.08	0.01
8-13	2.78	2.70	0.08	2.93	0.15	2.88	3.02	0.14	2.82	0.06	0.11	0.13	0.02
Av. Abs. Error			0.20		0.22			0.23		0.19			0.02

TABLE 3.3

AVERAGE PERCENT RELATIVE ERRORS FOR THE ANALYSES OF COPPER-BASE AND ALUMINUM-BASE ALLOYS

ELEMENT	RELATIVE ERROR,* %		
	COPPER-BASE ALLOY	ALUMINUM-BASE ALLOY	
		A	B
Magnesium	----	8.9	18.5
Silicon	----	2.4	9.6
Titanium	----	1.8	3.6
Chromium	----	1.5	3.1
Manganese	----	1.3	3.2
Iron	6.1	1.2	3.2
Nickel	8.4	1.5	2.0
Copper	0.31	0.4	3.8
Zinc	6.5	0.8	6.2
Tin	2.2	2.1	10.8
Lead	4.3	2.6	10.8
Bismuth	----	2.9	12.6

* calculations based on the weight percent of alloy compositions.

A α-correction method.

B direct ratio method.

This shows a higher accuracy for the α-correction method.

There is another source or error, which is due to the low intensities for lower concentrations of the analytes. A distribution of the percent relative error can be shown graphically, and can be found in Section (A.3). A general picture of this variation is shown as the hyperbola in Figure 3.1. Accordingly, the lower the concentration of the analyte, the higher will be the relative error.

The relative error also depends upon the element which analyzed. As the atomic number of the analyte decreases, the wavelength of the analyte-line increases, and:-

1) infinite thickness decreases;

2) fluorescent yield decreases;

3) matrix absorption increases.

Moreover, as the effective atomic number of the total specimen decreases, both coherent and incoherent scatter increase. Therefore, the analyte-line intensity is reduced, and a result is the higher relative error obtained for lower atomic number elements in XRF analysis. For instance, in this study, the analysis of iron (Z=26) in aluminum alloy has ±2% relative error when the

FIGURE 3.1 DISTRIBUTION OF RELATIVE ERROR

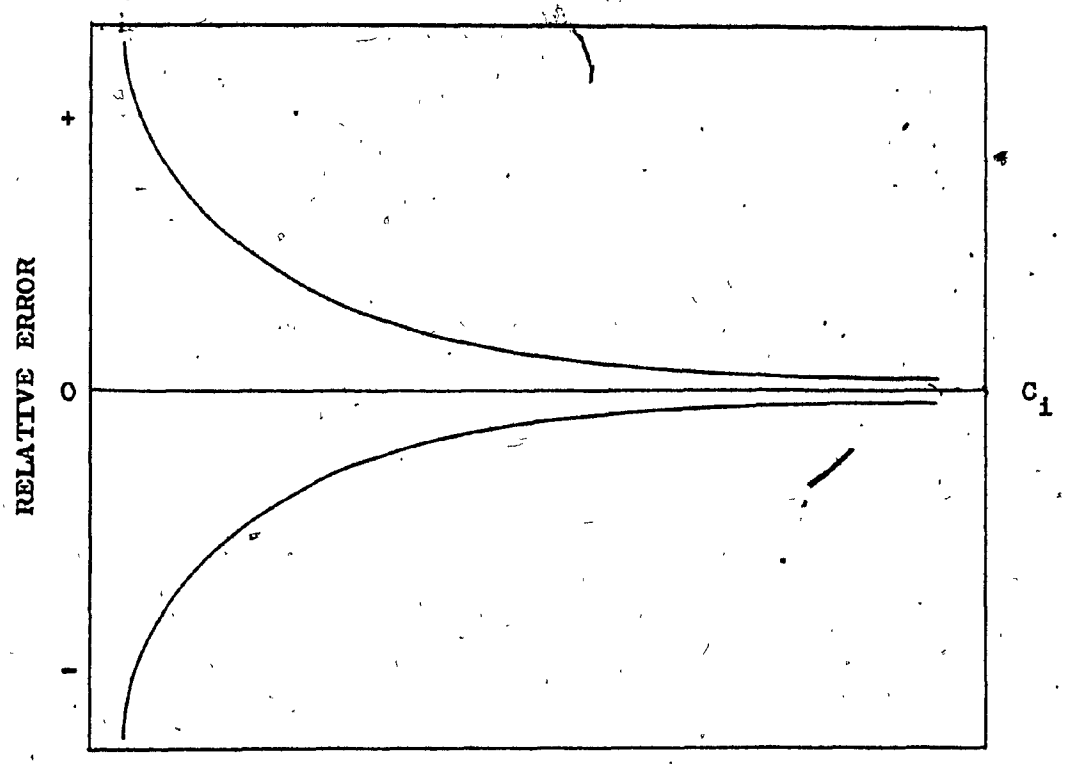

C_i : concentration of analyte

concentration of iron is at about 0.002 weight fraction. But for magnesium (Z=12), one can expect to obtain the same relative error (±2%) only with the analyte attaining at least a 0.02 weight fraction.

In addition, there are other problems which provide for increasing difficulty and inconvenience specific to the determination of the light elements by XRF analysis. These are summarized as follow:-

1) a reduction in excitation efficiency;
2) an increase in absorption for the fluorescent or emitted radiation throughout the optical path of the spectrometer from specimen to detector;
3) a resulting decrease in signal and in signal-to-noise ratio, and thus in sensitivity;
4) the specimen surface preparation becomes more critical;
5) the crystals used at long wavelengths are frequently less "reflective" than those applicable at shorter wavelengths.[50]
6) the higher value of the α-correction coefficients (e.g. $\alpha_{MgNi} = 8.68$ compared to $\alpha_{NiMg} = -0.69$) results in a higher value for the correction term, $\alpha \cdot C$. This means that any error in α-coefficient value will yield a higher error in the analyte C_i determination.

However, methodology of the present study uses the advantages of the numerical-correction methods, and minimizes most of their disadvantages. It is simple to apply and accurate at all investigated levels of concentration. Even for the lower atomic number elements (e.g. magnisum and silicon), the analyses give acceptable precision and accuracy, considering that the counting statistics is practically the only source of error.

Recently, Claisse and Thinh[51] have proposed a differential delta-coefficient method. This numerical method of matrix-effect correction in XRF analysis is obtained by derivation of the Lachance and Traill,[28] Rasberry and Heinrich,[20] and Claisse and Quintin[29] relationships. The authors calculated the α-coefficients and δ-coefficients by regression analysis from a set of binary systems. These expressions become highly complex because the δ-coefficients always depend on the composition of the sample. In such cases, a new set of δ-coefficients has to be recalculated when it is necessary to analyze samples with different compositions. Nevertheless, application of this technique[52] has been shown to be an accurate method of XRF analysis, especially in routine work where the sample composition varies only slightly.

4. CONCLUSION

In this study, the modified Lachance-Traill equation was improved. A total of more than 300 α-correction coefficients were determined from aqueous binary and ternary systems. The method offers a simple and rapid technique for the analysis of multicomponent systems such as copper-base alloys and aluminum-base alloys. The validity of this approach has been verified quite successfully on the basis of the analysis of synthetic solutions, as well as on the basis of the analysis of solutions obtained by dissolving known-composition copper-base alloys, solid specimens of these copper-base alloys and solid specimens of aluminum-base alloys.

In general, for copper-base alloys, the components copper, lead, tin, zinc, iron and nickel were determined with percent relative errors of 0.3, 4.3, 2.2, 6.5, 6.1 and 8.4. In general, the relative error increased with decreasing amount of the analyte determined.

Again, in general, for aluminum-base alloys, the components copper, zinc, iron, manganese, chromium, nickel, titanium, tin, silicon, lead, bismuth, and magnesium were determined with percent relative error of 0.4, 0.8, 1.2, 1.3, 1.5, 1.5, 1.8, 2.1, 2.4, 2.6, 2.9, and 8.9. In general, the relative error increased

with decreasing amount of the analyte determined, but increased with decreasing atomic number of the analyte.

This approach also provide several obvious advantages:-

1) Only one standard alloy is required in the computation of the chemical compositions of solutions of similar alloys of unknown compositions. Several binary/ternary specimens are required to determine the -coefficients, but such measurements are required to be made only initially.

2) The solution simultaneously of a series of linear equations yields in one operation the values for all of the elements of interest.

3) When the solution technique is used, a solution total weight of about 10 grams would have sufficed to fill the cell for examination purposes, with a corresponding total required analytes weight, or available sample weight, of only 0.1 to 1.5 grams.

In addition, for the further research about this study, such improvement may be indicated as:- (1) Increase the excitation efficiency of primary x-ray beam, hence a higher intensity can be measured, therefore, reduces the error from counting statistics; (2) Improve the reflective of analyzer crystal; (3) Improve the ability of the detector, especially in the analysis for those analyte-line having longer wavelength.

REFERENCES

1. Bertin, E.P., Principles and Practice of X-Ray Spectrometric Analysis, Plenum, N.Y. (1975)

2. Birks, L.S., X-Ray Spectrochemical Analysis, Interscience, (1969)

3. Kramers, H.A., Phil. Mag., 46, 836 (1923)

4. Lambert, M.C., Norelco Rep., 6, 37 (1959)

5. Compton, A.H., Phys. Rev., 21, 483 (1923)

6. Jenkins, R., An Introduction to X-Ray Spectrometry, Heyden, (1974)

7. Shiraiwa, T. and N. Fujino, Jap. J. App. Phys., 5, 886 (1966)

8. Shiraiwa, T. and N. Fujino, Bull. Chem. Soc. Jap., 40, 2289 (1967)

9. Shiraiwa, T. and N. Fujino, X-Ray Spectrom, 3, 64 (1974)

10. Mitchell, B.J. and J.E. Kellam, Appl. Spectrosc., 22, 742 (1968)

11. Muller. R.O., Spectrochemical Analysis by X-Ray Fluorescence, Pleunm, N.Y. (1972)

12. Sherman, J., Spectrochim Acta, 7, 283 (1955)

13. Sherman, J., Spectrochim Acta, 11, 466 (1959)

14. DiFruscia, R., J.G. Dick and C.C. Wan, X-Ray Spectrom., 7, 86 (1978)

15. Criss, J.W. and L.S. Birks, Anal. Chem., 40, 1080 (1968)

16. Gould. R.W. and S.R. Bates, X-Ray Spectrom., 1, 29 (1972)

17. de Jongh, W.K., X-Ray Spectrom., 2, 151 (1973)

18. Gilfrich, J.V. and L.S. Birks, Anal. Chem., 40, 1077 (1968)

19. Leibhafsky, H.A., X-Ray Absorption and Emission in Analytical Chemistry, John Wiley and Sons, N.Y. (1960)

20. Hienrich, K.F.J., The Electron Microprobe, Proceedings of The Symposium Sponsored by The Electrochemical Society, p.296, Oct., (1964)

21. Birks, L.S., Electronprobe Microanalysis, Interscience, N.Y. (1963)

22. Kalman, Z.M. and L. Heller, Anal. Chem., 34, 946 (1962)

23. Tertian, R., Spectrochim Acta, 270, 155 (1972)

24. Mencik, Z., X-Ray Spectrom., 4, 108 (1975)

25. Jenkins, R., Adv. in X-Ray Anal., 19, 1 (1975)

26. Stephenson, D.A., Anal. Chem., 43, 310 (1971)

27. Tertian, R., X-Ray Sepctrom., 2, 95 (1973)

28. Lachance, G.R, and R.J. Traill, Can. Specty., 11, 43 (1966)

29. Claisse, F. and M. Quintin, Can. Specty., 12, 129 (1967)

30. Rasberry, S.D. and K.F.J. Heinrich, Anal. Chem. 46, 81 (1974)

31. Noakes, G.E., ASTM Spec. Tech. Publ., 157, 57 (1954)

32. Dick, J.G. and A.D. Nguyen, Can Specty., 19, 110 (1974)

33. Wan, C.C., MSc Thesis, Dept. of Chem., Concordia Univ. Montreal, Canada (1975)

34. Lachance, G.R. and R.J. Traill, Can. Specty., 11, 63 (1966)

35. Sherman, J., ASTM Spec. Tech. Publ., 157, 27 (1956)

36. Beattie, M.J. and R.M. Brissey, Anal. Chem., 26, 980 (1954)

37. Marti, W., Spectrochim Acta, 18, 1499 (1962)

38. Lachance, G.R., Can. Specty., 15. 64 (1970)

39. Zimmerman, J.B. and J.C. Ingles, Dept. of Energy, Mines & Resources, Ottawa, Canada, Report N72-14

40. Bragg, W.H. and W.L. Bragg, Proc. Phys. Soc., (London) A88, 428 (1913)

41. Buwalda, J., Philips Serving Science and Industry, 10, 22 (1964)

42. Ruark, A. and F.E. Brammer, Phys. Rev., 52, 322 (1937)

43. Bowman, H.R., Science, 151, 562 (1966)

44. Gedke, D.A., X-Ray Spectrom., 1, 129 (1972)

45. Goulding, F.S., J.M. Jaklevic, B.V. Jarrett and D.A. Landis, Adv. X-Ray Anal., 15, 470 (1972)

46. Shirley, D.A., Nucleonics, 23(3), 62 (1965)

47. Dick, J.G., C.C. Wan and R. DiFruscia, X-Ray Spectrom., 6, 212 (1977)

48. Dick, J.G., and A.D. Nguyen, Can. Specty., 19, No. 5, 141 (1974)

49. DiFruscia, R., PhD Thesis, Department of Chemistry, Concordia University, Montreal, Canada

50. Jecht, U., and I. Petersohn, Siemens-Z, 41, 59 (1967)

51. Claisse, F., and T.P. Thinh, Anal. Chem. 51, 954 (1979)

52. Fréchette, G., J. Hébert, T.P. Thinh, R. Rousseau and F. Claisse, Anal. Cham., 51, 957 (1979)

APPENDICES

PRESENTATION OF DATA

Three groups of experimental data are presented in this chapter:-

Section (A.1) α-correction coefficients

Section (A.2) analysis of copper-base alloys

Section (A.3) analysis of aluminum-base alloys

Tables Involving "Effect of A on Elements"

Every coefficient was determined from a triplicate series of solutions, with a minimum of 50 data; their average values and standard deviations are given in these tables. K_α radiation for all elements except Hg, Pb, Th, and U where L_α used.

Tables Involving "Element Analysis"

The concentration (weight fraction) for each of the elements involved were expressed at a significant figure level, as based on the associated values from synthetic solution preparation or analyzed-standards basis.

The percent relative error was calculated as:-

$$\% \text{ Relative Error} = \frac{C\ (\text{cal.}) - C\ (\text{std.})}{C\ (\text{std.})}$$

Figures Involving "I_i vs C_i" and "Distribution of Relative Error"

The circles surrounding each experimentally determined locus on a curve are for identification of the locus only. They do not reflect the uncertainty parameters in measurement.

SECTION A.1

INTERELEMENT EFFECTS - α-CORRECTION COEFFICIENTS

Results from fundamental parameter approach - Reference 49

TABLE A.1.1 EFFECTS OF MATRIX(M) ON ELEMENTS

Element A	α_{AM} Mean	± Std. Dev.
# Magnesium	3.18	---
Aluminum	1.28	0.09
# Silicon	0.844	---
Phosphorus	-0.1^{4}	0.1^{0}
Chlorine	-0.39	0.02
Potassium	-0.71	0.04
Calcium	-0.79	0.03
# Titanium	-0.804	---
Chromium	-0.85	0.03
Manganese	-0.86	0.01
Iron	-0.90	0.01
Cobalt	-0.903	0.005
Nickel	-0.923	0.008
Copper	-0.924	0.002
Zinc	-0.943	0.008
Arsenic	-0.951	0.002
Bromine	-0.957	0.004
Strontium	-0.963	0.003
Molybdenum	-0.979	0.003
Silver	-0.963	0.007
Cadmium	-0.964	0.004
Tin	-0.962	0.004
Antimony	-0.964	0.005
Iodine	-0.939	0.009
Barium	-0.940	0.004
Lanthanum	-0.945	0.004
Cerium	-0.934	0.003
Mercury	-0.972	0.003
Lead	-0.974	0.004
Bismuth	-0.973	0.003
Thorium	-0.977	0.003
Uranium	-0.979	0.001

TABLE A.1.2 EFFECTS OF SODIUM ON ELEMENTS

Element A	σ_{ANa} Mean	± Std. Dev.
Phosphorus	1.2	0.2
Potassium	-0.22	0.05
Calcium	-0.34	0.05
Chromium	-0.56	0.02
Manganese	-0.600	0.009
Iron	-0.68	0.01
Cobalt	-0.716	0.009
Nickel	-0.773	0.004
Copper	-0.779	0.006
Zinc	-0.824	0.009

TABLE A.1.3 EFFECTS OF MAGNESIUM ON ELEMENTS

Element A	α_{AMg} Mean	± Std. Dev.
# Silicon	4.03	---
Phosphorus	1.5	0.7
Chlorine	1.6	0.3
Potassium	0.11	0.07
Calcium	-0.10	0.07
# Titanium	-0.37	---
Chromium	-0.35	0.03
Manganese	-0.46	0.04
Iron	-0.57	0.05
Cobalt	-0.64	0.03
Nickel	-0.69	0.04
Copper	-0.71	0.02
Zinc	-0.79	0.02
Cadmium	-0.93	0.05
# Tin	-0.949	---
# Lead	-0.896	---
# Bismuth	-0.903	---

TABLE A.I.4 EFFECTS OF ALUMINUM ON ELEMENTS

Element A	α_{AAl} Mean	± Std. Dev.
# Magnesium	-0.12	---
# Silicon	5.21	---
Phosphorus	3.6	0.4
Chlorine	1.8	0.2
Potassium	0.23	0.08
Calcium	0.03	0.07
# Titanium	-0.21	---
Chromium	-0.22	0.04
Manganese	-0.33	0.05
Iron	-0.49	0.03
Cobalt	-0.53	0.02
Nickel	-0.63	0.03
Copper	-0.64	0.03
Zinc	-0.70	0.02
Cadmium	-0.93	0.06
# Tin	-0.938	---
# Lead	-0.87	---
# Bismuth	-0.878	---

TABLE A.1.5 EFFECTS OF SILICON ON ELEMENTS

Element A	α_{AS} Mean	± Std. Dev.
# Magnesium	0.09	---
# Aluminum	-0.06	---
# Phosphorus	4.80	---
# Chlorine	1.71	---
# Potassium	0.41	---
# Calcium	-0.003	---
# Titanium	-0.03	---
# Chromium	-0.2	---
# Manganese	-0.31	---
# Iron	-0.38	---
# Cobalt	-0.48	---
# Nickel	-0.52	---
# Copper	-0.54	---
# Zinc	-0.61	---
# Tin	-0.923	---
# Lead	-0.85	---
# Bismuth	-0.861	---

TABLE A.1.6 EFFECTS OF PHOSPHORUS ON ELEMENTS

Element A	α_{AP} Mean	± Std. Dev.
# Magnesium	0.24	---
# Aluminum	0.085	---
# Silicon	-0.17	---
Chlorine	2.6	0.1
Potassium	0.83	0.05
Calcium	0.26	0.05
# Titanium	0.19	---
Chromium	0.08	0.02
Manganese	-0.01	0.02
Iron	-0.20	0.02
Cobalt	-0.26	0.01
Nickel	-0.411	0.007
Copper	-0.402	0.009
Zinc	-0.514	0.005

TABLE A.1.7 EFFECTS OF CHLORINE ON ELEMENTS

Element A	α_{ACl} Mean	± Std. Dev.
# Magnesium	0.49	---
# Aluminum	0.37	---
# Silicon	0.07	---
Phosphorus	-0.4	0.1
Potassium	1.36	0.06
Calcium	0.77	0.07
# Titanium	0.74	---
Chromium	0.52	0.05
Manganese	0.36	0.03
Iron	0.065	0.004
Cobalt	0.03	0.03
Nickel	-0.14	0.03
Copper	-0.16	0.02
Zinc	-0.23	0.05
Tin	-0.82	0.05

TABLE A.1.8 EFFECTS OF POTASSIUM ON ELEMENTS

Element A	α_{AK} Mean	± Std. Dev.
# Magnesium	0.87	---
# Aluminum	0.71	---
# Silicon	0.35	---
Phosphorus	-0.4	0.3
Chlorine	-0.2	0.2
Calcium	1.5	0.1
# Titanium	1.57	---
Chromium	1.01	0.02
Manganese	0.86	0.02
Iron	0.39	0.05
Cobalt	0.40	0.02
Nickel	0.16	0.01
Copper	0.15	0.01
Zinc	-0.08	0.01

TABLE A.1.9 EFFECTS OF CALCIUM ON ELEMENTS

Element A	α_{ACa} Mean	±Std. Dev.
# Magnesium	1.29	---
# Aluminum	1.74	---
# Silicon	0.48	---
Phosphorus	0.2	0.4
Chlorine	-0.0	0.2
Potassium	-0.35	0.04
# Titanium	2.10	---
Chromium	1.37	0.08
Manganese	1.19	0.02
Iron	0.83	0.02
Cobalt	0.64	0.01
Nickel	0.38	0.02
Copper	0.38	0.02
Zinc	0.11	0.01

TABLE A.1.10 EFFECTS OF TITANIUM ON ELEMENTS

Element A	α_{ATi} Mean	±Std. Dev.
# Magnesium	2.52	---
# Aluminum	1.67	---
# Silicon	0.83	---
# Phosphorus	0.33	---
# Chlorine	-0.24	---
# Potassium	-0.51	---
# Calcium	-0.56	---
# Chrominm	1.62	---
# Manganese	1.30	---
# Iron	1.11	---
# Cobalt	0.80	---
# Nickel	0.69	---
# Copper	0.61	---
# Zinc	0.41	---
# Tin	-0.734	---
# Lead	-0.45	---
# Bismuth	-0.49	---

TABLE A.1.11 EFFECTS OF CHROMIUM ON ELEMENTS

Element A	α_{ACr} Mean	±Std. Dev.
# Magnesium	4.88	---
# Aluminum	3.28	---
# Silicon	1.81	---
Phosphorus	1.2	0.1
Chlorine	0.4	0.1
Potassium	-0.31	0.03
Calcium	-0.49	0.04
# Titanium	-0.57	---
# Manganese	-0.54	---
Iron	1.74	0.03
Cobalt	1.42	0.04
Nickel	0.96	0.02
Copper	1.00	0.04
Zinc	2.17	0.06
Cadmium	-0.54	0.02
Tin	-0.58	0.05
# Lead	-0.29	---
# Bismuth	-0.34	---

TABLE A.1.12 EFFECTS OF MANGANESE ON ELEMENTS

Element A	α_{AMn} Mean	±Std. Dev.
# Magnesium	5.94	---
Aluminum	4.02	0.03
# Silicon	2.29	---
Phosphorus	1.3	0.1
Chlorine	0.6	0.1
Potassium	-0.16	0.04
Calcium	-0.46	0.04
# Titanium	-0.56	---
Chromium	-0.18	0.03
Iron	-0.23	0.06
Cobalt	1.6	0.1
Nickel	1.12	0.05
Copper	1.16	0.09
Zinc	0.70	0.09
Cadmium	-0.50	0.03
Tin	-0.54	0.04
# Lead	-0.23	---
# Bismuth	-0.28	---

TABLE A.1.13 EFFECTS OF IRON ON ELEMENTS

Element A	α_{AFe} Mean	±Std. Dev.
# Magnesium	7.67	---
Aluminum	5.2[2]	0.3[6]
# Silicon	3.06	---
Phosphorus	1.5	0.2
Chlorine	1.00	0.07
Potassium	-0.12	0.09
Calcium	-0.41	0.07
# Titanium	-0.52	---
Chromium	-0.58	0.05
Manganese	0.00	0.03
Cobalt	-0.02	0.08
Nickel	1.46	0.09
Copper	1.47	0.06
Zinc	1.04	0.08
Cadmium	-0.45	0.06
Tin	-0.47	0.03
# Lead	-0.14	---
# Bismuth	-0.19	---

TABLE A.1.14 EFFECTS OF COBALT ON ELEMENTS

Element A	α_{ACo} Mean	± Std. Dev.
# Magnesium	8.72	---
# Aluminum	6.04	---
# Silicon	3.62	---
Phosphorus	1.5	0.4
Chlorine	1.0	0.1
Potassium	-0.03	0.05
Calcium	-0.25	0.02
# Titanium	-0.45	---
Chromium	-0.60	0.01
Manganese	-0.59	0.04
Iron	-0.030	0.005
Nickel	-0.11	0.02
Copper	1.63	0.06
Zinc	1.20	0.05
Cadmium	-0.42	0.06
Tin	-0.43	0.05

TABLE A.1.15 EFFECTS OF NICKEL ON ELEMENTS

Element A	α_{ANi} Mean	± Std. Dev.
# Magnesium	8.68	---
Aluminum	7.2	0.1
# Silicon	3.75	---
Phosphorus	2.3	0.5
Chlorine	1.4	0.2
Potassium	0.06	0.04
Calcium	-0.17	0.04
# Titanium	-0.40	---
Chromium	-0.39	0.09
Manganese	-0.52	0.07
Iron	-0.54	0.04
Cobalt	-0.05	0.03
Copper	-0.05	0.04
Zinc	1.51	0.09
Cadmium	-0.27	0.07
Tin	-0.34	0.04
# Lead	0.044	---
# Bismuth	-0.014	---

TABLE A.1.16 EFFECTS OF COPPER ON ELEMENTS

Element A	α_{ACu} Mean	± Std. Dev.
# Magnesium	9.39	---
Aluminum	7.4	0.2
# Silicon	4.10	---
Chlorine	1.5	0.1
Potassium	0.24	0.05
Calcium	-0.14	0.04
# Titanium	-0.36	---
Chromium	-0.39	0.04
Manganese	-0.65	0.05
Iron	-0.58	0.03
Cobalt	-0.59	0.03
Nickel	-0.34	0.05
Zinc	-0.17	0.05
Cadmium	-0.22	0.07
Tin	-0.28	0.04
# Lead	0.10 8	---
# Bismuth	0.04	---

TABLE A.1.17 EFFECTS OF ZINE ON ELEMENTS

Element A	α_{AZn} Mean	Std. Dev.
# Magnesium	11.2	---
# Aluminum	8.0	---
# Silicon	4.98	---
Phosphorus	3.0	0.3
Chlorine	1.7	0.2
Potassium	0.38	0.07
Calcium	0.05	0.04
# Titanium	-0.25	---
Chromium	-0.35	0.06
Manganese	-0.42	0.06
Iron	-0.53	0.06
Cobalt	-0.53	0.04
Nickel	-0.59	0.03
Copper	-0.10	0.05
Cadmium	-0.09	0.03
Tin	-0.17	0.03
# Lead	0.29	---
# Bismuth	0.21	---

TABLE A.1.18 EFFECTS OF CADMIUM ON ELEMENTS

Element A	α_{ACd} Mean	± Std. Dev.
Chlorine	1.1	0.1
Calcium	1.41	0.07
Chromium	2.07	0.04
Manganese	1.84	0.07
Iron	1.29	0.03
Cobalt	1.15	0.04
Nickel	0.77	0.04
Copper	0.79	0.02
Zinc	0.40	0.02

TABLE A.1.19 EFFECT OF TIN ON ELEMENTS

Element A	α_{ASn} Mean	± Std. Dev.
# Magnesium	12.0	---
# Aluminum	5.02	---
# Silicon	3.35	---
# Chlorine	1.80	---
# Titanium	2.67	---
# Chromium	2.11	---
# Manganese	1.74	---
# Iron	1.51	---
# Nickel	1.00	---
# Copper	0.88	---
# Zinc	0.65	---
# Lead	-0.484	---
# Bismuth	-0.48	---

TABLE A.1.20 EFFECT OF LEAD ON ELEMENTS

Element A	α_{APb} Mean	± Std. Dev.
# Magnesium	12.83	---
# Aluminum	4.66	---
# Silicon	3.33	---
# Chlorine	2.07	---
Calcium	2.17	0.09
# Titanium	2.34	---
# Chromium	1.96	---
Manganese	1.66	0.04
Iron	1.09	0.03
Cobalt	1.09	0.03
Nickel	0.67	0.03
Copper	0.71	0.02
Zinc	0.40	0.03
Cadmium	1.3	0.1
# Tin	0.52	---
# Bismuth	-0.04	---

TABLE A.1.21 EFFECTS OF BISMUTH ON ELEMENTS

Element A	α_{ABi} Mean	± Std. Dev.
# Magnesium	13.29	---
# Silicon	7.62	---
# Titanium	2.50	---
# Chromium	1.82	---
# Manganese	1.79	---
# Iron	1.70	---
# Nickel	1.20	---
# Copper	1.16	---
# Zinc	0.95	---
# Tin	0.594	---
# Lead	0.011	---

SECTION A.2

ANALYSIS OF COPPER-BASE ALLOYS

SECTION A.2.1

SYNTHETIC COPPER-BASE ALLOYS - SERIES SC

TABLE A.2.1.1 COPPER ANALYSIS - SERIES SC

Sample	C_{Cu}(std.)	$I^{meas.}_{CuK\alpha}$ (cps)	$I^{cor.}_{CuK\alpha}$ (cps)	C_{Cu}(cal.)	Relative Error %
SC-1	0.039290	59048	8341	0.038195	-2.8
SC-2	0.041710	62689	8779	0.039926	-4.3
SC-3	0.044290	66475	9416	0.043002	-2.9
SC-4	0.042350	64081	8946	0.041011	-3.2
SC-5	0.043710	70347	9847	0.047705	9.1
SC-6	0.045000	67987	9601	0.043972	-2.3
SC-7	0.046410	70118	9858	0.045243	-2.5
SC-8	0.047610	74820	10562	0.050338	5.7

TABLE A.2.1.2 LEAD ANALYSIS - SERIES SC

Sample	C_{Pb}(std.)	$I^{meas.}_{PbL\alpha}$ (cps)	$I^{cor.}_{PbL\alpha}$ (cps)	C_{Pb}(cal.)	Relative Error %
SC-1	0.002579	1827	198	0.002095	-18.7
SC-2	0.001421	1027	110	0.001167	-17.8
SC-3	0.002143	1540	165	0.001797	-16.1
SC-4	0.000286	229	25	0.000264	-7.7
SC-5	0.000714	529	57	0.000670	-6.2
SC-6	0.001750	1254	135	0.001472	-15.8
SC-7	0.001429	1039	111	0.001224	-14.3
SC-8	0.001386	1017	109	0.001282	-7.5

TABLE A.2.1.3 IRON ANALYSIS - SERIES SC

Sample	C_{Fe}(std.)	$I^{meas.}_{FeK\alpha}$ (cps)	$I^{cor.}_{FeK\alpha}$ (cps)	C_{Fe}(cal.)	Relative Error %
SC-1	0.000286	1405	181	0.000322	12.6
SC-2	0.000286	1173	148	0.000264	-7.7
SC-3	0.000400	1662	213	0.000378	-5.5
SC-4	0.000136	653	82	0.000145	6.6
SC-5	0.000107	504	63	0.000114	6.5
SC-6	0.000279	1148	146	0.000260	-6.8
SC-7	0.000143	610	77	0.000137	-4.2
SC-8	0.000271	1163	147	0.000265	-2.2

TABLE A.2.1.4 ZINC ANALYSIS - SERIES SC

Sample	C_{Zn}(std.)	$I^{meas.}_{ZnK_\alpha}$ (cps)	$I^{cor.}_{ZnK_\alpha}$ (cps)	C_{Zn}(cal)	Relative Error %
SC-1	0.029200	54340	6463	0.028919	-0.9
SC-2	0.027300	50575	5940	0.026279	-3.7
SC-3	0.024600	45426	5365	0.023952	-2.6
SC-4	0.028730	53438	6278	0.027710	-3.6
SC-5	0.026900	53393	6264	0.029152	8.3
SC-6	0.024400	45189	5318	0.023755	-2.6
SC-7	0.023090	43501	5083	0.022748	-1.5
SC-8	0.022160	43444	5087	0.023535	6.2

SECTION A.2.2

COPPER-BASE ALLOY - SOLID SPECIMEN

TABLE A.2.2.1 TIN ANALYSIS - COPPER-BASE ALLOYS

Sample	C_{Sn}(std.)	$I^{meas.}_{SnK\alpha}$ (cps)	$I^{cor.}_{SnK\alpha}$ (cps)	C_{Sn}(cal.)	Relative Error %
2-1	0.042200	7448	5703	0.041300	-2.1
2-2	0.048400	9156	7044	0.051000	5.4
2-3	0.060500	10769	8315	0.060300	-0.3
2-4	0.059700	10627	8251	0.059800	0.2
2-5	0.060000	10531	8213	0.059100	-1.5
2-6	0.060000	10398	8158	0.059100	-1.5
2-7	0.059200	4511	----	----	---
2-8	0.049300	8521	6624	0.048200	-2.2
2-9	0.048000	8485	6650	0.048200	0.4
2-10	0.049400	8465	6659	0.048300	-2.2
2-11	0.058600	9990	7892	0.057100	-2.6
8-1	0.048300	9054	6700	0.047500	-1.7
8-2	0.060100	10656	7928	0.056200	-6.5
8-5	0.059700	12157	9191	0.065300	9.4
8-6	0.063800	11890	9060	0.064200	0.6
8-8	0.056300	10120	7599	0.054000	-4.1
8-10	0.053000	10007	7573	0.053500	0.6
8-11	0.053100	9946	7560	0.053600	0.9
8-12	0.058400	10417	7919	0.056100	-3.8
8-13	0.066100	11527	8802	0.062100	-6.1

TABLE A.2.2.2 LEAD ANALYSIS - COPPER-BASE ALLOYS

Sample	C_{Pb}(std.)	$I^{meas.}_{PbL\alpha}$ (cps)	$I^{cor.}_{PbL\alpha}$ (cps)	C_{Pb}(cal.)	Relative Error %
2-1	0.040100	2637	2857	0.039700	-0.1
2-2	0.039500	2577	2788	0.038700	-2.0
2-3	0.039600	2593	2791	0.038800	-2.0
2-4	0.043700	2957	3180	0.044200	1.1
2-5	0.048700	2793	3002	0.041700	-14.3
2-6	0.054600	3618	3883	0.054000	-1.1
2-8	0.055700	3677	3963	0.055100	-1.1
2-9	0.061600	3916	4222	0.058600	-4.9
2-10	0.062500	4230	4554	0.063300	1.3
2-11	0.062200	4141	4443	0.061700	-0.8
8-1	0.006000	332	359	0.006000	0.0
8-2	0.005400	334	359	0.006000	11.1
8-5	0.017900	1078	1163	0.019200	7.3
8-6	0.025200	1411	1516	0.025200	0.0
8-8	0.018100	1033	1115	0.018500	2.2
8-10	0.024300	1153	1243	0.020600	-15.2
8-11	0.029000	1600	1739	0.028600	-1.4
8-12	0.027800	1527	1639	0.027300	-1.8
8-13	0.027800	1306	1399	0.023300	-16.2

TABLE A.2.2.3 IRON ANALYSIS - COPPER-BASE ALLOYS

Sample	C_{Fe}(std.)	$I^{meas.}_{FeK\alpha}$ (cps)	$I^{cor.}_{FeK\alpha}$ (cps)	C_{Fe}(cal.)	Relative Error %
2-1	0.001000	863	495	0.000900	-10.0
2-2	0.001100	1101	647	0.001200	9.1
2-3	0.001200	1038	632	0.001200	0.0
2-4	0.001300	1138	705	0.001300	0.0
2-5	0.001300	1126	704	0.001300	0.0
2-6	0.001300	1116	711	0.001300	0.0
2-8	0.001200	1005	620	0.001200	0.0
2-9	0.001200	939	582	0.001100	-8.3
2-10	0.001200	893	561	0.001100	-8.3
2-11	0.001200	1026	664	0.001300	8.3
8-1	0.000100	140	74	0.000100	0.0
8-2	0.000200	201	111	0.000200	0.0
8-5	0.000300	228	131	0.000200	-33.3
8-6	0.000300	165	98	0.000200	-33.3
8-8	0.000200	165	92	0.000200	0.0
8-10	0.000200	163	93	0.000200	0.0
8-11	0.000100	155	90	0.000200	100.0
8-12	0.000100	161	95	0.000200	100.0
8-13	0.000300	148	89	0.000100	-66.7

TABLE A.2.2.4 NICKEL ANALYSIS - COPPER-BASE ALLOYS

Sample	C_{Ni}(std.)	$I^{meas.}_{NiK\alpha}$ (cps)	$I^{cor.}_{NiK\alpha}$ (cps)	C_{Ni}(cal.)	Relative Error %
2-1	0.002200	3245	2438	0.002700	22.7
2-2	0.002400	3074	2327	0.002600	8.1
2-3	0.002600	2948	2269	0.002500	-3.8
2-4	0.002900	2958	2295	0.002500	-13.8
2-5	0.002700	2981	2327	0.002500	-7.4
2-6	0.002800	2931	2311	0.002500	-10.7
2-8	0.003400	4251	3307	0.003600	5.9
2-9	0.003800	4660	3634	0.004000	5.3
2-10	0.004000	4755	3735	0.004100	2.5
2-11	0.003100	4615	3669	0.004000	29.0
8-1	0.000100	26	19	0.000100	0.0
8-2	0.0	---	---	0.0	0.0
8-5	0.0	---	---	0.0	0.0
8-6	0.000100	36	27	0.000000	-100.0
8-8	0.000700	628	333	0.000700	0.0
8-10	0.001100	906	680	0.001000	-9.1
8-11	0.001200	1052	796	0.001200	0.0
8-12	0.001400	1176	898	0.001300	-7.1
8-13	0.001100	1205	927	0.001400	27.3

TABLE A.2.2.5 ZINC ANALYSIS - COPPER-BASE ALLOYS

Sample	C_{Zn}(std.)	$I^{meas.}_{ZnK\alpha}$ (cps)	$I^{cor.}_{ZnK\alpha}$ (cps)	C_{Zn}(cal.)	Relative Error %
2-1	0.024000	18093	17305	0.025700	7.1
2-2	0.039200	27640	26735	0.039600	1.0
2-3	0.046500	32567	31773	0.048600	1.1
2-4	0.043000	32132	31551	0.046500	8.1
2-5	0.043400	30767	30328	0.044400	2.3
2-6	0.038400	29822	29589	0.045400	7.8
2-8	0.028200	20855	20539	0.030100	6.7
2-9	0.025800	20231	19992	0.029300	13.6
2-10	0.028600	19682	19533	0.028600	0.0
2-11	0.037700	25066	25035	0.036700	-2.7
8-1	0.014900	4392	3800	0.016800	12.7
8-2	0.026000	7833	6817	0.030100	15.8
8-5	0.045900	8894	7834	0.034800	-24.2
8-6	0.036900	8496	7524	0.033300	-9.7
8-8	0.022700	5694	4985	0.022100	-2.6
8-10	0.022800	5457	4802	0.021200	-7.0
8-11	0.019500	5168	4549	0.020200	3.6
8-12	0.015500	5959	5259	0.023300	50.3
8-13	0.028800	7521	6675	0.029400	2.1

SECTION A.2.3

COPPER-BASE ALLOYS - LIQUID SPECIMEN

TABLE A.2.3.1 COPPER ANALYSIS - COPPER-BASE ALLOYS

Sample	C_{Cu}(std.)	$I^{meas.}_{CuK\alpha}$ (cps)	$I^{cor.}_{CuK\alpha}$ (cps)	C_{Cu}(cal.)	Relative Error %
2-1	0.018188	35211	4300	0.017992	-1.1
2-2	0.017373	32737	4082	0.017079	-1.7
2-3	0.017637	33737	4171	0.017452	-1.0
2-4	0.017337	34204	4180	0.017490	0.9
2-5	0.017615	34316	4222	0.017665	0.3
2-6	0.017673	34892	4244	0.017757	0.5
2-7	0.016915	39022	4053	0.016958	0.3
2-8	0.017563	31552	4204	0.017590	0.2
2-9	0.017605	37477	4072	0.017029	-3.3
2-10	0.017143	38801	4131	0.017280	0.8
2-11	0.017116	40098	4099	0.017151	0.2
8-1	0.018552	29572	4206	0.018611	0.3
8-2	0.018119	31063	4111	0.018190	0.4
8-5	0.017574	29119	3976	0.017593	0.1
8-6	0.017731	31308	4029	0.017788	0.3
8-8	0.018127	30779	4103	0.018155	0.2
8-10	0.017958	32639	4077	0.018040	0.5
8-11	0.017698	33246	4027	0.017819	0.7
8-12	0.017972	33611	3993	0.017668	-1.7
8-13	0.017694	29007	3986	0.017637	-0.3

TABLE A.2.3.2 TIN ANALYSIS - COPPER-BASE ALLOYS

Sample	C_{Sn}(std.)	$I^{meas.}_{SnK\alpha}$ (cps)	$I^{cor.}_{SnK\alpha}$ (cps)	C_{Sn}(cal.)	Relative Error %
2-1	0.000865	2503	146	0.000854	-1.3
2-2	0.000969	2968	172	0.001006	3.8
2-3	0.001222	3460	202	0.001181	-3.4
2-4	0.001222	3609	209	0.001222	0.0
2-5	0.001232	3664	214	0.001251	1.5
2-6	0.001261	3623	211	0.001234	-2.1
2-7	0.001198	3735	204	0.001193	-0.4
2-8	0.001007	2796	168	0.000982	-2.5
2-9	0.000972	3109	172	0.001006	3.5
2-10	0.000992	3100	170	0.000994	-0.2
2-11	0.001198	3773	205	0.001199	0.1
8-1	0.000976	2762	168	0.000951	-2.6
8-2	0.001199	3399	200	0.001133	-5.5
8-5	0.001196	3904	234	0.001325	10.8
8-6	0.001295	3898	229	0.001297	0.2
8-8	0.001051	3296	195	0.001104	5.0
8-10	0.001059	3310	191	0.001082	2.2
8-11	0.001048	3105	177	0.001002	-4.4
8-12	0.001170	3435	195	0.001104	-5.6
8-13	0.001311	3800	229	0.001297	-1.1

TABLE A.2.3.3 LEAD ANALYSIS - COPPER-BASE ALLOYS

Sample	C_{Pb}(std.)	$I^{meas.}_{Pb L\alpha}$ (cps)	$I^{cor.}_{Pb L\alpha}$ (cps)	C_{Pb}(cal.)	Relative Error %
2-1	0.000797	1111	62	0.000824	3.4
2-2	0.000791	1076	60	0.000804	1.6
2-3	0.000798	1056	59	0.000789	-1.1
2-4	0.000897	1113	61	0.000823	-8.2
2-5	0.001015	1323	74	0.000987	-2.8
2-6	0.001148	1359	76	0.001007	-12.3
2-7	0.001198	1792	89	0.001184	-1.2
2-8	0.001140	1503	88	0.001179	3.4
2-9	0.001171	1909	97	0.001296	10.7
2-10	0.001255	2067	104	0.001385	10.4
2-11	0.001271	1961	96	0.001285	1.1
8-1	0.000109	131	8	0.000117	7.3
8-2	0.000108	124	7	0.000104	-3.7
8-5	0.000358	422	25	0.000365	2.0
8-6	0.000511	607	35	0.000504	-1.4
8-8	0.000344	412	24	0.000351	2.0
8-10	0.000486	594	33	0.000483	-0.6
8-11	0.000571	686	38	0.000543	-4.9
8-12	0.000557	705	38	0.000552	-0.9
8-13	0.000565	638	38	0.000554	-1.9

TABLE A.2.3.4 IRON ANALYSIS - COPPER-BASE ALLOYS

Sample	C_{Fe}(std.)	$I^{meas.}_{FeK\alpha}$ (cps)	$I^{cor.}_{FeK\alpha}$ (cps)	C_{Fe}(cal.)	Relative Error %
2-1	0.000021	129	18	0.000022	4.8
2-2	0.000022	149	22	0.000026	18.2
2-3	0.000025	147	21	0.000025	0.0
2-4	0.000027	155	22	0.000027	0.0
2-5	0.000027	161	23	0.000028	3.7
2-6	0.000027	156	22	0.000027	0.0
2-7	0.000026	176	21	0.000025	-3.8
2-8	0.000025	134	21	0.000025	0.0
2-9	0.000024	157	20	0.000024	0.0
2-10	0.000024	150	19	0.000022	-8.3
2-11	0.000025	173	21	0.000024	-4.0
8-1	0.000002	64	15	0.000003	50.0
8-2	0.000004	74	13	0.000003	-25.0
8-5	0.000005	78	14	0.000003	-40.0
8-6	0.000005	74	13	0.000003	-40.0
8-8	0.000003	70	13	0.000003	0.0
8-10	0.000003	82	14	0.000003	0.0
8-11	0.000003	76	13	0.000003	0.0
8-12	0.000003	84	14	0.000003	0.0
8-13	0.000006	68	13	0.000003	-50.0

TABLE A.2.3.5 NICKEL ANALYSIS - COPPER-BASE ALLOYS

Sample	C_{Ni}(std.)	$I^{meas.}_{NiK\alpha}$ (cps)	$I^{cor.}_{NiK\alpha}$ (cps)	C_{Ni}(cal.)	Relative Error %
2-1	0.000045	364	43	0.000053	17.8
2-2	0.000048	343	41	0.000052	8.3
2-3	0.000054	361	43	0.000054	0.0
2-4	0.000059	363	43	0.000053	-10.2
2-5	0.000056	368	44	0.000055	-1.8
2-6	0.000059	367	43	0.000054	-8.5
2-7	0.000043	412	41	0.000051	18.6
2-8	0.000069	462	60	0.000075	8.7
2-9	0.000076	606	63	0.000079	3.9
2-10	0.000080	638	65	0.000081	1.3
2-11	0.000063	673	66	0.000082	30.2
8-1	0.000001	27	4	0.000005	400.0
8-2	0.000000	20	--	--	---
8-5	0.000000	26	--	--	---
8-6	0.000001	26	3	0.000004	300.0
8-8	0.000013	80	10	0.000015	15.4
8-10	0.000021	117	14	0.000020	-4.8
8-11	0.000024	140	16	0.000023	-4.2
8-12	0.000027	146	17	0.000024	-11.1
8-13	0.000023	131	18	0.000025	8.7

TABLE A.2.3.6 ZINC ANALYSIS - COPPER-BASE ALLOYS

Sample	C_{Zn}(std.)	$I^{meas.}_{ZnK\alpha}$ (cps)	$I^{cor.}_{ZnK\alpha}$ (cps)	C_{Zn}(cal.)	Relative Error %
2-1	0.000576	3473	367	0.000535	-7.1
2-2	0.000825	5134	553	0.000806	-2.3
2-3	0.000941	6465	686	0.001000	6.3
2-4	0.000932	6483	683	0.000996	6.9
2-5	0.000903	6211	656	0.000956	5.7
2-6	0.000856	6134	639	0.000931	8.8
2-7	0.000862	6690	580	0.000845	-2.0
2-8	0.000627	3567	416	0.000606	-3.3
2-9	0.000649	4346	400	0.000583	-10.2
2-10	0.000578	4445	401	0.000585	1.2
2-11	0.000771	6017	512	0.000746	-3.2
8-1	0.000360	1981	232	0.000351	-2.5
8-2	0.000519	3879	418	0.000633	21.9
8-5	0.000919	4344	485	0.000735	-20.0
8-6	0.000749	4722	492	0.000746	-0.4
8-8	0.000450	2893	315	0.000476	5.8
8-10	0.000456	2885	291	0.000440	-3.5
8-11	0.000385	2892	282	0.000426	10.6
8-12	0.000311	3404	324	0.000490	57.5
8-13	0.000567	3651	411	0.000622	9.7

TABLE A.2.3.7 CHLORINE ANALYSIS - COPPER-BASE ALLOYS

Sample	C_{Cl}(std.)	$I^{meas.}_{ClK\alpha}$ (cps)	$I^{cor.}_{ClK\alpha}$ (cps)	C_{Cl}(cal.)	Relative Error %
2-1	0.034147	10625	7042	0.033533	-1.8
2-2	0.038000	12294	8156	0.038838	2.2
2-3	0.035600	11194	7431	0.035386	-0.6
2-4	0.033900	10311	6834	0.032543	-4.0
2-5	0.034400	10789	7162	0.034105	-0.9
2-6	0.032200	10230	6786	0.032314	0.4
2-7	0.009900	2558	1671	0.007957	-19.6
2-8	0.048300	15686	10485	0.049929	3.4
2-9	0.016700	4710	3086	0.014695	-12.0
2-10	0.013600	3200	2093	0.010000	-26.5
2-11	0.007400	1681	1097	0.005224	-29.4
8-1	0.061570	19313	12982	0.062413	1.4
8-2	0.048510	15123	10088	0.048500	0.0
8-5	0.053760	16605	11116	0.053442	-0.6
8-6	0.042870	12997	8654	0.041606	-2.9
8-8	0.049640	15137	10107	0.048591	-2.1
8-10	0.038500	11981	7948	0.038211	-0.8
8-11	0.033780	10663	7050	0.033894	0.3
8-12	0.030260	9730	6425	0.030889	2.1
8-13	0.054390	17104	11461	0.055101	1.3

SECTION A.3

ANALYSIS OF ALUMINUM-BASE ALLOYS

A.3.1 Synthetic Aluminum Alloys - Liquid Specimen

A.3.2 Aluminum Alloys - Solid Specimen

SECTION A.3.1

SYNTHETIC ALUMINUM ALLOYS - LIQUID SPECIMEN

A calculated concentration - α-correction method
B calculated concentration - direct ratio method
C relative error - α-correction method
D relative error - direct ratio method

* standard sample for the direct ratio method

TABLE A.3.1.1 ALUMINUM ANALYSIS - SERIES S

SAMPLE	C_{Al} (std.)	$I_{AlK\alpha}$ (cps)	$I_{AlK\alpha}$ (corrected) (cps)	C_{Al} (calculated) A	B	Relative Error (%) C	D
* S-1	0.01210	352	789	0.01161	0.01210	-4.0	---
S-2	0.01272	433	976	0.01435	0.01488	12.8	17.0
S-3	0.01319	411	918	0.01349	0.01413	2.3	7.1
S-4	0.01362	400	892	0.01310	0.01375	-3.8	1.0
S-5	0.01412	437	975	0.01433	0.01502	1.5	6.4
S-6	0.01156	344	771	0.01134	0.01183	-1.9	2.3
S-7	0.01097	349	787	0.01157	0.01200	5.5	9.4
S-8	0.01445	449	998	0.01468	0.01543	1.6	6.8

FIGURE A.3.1.1 INTENSITY I_{AlK_α} VS CONCENTRATION C_{Al}

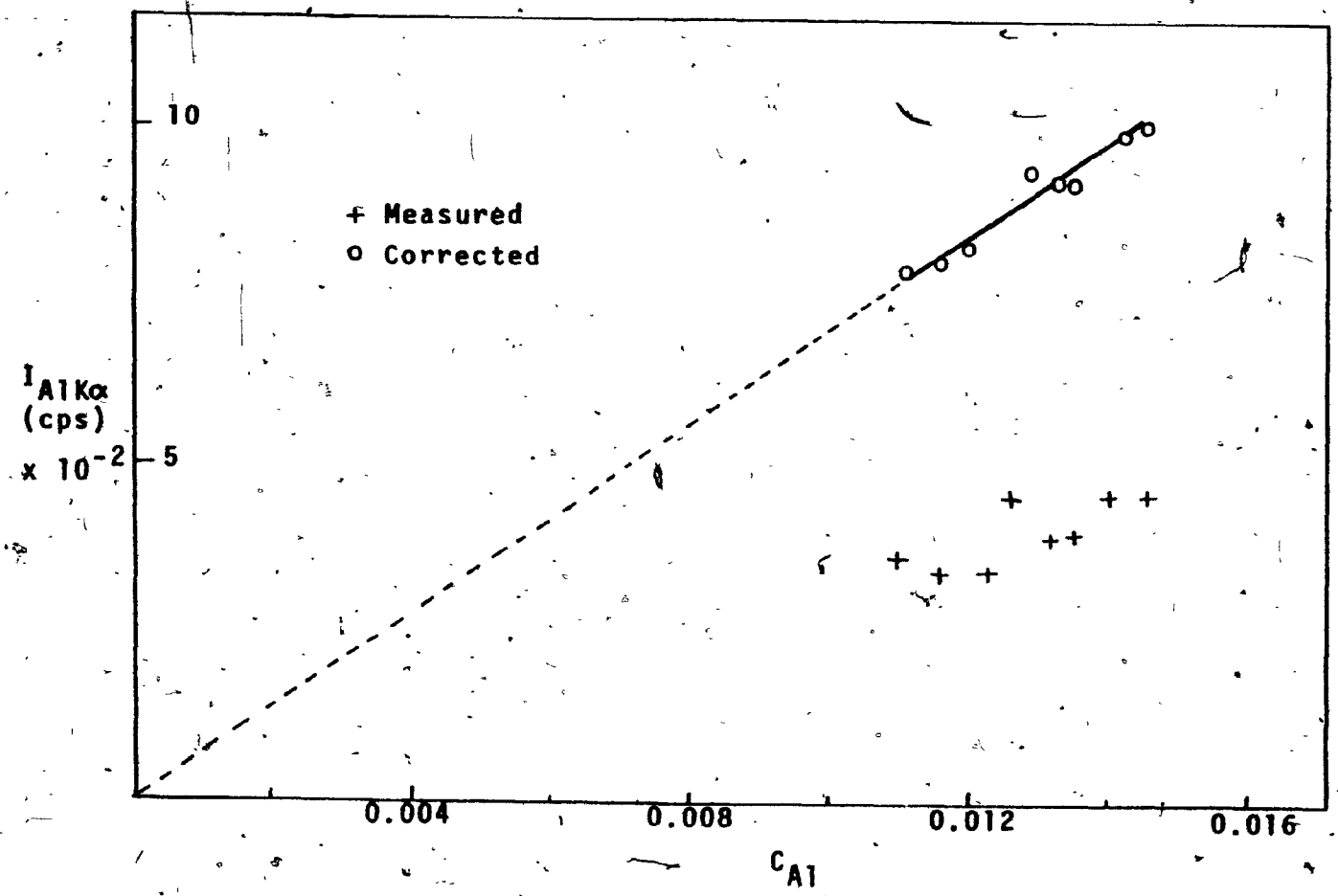

TABLE A.3.1.2 MANGANESE ANALYSIS - SERIES S

SAMPLE	C_{Mn}(std.)	$I_{MnK\alpha}$ (cps)	$I_{MnK\alpha}$(corrected) (cps)	C_{Mn}(calculated) A	B	Relative Error(%) C	D
S-1	0.00172	2590	604	0.00164	0.00172	-4.7	---
S-2	0.00215	3676	788	0.00218	0.00244	1.4	13.5
S-3	0.00280	4359	1000	0.00281	0.00289	0.4	3.2
S-4	0.00325	5041	1178	0.00330	0.00335	1.5	3.1
S-5	0.00118	1893	445	0.00122	0.00126	3.4	6.8
S-6	0.00079	1181	283	0.00078	0.00078	-1.3	-1.3
S-7	0.00194	3002	702	0.00195	0.00199	0.5	2.6
S-8	0.00080	1205	292	0.00081	0.00080	1.3	0.0

FIGURE A.3.1.2 INTENSITY $I_{MnK\alpha}$ VS CONCENTRATION C_{Mn}

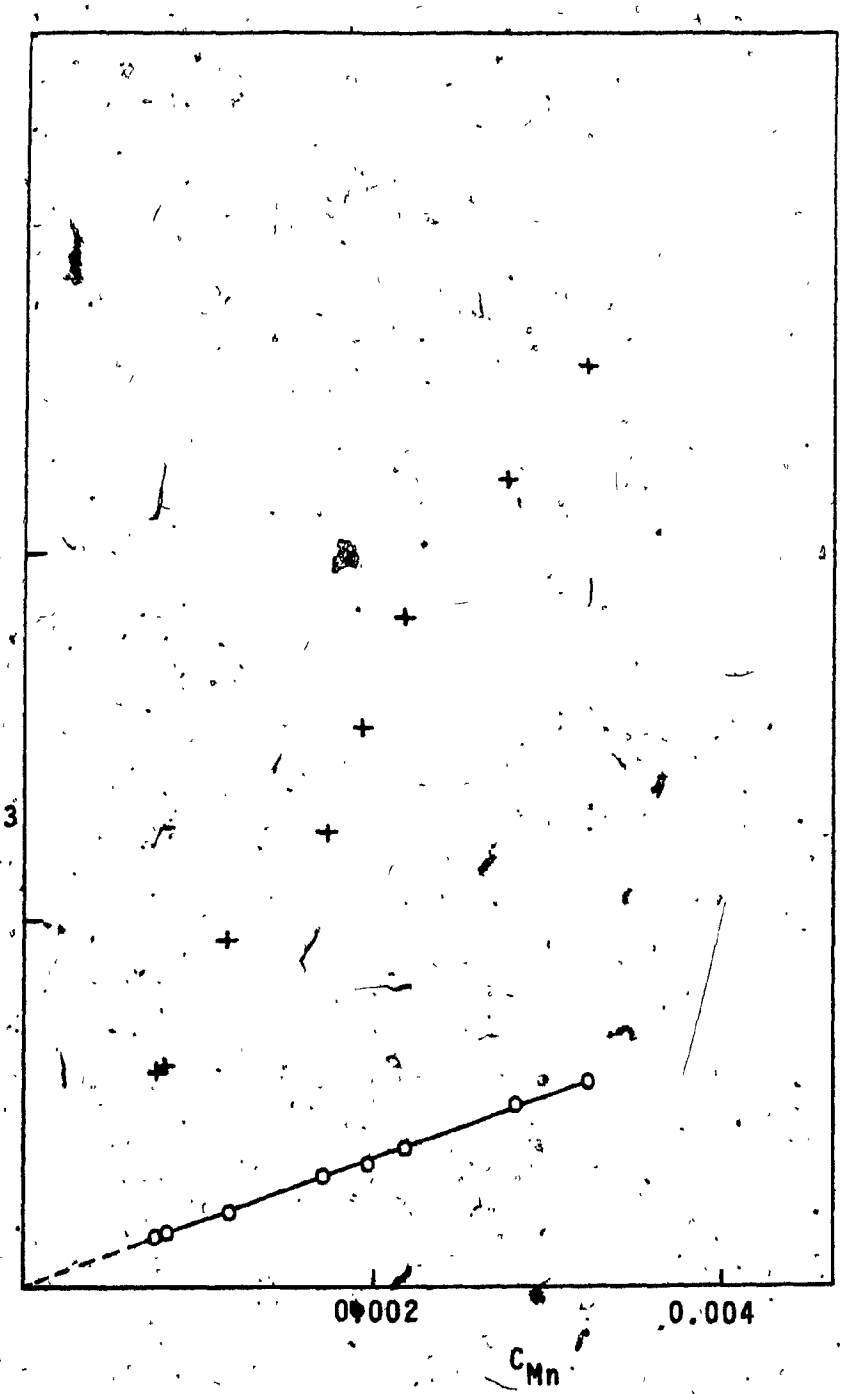

TABLE A.3.1.3 IRON ANALYSIS - SERIES S

SAMPLE	C_{Fe}(std.)	$I_{FeK\alpha}$ (cps)	$I_{FeK\alpha}$(corrected) (cps)	C_{Fe}(calculated) A	B	Relative Error(%) C	D
* S-1	0.00170	4285	748	0.00163	0.00170	-4.1	---
S-2	0.00120	3418	546	0.00121	0.00136	0.8	13.3
S-3	0.00159	4163	713	0.00161	0.00165	1.3	3.8
S-4	0.00100	2594	453	0.00102	0.00103	2.0	3.0
S-5	0.00219	5642	993	0.00217	0.00224	-0.9	2.3
S-6	0.00160	3994	719	0.00158	0.00158	-1.3	-1.3
S-7	0.00241	6191	1086	0.00241	0.00246	0.0	2.1
S-8	0.00040	1019	185	0.00041	0.00040	2.5	0.0

FIGURE A.3.1.3 INTENSITY $I_{FeK\alpha}$ VS CONCENTRATION C_{Fe}.

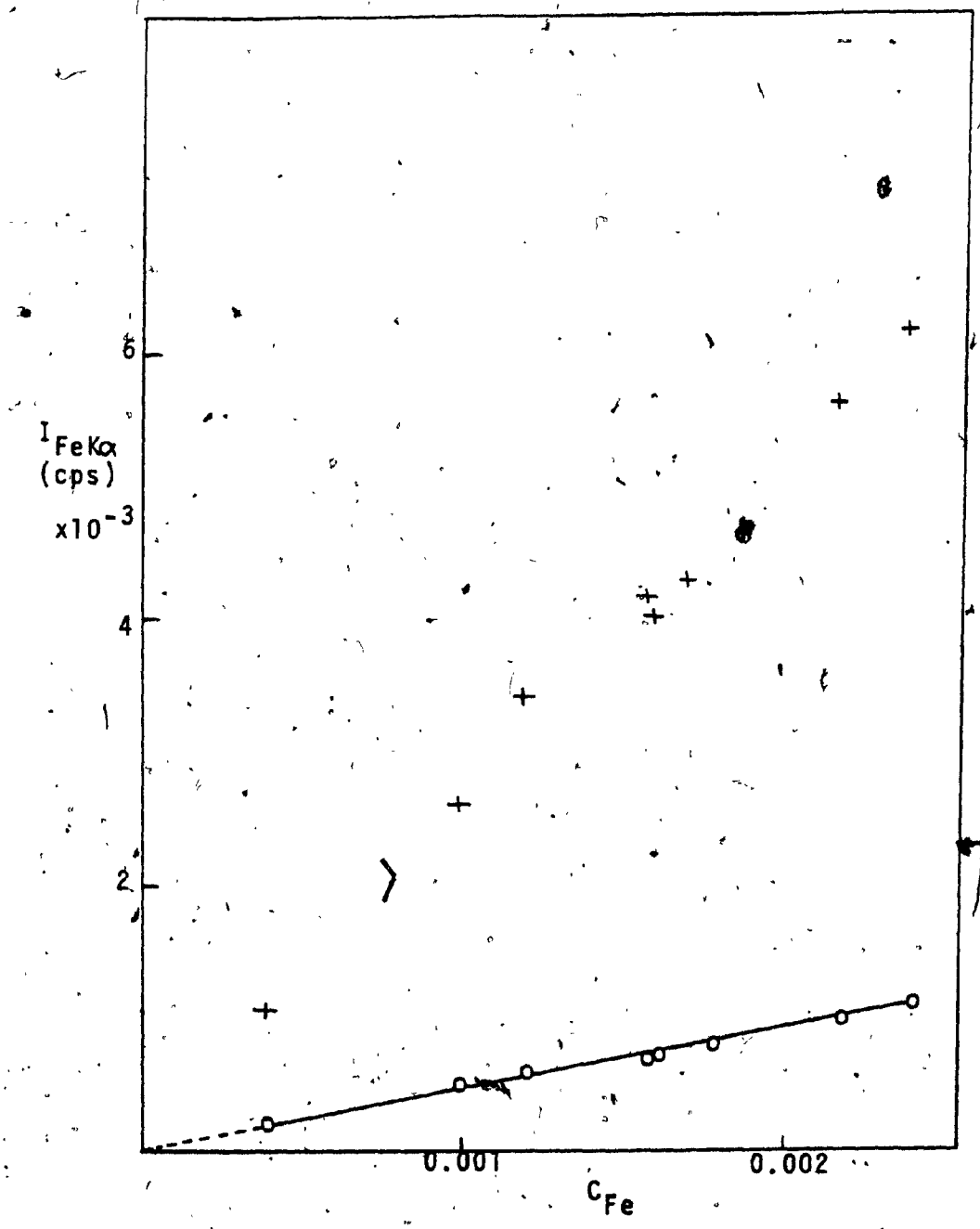

TABLE A.3.1.4 - NICKEL ANALYSIS - SERIES S

SAMPLE	C_{Ni} (std.)	$I_{NiK\alpha}$ (cps)	$I_{NiK\alpha}$ (corrected) (cps)	C_{Ni} (calculated) A	C_{Ni} (calculated) B	Relative Error (%) C	Relative Error (%) D
* S-1	0.00116	5999	861	0.00108	0.00116	-6.9	---
S-2	0.00172	10107	1328	0.00170	0.00195	-1.2	13.4
S-3	0.00040	2246	318	0.00041	0.00043	2.5	7.5
S-4	0.00080	4413	636	0.00083	0.00085	3.7	6.3
S-5	0.00038	2173	314	0.00040	0.00042	5.3	10.5
S-6	0.00200	10484	1542	0.00196	0.00203	2.0	1.5
S-7	0.00105	5614	820	0.00105	0.00109	0.0	3.8
S-8	0.00122	6523	949	0.00121	0.00126	-0.8	3.3

FIGURE A.3.1.4 INTENSITY $I_{NiK\alpha}$ VS CONCENTRATION C_{Ni}

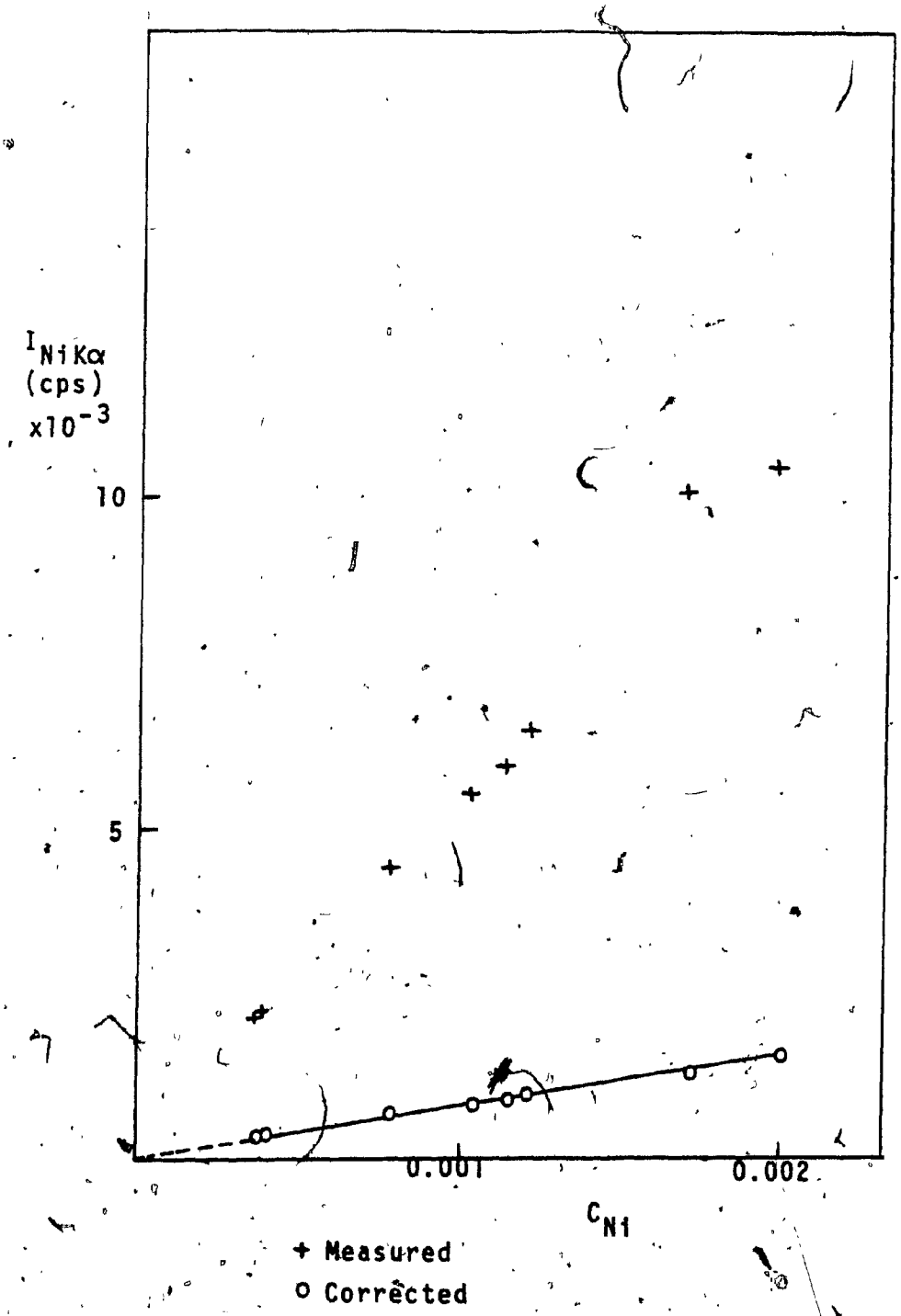

TABLE A.3.1.5 COPPER ANALYSIS - SERIES S

SAMPLE	C_{Cu}(std.)	$I_{CuK\alpha}$ (cps)	$I_{CuK\alpha}$(corrected) (cps)	C_{Cu}(calculated) A	B	Relative Error(%) C	D
* S-1	0.00110	4678	664	0.00103	0.00110	-6.4	---
S-2	0.00073	3497	454	0.00072	0.00082	-1.4	12.3
S-3	0.00093	4180	586	0.00094	0.00098	1.1	5.3
S-4	0.00039	1800	256	0.00041	0.00042	5.1	7.7
S-5	0.00203	7027	1004	0.00157	0.00165	-22.6	-18.7
S-6	0.00157	6616	963	0.00151	0.00156	3.8	-0.6
S-7	0.00205	8613	1249	0.00198	0.00203	-3.4	-1.0
S-8	0.00039	1868	267	0.00042	0.00044	7.7	12.8

FIGURE A.3.1.5 INTERSITY I_{CuK} VS CONCENTRATION C_{Cu}

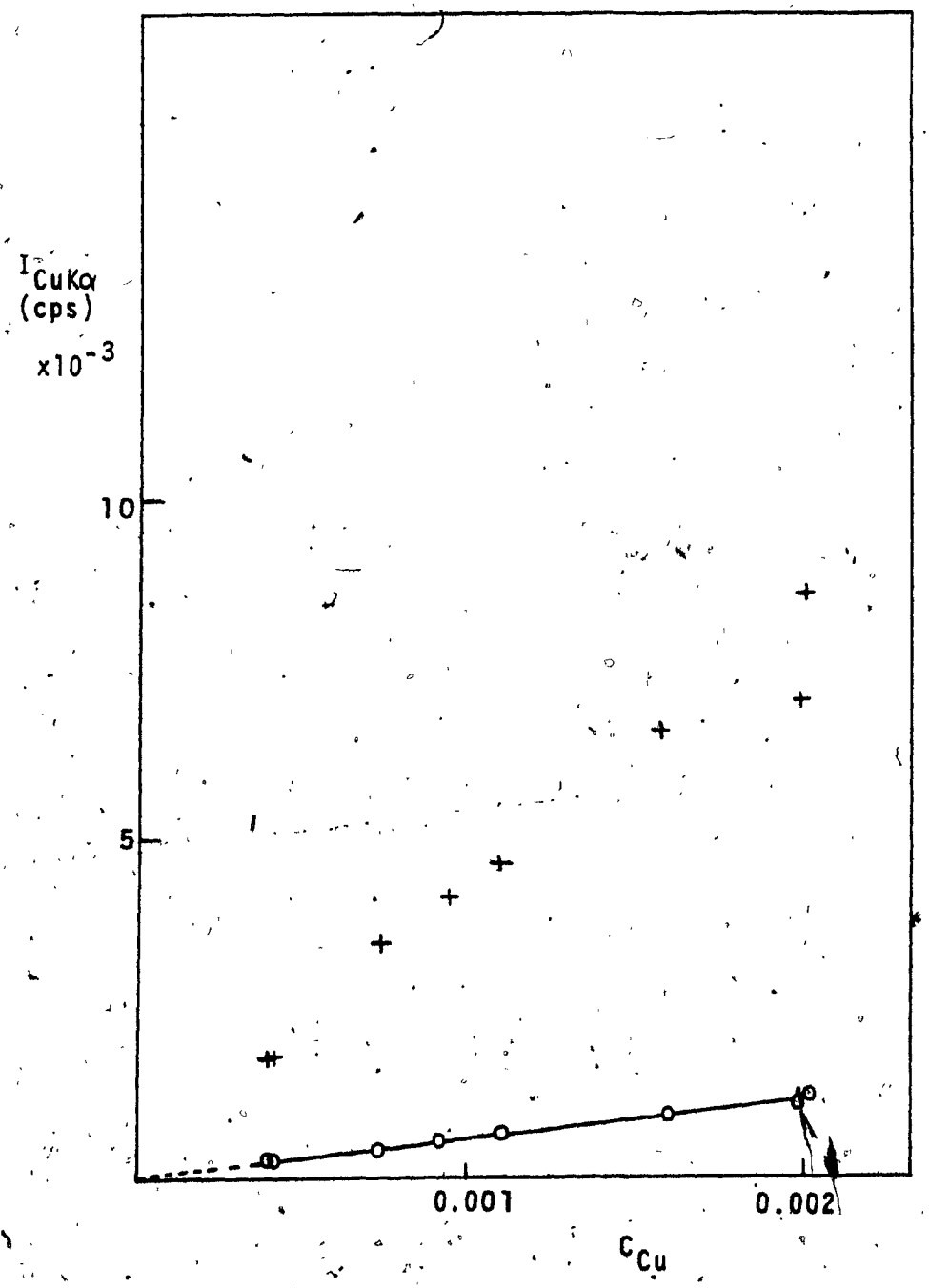

TABLE A.3.1.6 ZINE ANALYSIS - SERIES S

SAMPLE	C_{Zn}(std.)	$I_{ZnK\alpha}$ (cps)	$I_{ZnK\alpha}$(corrected) (cps)	C_{Zn}(calculated) A	B	Relative Error(%) C	D
* S-1	0.00117	6403	764	0.00112	0.00117	-4.3	---
S-2	0.00081	5127	558	0.00083	0.00094	2.5	16.0
S-3	0.00080	4481	520	0.00079	0.00082	-1.3	2.5
S-4	0.00039	2124	251	0.00038	0.00039	-2.6	0.0
S-5	0.00048	2747	326	0.00048	0.00050	0.0	4.2
S-6	0.00120	6819	810	0.00120	0.00119	0.0	-0.8
S-7	0.00158	8677	1056	0.00158	0.00159	0.0	0.6
S-8	0.00094	5149	624	0.00093	0.00094	-1.1	0.0

FIGURE A.3.1.6 INTENSITY $I_{ZnK\alpha}$ VS CONCENTRATION C_{Zn}

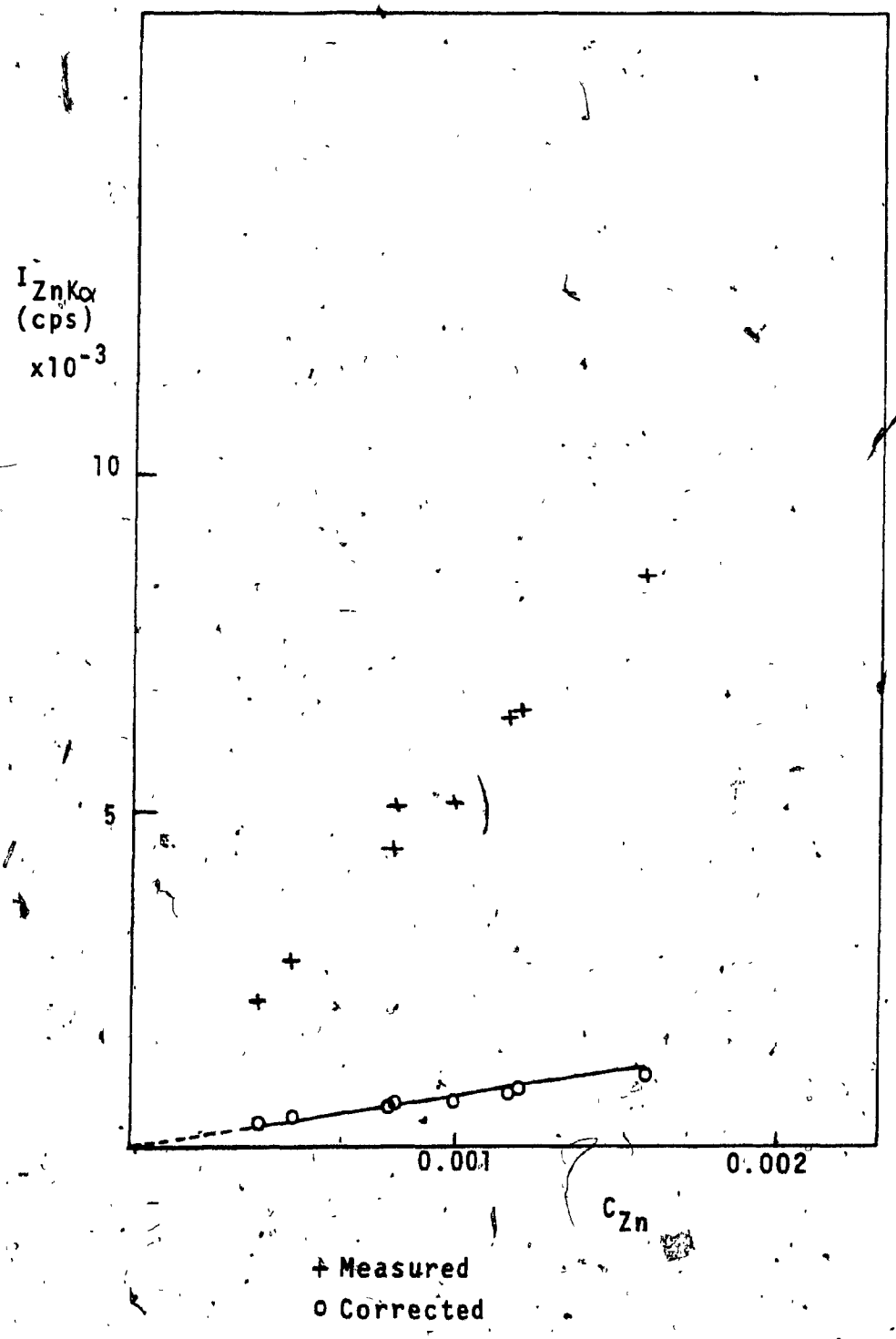

TABLE A.3.1.7 TIN ANALYSIS - SERIES S

SAMPLE	C_{Sn}(std.)	$I_{SnK\alpha}$ (cps)	$I_{SnK\alpha}$(corrected) (cps)	C_{Sn}(calculated) A	B	Relative Error(%) C	D
* S-1	0.00112	3266	188	0.00116	0.00112	3.6	---
S-2	0.00120	4176	210	0.00131	0.00143	9.2	19.2
S-3	0.00040	1286	66	0.00041	0.00044	2.5	10.0
S-4	0.00087	2632	135	0.00085	0.00090	-2.3	3.4
S-5	0.0[illegible]47	1345	70	0.00043	0.00046	-8.5	-2.1
S-6	0.00113	3202	173	0.00107	0.00109	-5.3	-3.5
S-7	0.00120	3475	188	0.00117	0.00119	-2.5	-0.8
S-8	0.00202	6085	321	0.00201	0.00209	-0.5	3.5

FIGURE A.3.1.7 INTENSITY $I_{SnK\alpha}$ VS CONCENTRATION C_{Sn}

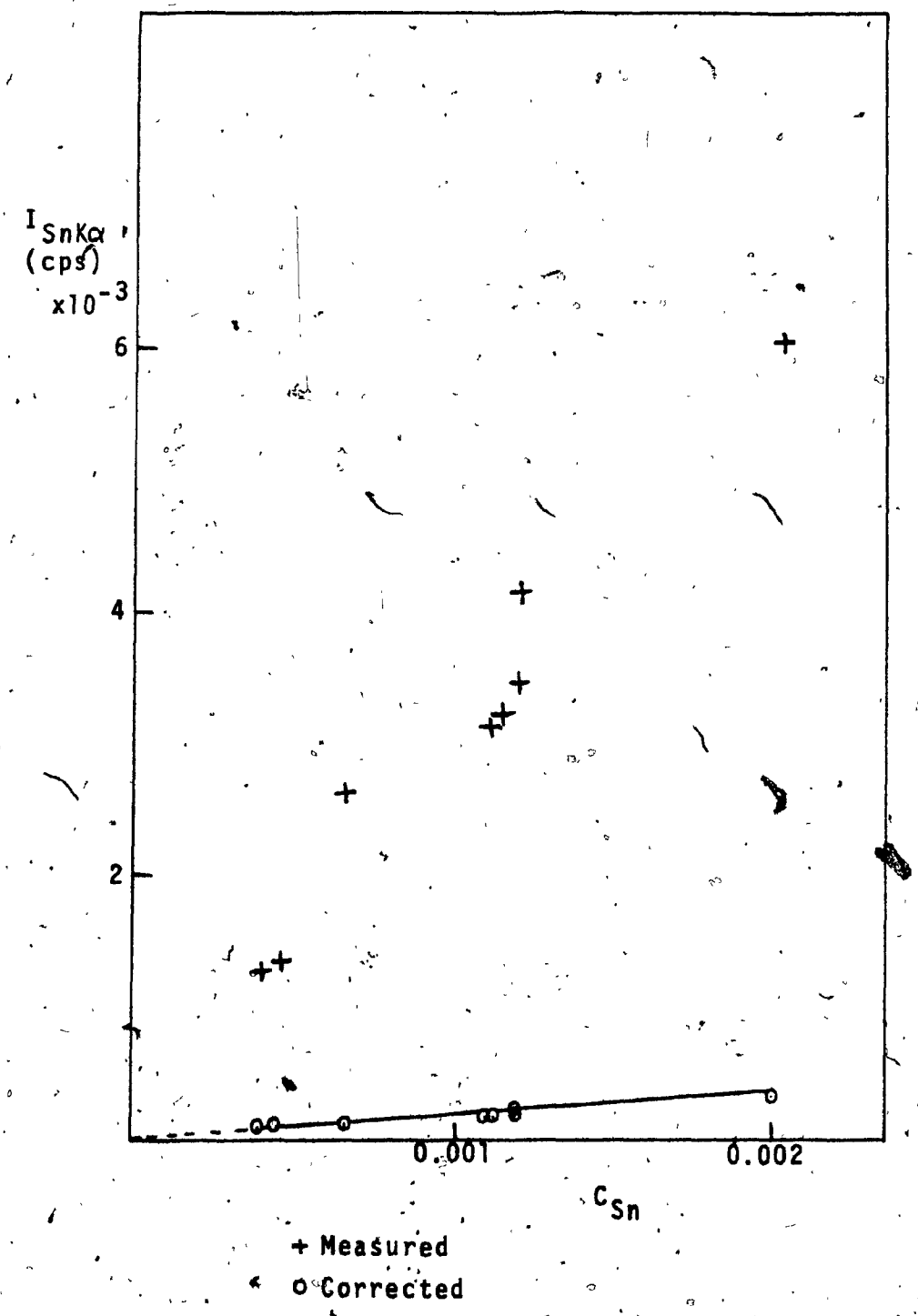

TABLE A.3.2.2 SILICON ANALYSIS - ALUMINUM ALLOYS

SAMPLE	C_{Si}(std.)	$I_{SiK\alpha}$ (cps)	$I_{SiK\alpha}$(corrected) (cps)	C_{Si}(calculated) A	B	Relative Error(%) C	D
117-AD	0.04700	977	5764	0.04762	0.04961	1.3	5.6
125-AI	0.05550	1150	6770	0.05593	0.05840	0.7	5.2
225-AG	0.00810	172	1049	0.00867	0.00873	7.0	7.8
226-AC	0.00170	30	184	0.00152	0.00152	10.6	-10.6
125-AL	0.04950	1020	6043	0.04992	0.05180	8.5	4.6
125-AN	0.05120	1044	6166	0.05097	0.05302	-0.5	3.6
B143-AA	0.09240	2001	11329	0.09353	0.10161	1.2	10.0
143-AF	0.08500	2766	15800	0.12572	0.14046	47.9	65.2
A143-AT	0.10000	2103	11810	0.09780	0.10679	-2.2	6.8
236-AC	0.02050	409	2448	0.02024	0.02077	-1.3	1.3
6165-AA-D	0.18000	4200	21923	0.18103	0.21328	0.6	18.5
24S-AT	0.00170	33	201	0.00166	0.00168	-2.4	-1.2
218-AQ	0.00200	40	243	0.00201	0.00203	0.5	1.5
162-AZ	0.12100	2702	14883	0.12290	0.13721	1.6	13.4
38S-AI-D	0.11430	2540	14136	0.11657	0.12898	2.0	12.8
135-AM	0.07060	1482	8636	0.07133	0.07526	1.0	6.6
135-AN	0.07310	1536	8921	0.07370	0.07800	0.8	6.7
A35-AJ	0.00110	20	122	0.00101	0.00102	-8.1	-7.3
A56S-AB	0.00160	32	195	0.00162	0.00163	1.3	1.9
M57S-AC	0.00280	57	350	0.00289	0.00289	3.2	3.2
A135-AM	0.00120	26	158	0.00131	0.00132	9.2	10.0

TABLE A.3.2.2 cont'd

SAMPLE	C_{Si}(std.)	$I_{SiK\alpha}$ (cps)	$I_{SiK\alpha}$(corrected) (cps)	C_{Si}(calculated) A	C_{Si}(calculated) B	Relative Error(%) C	Relative Error(%) D
340-AA-D	0.00250	50	303	0.00252	0.00254	0.8	1.6
350-AQ	0.00120	24	146	0.00121	0.00122	0.8	1.7
350-AS	0.00150	30	182	0.00151	0.00152	0.7	1.3
123-AJ	0.05000	1041	6179	0.05102	0.05286	2.0	14.3
161-AB	0.09680	2110	11965	0.09871	0.10715	2.0	10.7
161-AE	0.11700	2601	14476	0.11937	0.13208	2.0	12.9
B160-AA	0.12270	2729	15137	0.12485	0.13858	1.8	12.9
160-DB	0.12230	2714	15085	0.12442	0.13782	1.7	12.7
F40E-AG	0.00150	32	197	0.00163	0.00163	8.7	8.7
6235-AA	0.00100	20	124	0.00102	0.00102	2.0	2.0
6392-AA	0.00150	30	185	0.00153	0.00152	2.0	1.3
79S-AD-D	0.00150	30	184	0.00152	0.00152	1.3	1.3
79S-AE	0.00180	37	226	0.00187	0.00188	3.9	4.4
6448-AA	0.00070	15	92	0.00076	0.00076	8.6	8.6
LM24-AA	0.07800	1693	9690	0.07994	0.08597	2.5	10.2
6195-AA-D	0.10620	2350	13107	0.10813	0.11934	1.8	12.4
6195-AC	0.09500	2081	11715	0.09667	0.10568	1.8	11.2
6252-AD	0.05500	1159	6772	0.05621	0.05886	2.2	7.0
6363-AA	0.00360	74	444	0.00368	0.00376	2.2	4.4
B51S-AF-D	0.01000	200	1225	0.01012	0.01016	1.2	1.6
* 6449-AA-D	0.00650	128	787	0.00650	0.00650	0.0	---

FIGURE A.3.2.2 (A) I_{SiK} VS C_{Si} - ALUMINUM ALLOYS

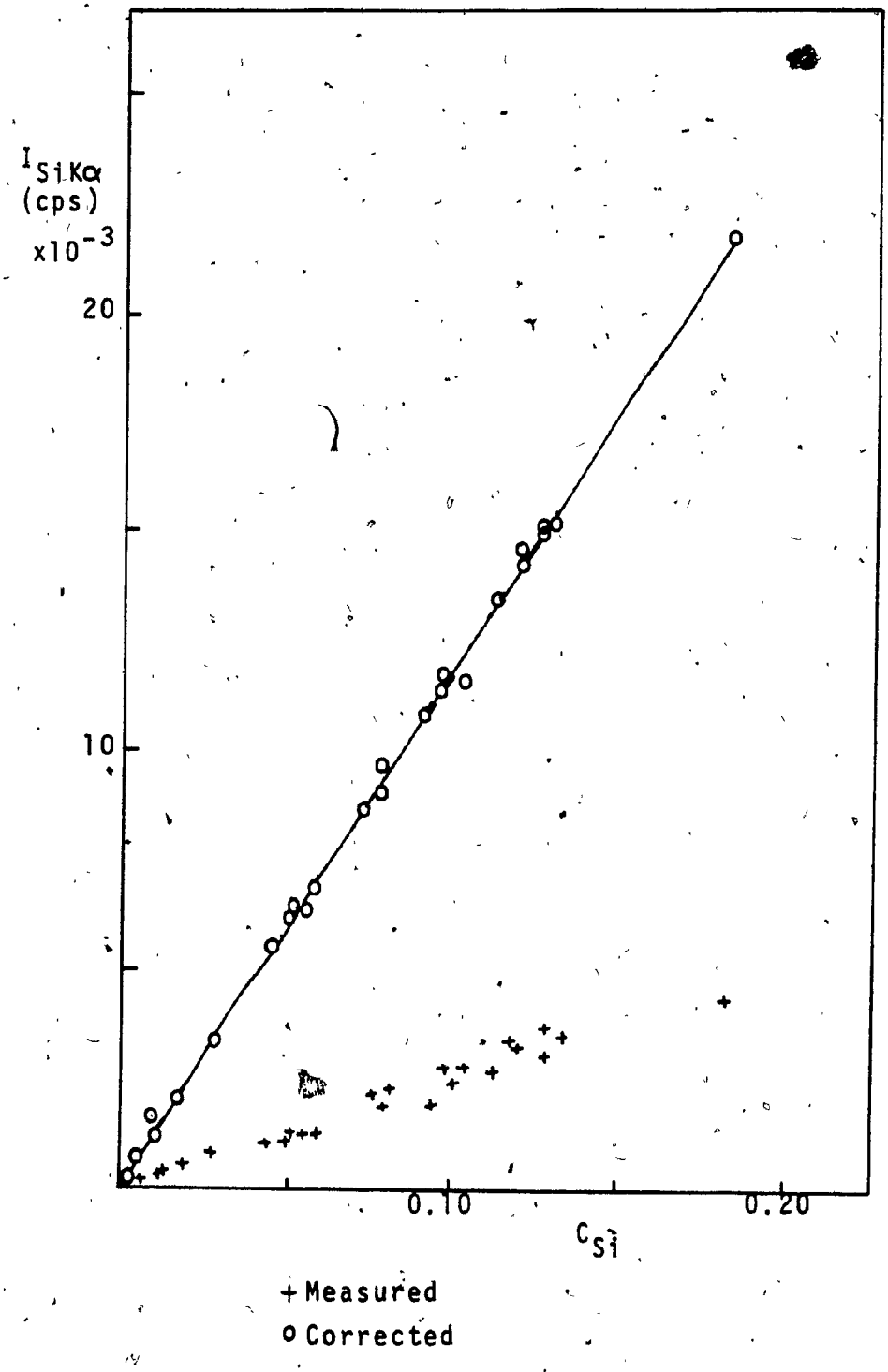

FIGURE A.3.2.2 (B) DISTRIBUTION OF RELATIVE ERROR OF C_{Si}

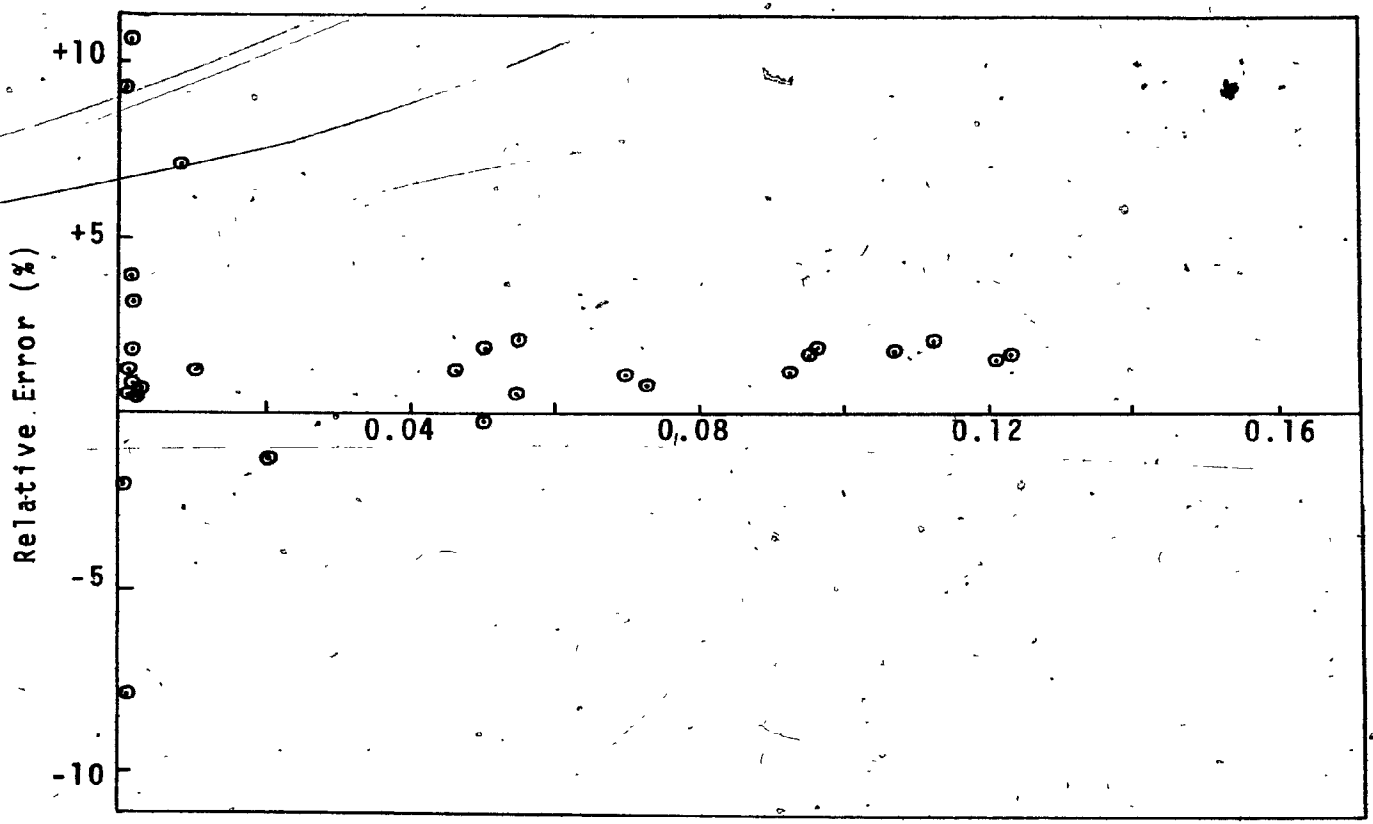

TABLE A.3.2.3 TITANIUM ANALYSIS - ALUMINUM ALLOYS

SAMPLE	C_{Ti}(std.)	$I_{TiK\alpha}$ (cps)	$I_{TiK\alpha}$(corrected) (cps)	C_{Ti}(calculated) A	B	Relative Error(%) C	D
117-AD	0.00036	593	470	0.00036	0.00037	0.0	2.8
125-AI	0.00120	1984	1585	0.00121	0.00123	0.8	2.5
225-AG	0.00150	2531	1989	0.00152	0.00157	1.3	4.7
226-AC	0.00150	2491	1960	0.00149	0.00154	-0.7	2.7
125-AL	0.00150	2473	1975	0.00151	0.00153	0.7	2.0
125-AN	0.00170	2802	2239	0.00171	0.00174	0.6	2.4
B143-AA	0.00110	1793	1438	0.00109	0.00111	-0.9	0.9
143-AF	0.00041	681	546	0.00042	0.00042	2.4	2.4
A143-AT	0.00042	689	551	0.00042	0.00043	0.0	2.4
236-AC	0.00150	2502	1955	0.00149	0.00155	-0.7	3.3
6165-AA-D	0.00025	407	332	0.00025	0.00025	0.0	0.0
24S-AT	0.00016	273	213	0.00016	0.00017	0.0	6.3
218-AQ	0.00150	1896	1477	0.00113	0.00118	-24.6	-21.3
162-AZ	0.00034	561	451	0.00035	0.00035	2.9	2.9
38S-AI-D	0.00060	987	796	0.00061	0.00061	1.7	1.7
135-AM	0.00190	3102	2496	0.00190	0.00192	0.0	1.1
135-AN	0.00180	2940	2365	0.00180	0.00182	0.0	1.1
A35-AJ	0.00160	2701	2127	0.00161	0.00168	0.6	5.0
A56S-AB	0.00053	888	694	0.00053	0.00055	0.0	3.8
M57S-AC	0.00032	533	419	0.00032	0.00033	0.0	3.1
A135-AM	0.00160	2672	2089	0.00159	0.00166	-0.6	3.8

TABLE A.3.2.3 cont'd

SAMPLE	C_{Ti}(std.)	$I_{TiK\alpha}$ (cps)	$I_{TiK\alpha}$(corrected) (cps)	C_{Ti}(calculated) A	B	Relative Error(%) C	D
340-AA-D	0.00090	1523	1182	0.00091	0.00094	1.1	4.4
350-AQ	0.00029	483	375	0.00029	0.00030	0.0	3.4
350-AS	0.00110	1850	1436	0.00110	0.00115	0.0	4.5
123-AJ	0.00110	1801	1442	0.00110	0.00112	0.0	1.8
161-AB	0.00045	727	587	0.00045	0.00045	0.0	0.0
161-AE	0.00042	681	552	0.00042	0.00042	0.0	0.0
B160-AA	0.00041	660	536	0.00041	0.00041	0.0	0.0
160-DB	0.00042	672	547	0.00042	0.00042	0.0	0.0
F40E-AG	0.00200	3293	2592	0.00200	0.00204	0.0	2.0
6235-AA	0.00040	660	521	0.00040	0.00041	0.0	2.5
6392-AA	0.00080	1326	1045	0.00079	0.00082	-1.3	2.5
79S-AD-D	0.00070	1170	916	0.00069	0.00073	-1.4	4.3
79S-AE	0.00060	1000	783	0.00059	0.00062	-1.7	3.3
6448-AA	0.00040	706	552	0.00042	0.00044	5.0	10.0
LM24-AA	0.00170	2801	2243	0.00171	0.00174	0.6	2.4
6195-AA-D	0.00090	1449	1163	0.00088	0.00090	-2.2	0.0
6195-AC	0.00045	729	583	0.00044	0.00045	-2.2	0.0
6252-AD	0.00140	2300	1827	0.00140	0.00143	0.0	2.1
6363-AA	0.00040	525	521	0.00039	0.00033	-2.5	-17.5
B51S-AF-D	0.00045	743	588	0.00045	0.00046	0.0	2.2
* 6449-AA-D	0.00080	1290	1049	0.00080	0.00080	0.0	---

FIGURE A.3.2.3 (A) I_{TiK} VS C_{Ti} - ALUMINUM ALLOYS

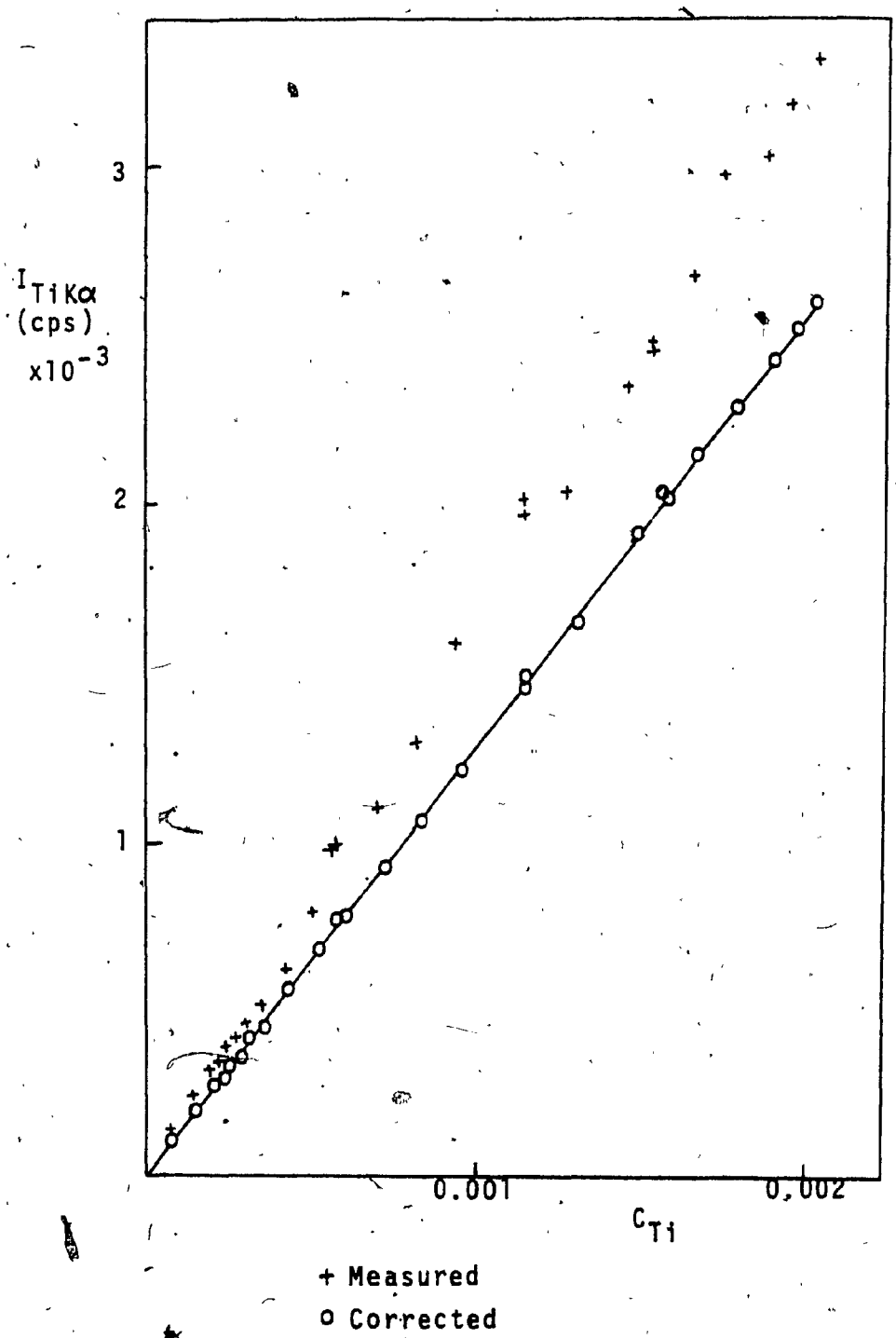

FIGURE A.3.2.3 (B) DISTRIBUTION OF RELATIVE ERROR OF C_{Ti}

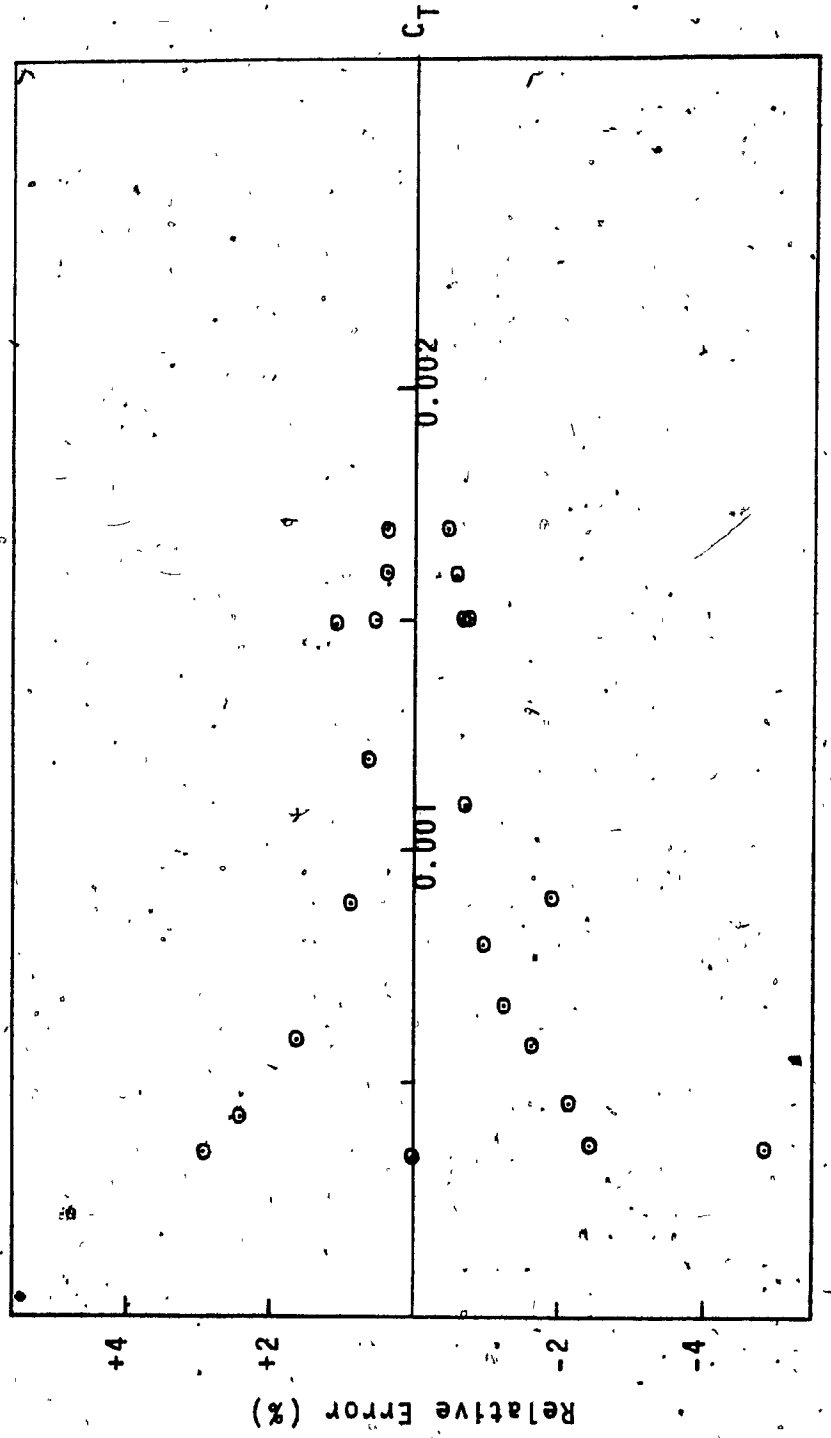

TABLE A.3.2.4 CHROMIUM ANALYSIS - ALUMINUM ALLOYS

SAMPLE	C_{Cr}(std.)	$I_{CrK\alpha}$ (cps)	$I_{CrK\alpha}$ (corrected) (cps)	C_{Cr}(calculated) A	C_{Cr}(calculated) B	Relative Error(%) C	Relative Error(%) D
147-AD	0.00030	130	101	0.00028	0.00029	-6.7	-3.3
125-AI	0.00034	160	125	0.00035	0.00036	2.9	5.9
225-AG	0.00015	68	52	0.00015	0.00015	0.0	0.0
226-AC	0.00035	168	130	0.00037	0.00038	5.7	8.6
125-AL	0.00032	144	113	0.00032	0.00032	0.0	0.0
125-AN	0.00042	190	148	0.00042	0.00043	0.0	2.4
B143-AA	0.00050	231	180	0.00051	0.00052	2.0	4.0
143-AF	0.00046	209	162	0.00046	0.00047	0.0	2.2
A143-AT	0.00025	117	91	0.00025	0.00026	0.0	4.0
236-AC	0.00023	100	77	0.00022	0.00023	-4.3	0.0
6165-AA-D	0.00020	96	75	0.00021	0.00022	5.0	10.0
24S-AT	0.00028	131	101	0.00028	0.00029	0.0	3.6
218-AQ	0.00025	112	86	0.00024	0.00025	-4.0	0.0
162-AZ	0.00027	123	96	0.00027	0.00028	0.0	3.7
38S-AI-D	0.00034	155	121	0.00034	0.00035	0.0	2.9
135-AM	0.00024	107	84	0.00024	0.00024	0.0	0.0
135-AN	0.00032	143	112	0.00032	0.00032	0.0	0.0
A35-AJ	0.00010	45	35	0.00009	0.00010	-10.0	0.0
A56S-AB	0.00038	182	141	0.00040	0.00041	5.3	7.9
M57S-AC	0.00026	119	93	0.00026	0.00027	0.0	3.8
A135-AM	0.00047	214	166	0.00047	0.00048	0.0	2.1

TABLE A.3.2.4 cont'd

SAMPLE	C_{Cr}(std.)	$I_{CrK\alpha}$ (cps)	$I_{CrK\alpha}$(corrected) (cps)	C_{Cr}(calculated) A	B	Relative Error(%) C	D
340-AA-D	0.00027	131	101	0.00029	0.00029	7.4	7.4
350-AQ	0.00022	100	77	0.00022	0.00023	0.0	4.5
350-AS	0.00035	163	126	0.00035	0.00037	0.0	5.7
123-AJ	0.00025	108	85	0.00024	0.00024	-4.0	-4.0
161-AB	0.00049	222	173	0.00049	0.00050	0.0	2.0
161-AE	0.00033	147	115	0.00032	0.00033	-3.0	0.0
B160-AA	0.00030	132	103	0.00029	0.00030	-3.3	0.0
160-DB	0.00052	234	184	0.00052	0.00053	0.0	1.9
F40E-AG	0.00420	1908	1483	0.00418	0.00429	-0.5	2.1
6235-AA	0.00030	137	106	0.00030	0.00031	0.0	3.3
6392-AA	0.00100	456	354	0.00099	0.00103	-1.0	3.0
79S-AD-D	0.00160	733	565	0.00159	0.00165	-0.6	3.1
79S-AE	0.00200	909	702	0.00197	0.00205	-1.5	2.5
6448-AA	0.00210	981	752	0.00212	0.00221	1.0	0.5
LM24-AA	0.00020	90	70	0.00019	0.00020	-5.0	0.0
6195-AA-D	0.00040	183	142	0.00040	0.00041	0.0	2.5
6195-AC	0.00047	214	166	0.00047	0.00048	0.0	2.1
6252-AD	0.00048	223	173	0.00049	0.00050	2.1	4.2
6363-AA	0.00040	148	140	0.00039	0.00033	-2.5	-17.5
B51S-AF-D	0.00042	190	149	0.00042	0.00043	0.0	2.4
* 6449-AA-D	0.00090	400	320	0.00090	0.00090	0.0	---

FIGURE A.3.2.4 (A) I_{CrK} VS C_{Cr} - ALUMINUM ALLOYS

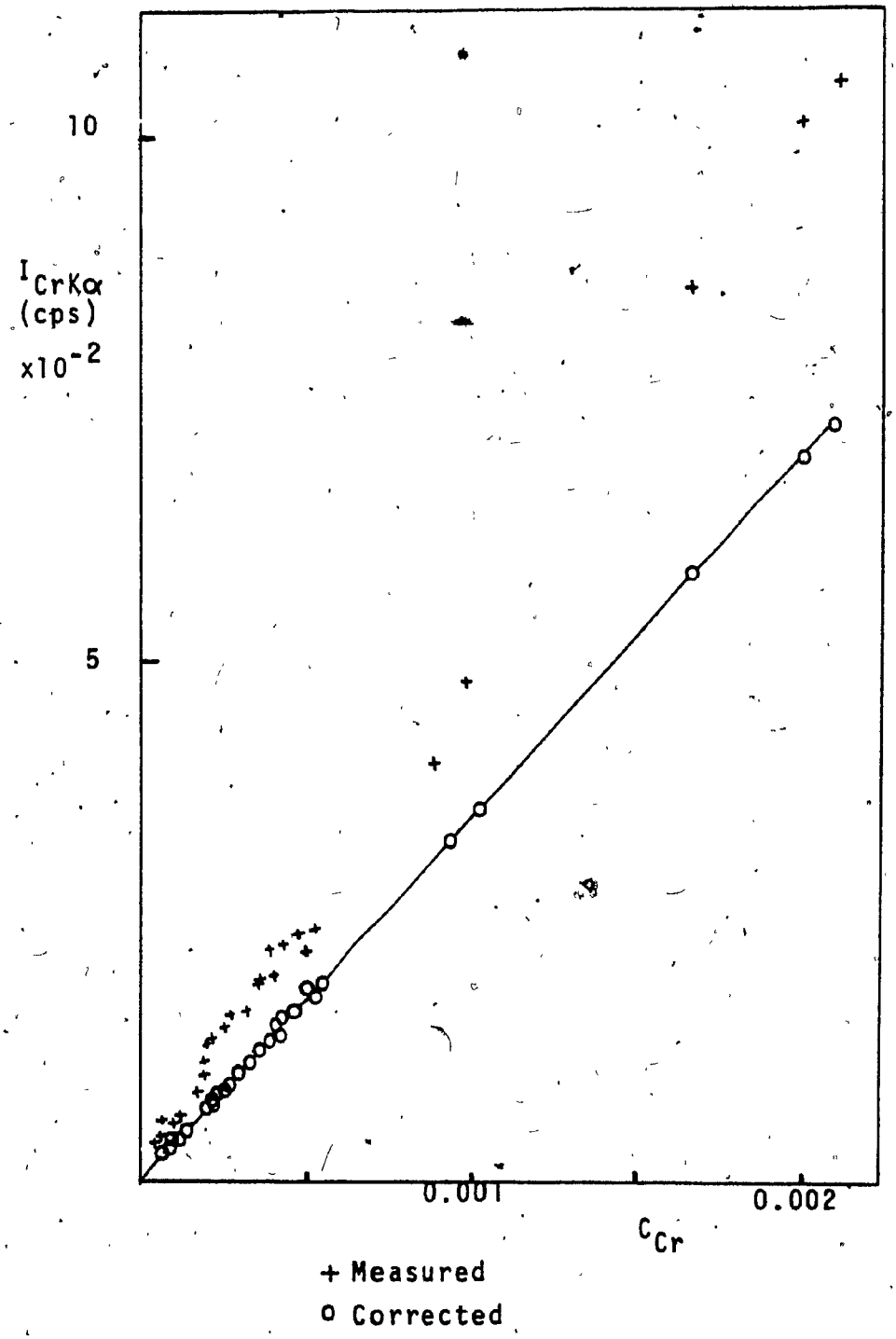

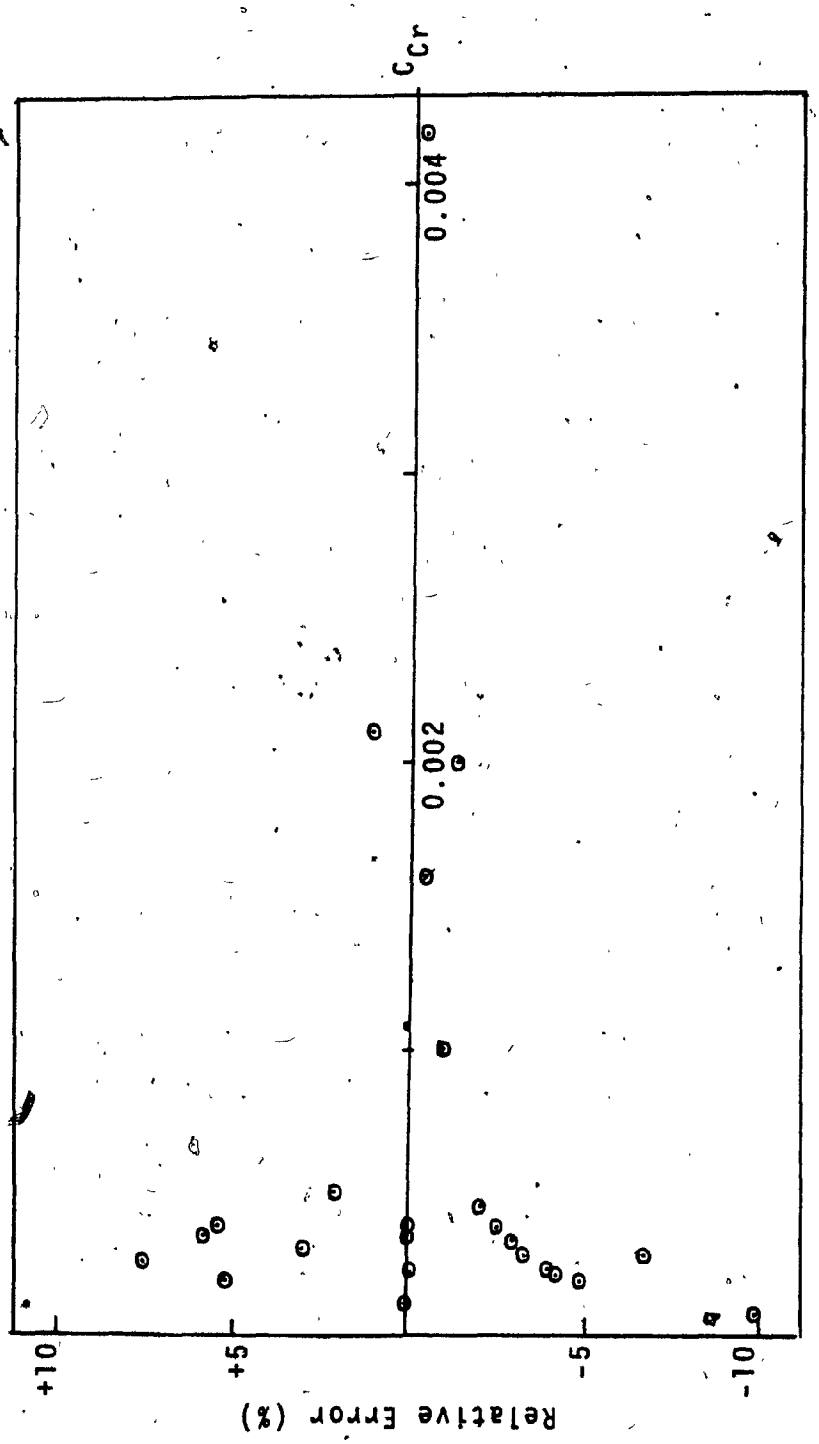

FIGURE A.3.2.4 (B) DISTRIBUTION OF RELATIVE ERROR - C_{Cr}

TABLE A.3.2.5 MANGANESE ANALYSIS - ALUMINUM ALLOYS

SAMPLE	C_{Mn}(std)	$I_{MnK\alpha}$ (cps)	$I_{MnK\alpha}$(corrected) (cps)	C_{Mn}(calculated) A	B	Relative Error(%) C	D
117-AD	0.00660	3837	2561	0.00664	0.00687	0.6	4.1
125-AI	0.00023	130	87	0.00023	0.00023	0.0	0.0
225-AG	0.00040	229	151	0.00039	0.00041	-2.5	2.5
226-AC	0.00090	532	352	0.00091	0.00095	1.1	5.6
125-AL	0.00040	231	155	0.00040	0.00041	0.0	2.5
125-AN	0.00042	242	163	0.00042	0.00043	0.0	2.4
B143-AA	0.00270	1567	1047	0.00271	0.00280	0.4	3.7
143-AF	0.00110	632	421	0.00109	0.00113	-0.9	2.7
A143-AT	0.00250	1428	949	0.00246	0.00256	-1.6	2.4
236-AC	0.00110	640	420	0.00109	0.00115	-0.9	4.5
6165-AA-D	0.00040	221	148	0.00038	0.00040	-5.0	0.0
24S-AT	0.00720	4238	2793	0.00723	0.00759	0.4	5.4
218-AQ	0.00035	200	131	0.00034	0.00036	-2.8	2.8
162-AZ	0.00037	207	138	0.00036	0.00037	-2.7	0.0
38S-AI-D	0.00055	328	220	0.00057	0.00059	3.6	7.3
135-AM	0.00030	171	116	0.00030	0.00031	0.0	3.3
135-AN	0.00042	237	160	0.00042	0.00042	0.0	0.0
A35-AJ	0.00160	923	620	0.00159	0.00165	-0.6	3.1
A56S-AB	0.00630	3701	2477	0.00642	0.00662	1.9	5.1
M57S-AC	0.00350	2091	1405	0.00364	0.00374	4.0	6.8
A135-AM	0.00170	982	655	0.00170	0.00176	0.0	2.8

TABLE A.3.2.5 cont'd

SAMPLE	C_{Mn}(std.)	$I_{MnK\alpha}$ (cps)	$I_{MnK\alpha}$(corrected) (cps)	C_{Mn}(calculated) A	B	Relative Error(%) C	D
340-AA-D	0.00036	208	139	0.00036	0.00037	0.0	2.8
350-AQ	0.00031	180	119	0.00031	0.00032	0.0	3.2
350-AS	0.00035	214	141	0.00037	0.00038	5.7	8.6
123-AJ	0.00023	139	94	0.00024	0.00025	4.7	8.7
161-AB	0.00070	402	273	0.00071	0.00072	1.4	2.9
161-AE	0.00510	2901	1965	0.00509	0.00519	-0.4	1.8
B160-AA	0.00043	244	165	0.00043	0.00044	0.0	2.3
160-DB	0.00039	221	149	0.00039	0.00040	0.0	2.6
F40E-AG	0.00036	206	138	0.00036	0.00037	0.0	2.8
6235-AA	0.00036	206	138	0.00035	0.00037	-2.8	2.8
6392-AA	0.00160	920	615	0.00159	0.00165	-0.6	3.1
79S-AD-D	0.00200	1170	778	0.00201	0.00209	0.5	4.5
79S-AE	0.00220	1276	849	0.00220	0.00228	0.0	3.6
6448-AA	0.00038	228	150	0.00038	0.00041	0.0	7.9
LM24-AA	0.00430	2496	1672	0.00433	0.00447	0.7	4.0
6195-AA-D	0.00280	1620	1080	0.00279	0.00290	-0.4	3.6
6195-AC	0.00420	2393	1594	0.00413	0.00428	-1.7	1.9
6252-AD	0.00630	3687	2458	0.00644	0.00660	2.2	4.8
6363-AA	0.00040	189	154	0.00039	0.00034	-2.5	-15.0
B51S-AF-D	0.00540	3086	2083	0.00539	0.00552	-0.2	2.2
* 6449-AA-D	0.00150	838	579	0.00149	0.00150	-0.7	---

FIGURE A.3.2.5 (A) I_{MnK} VS C_{Mn} - ALUMINUM ALLOYS

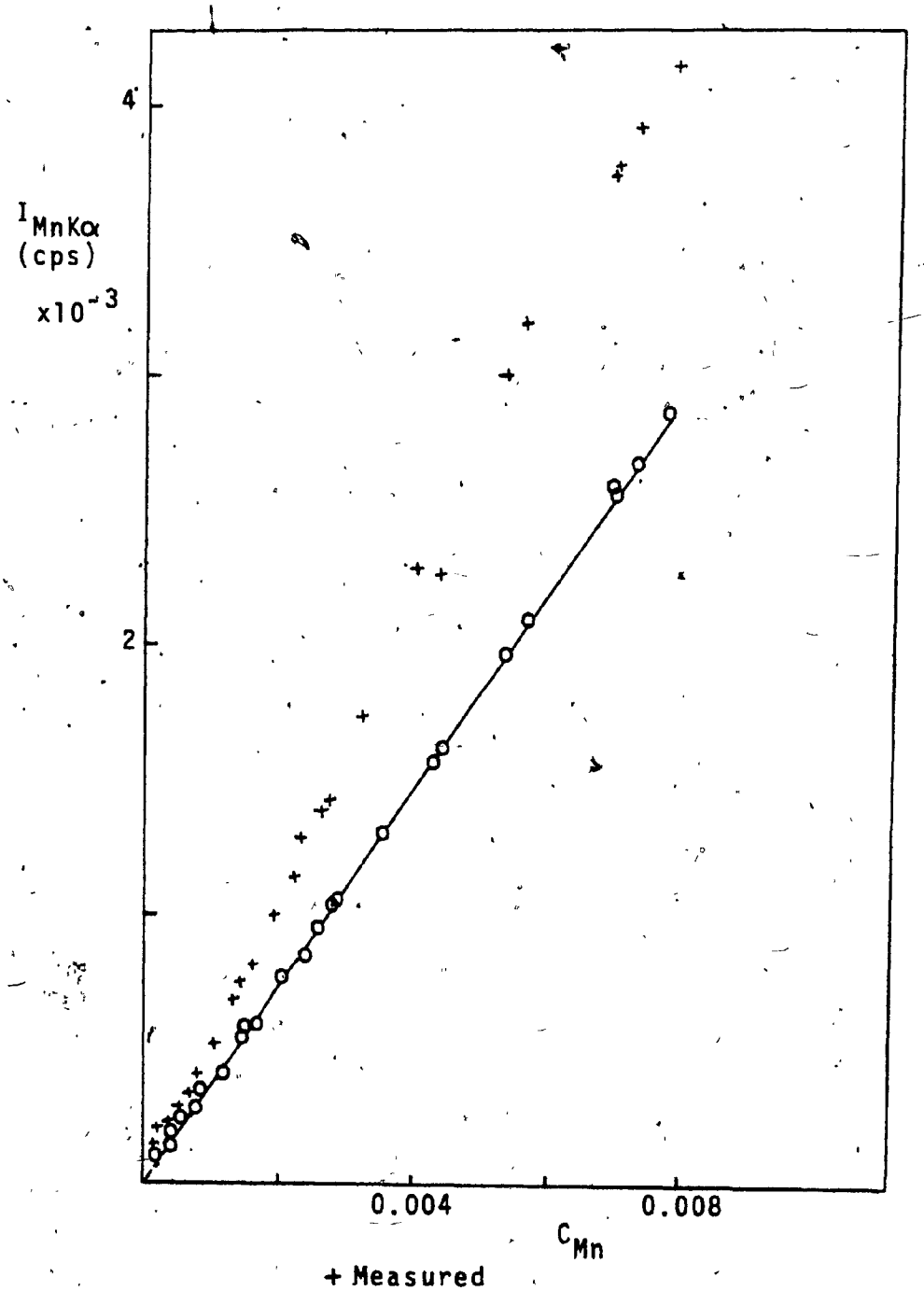

FIGURE A.3.2.5 (B) DISTRIBUTION OF RELATIVE ERROR - C_{Mn}

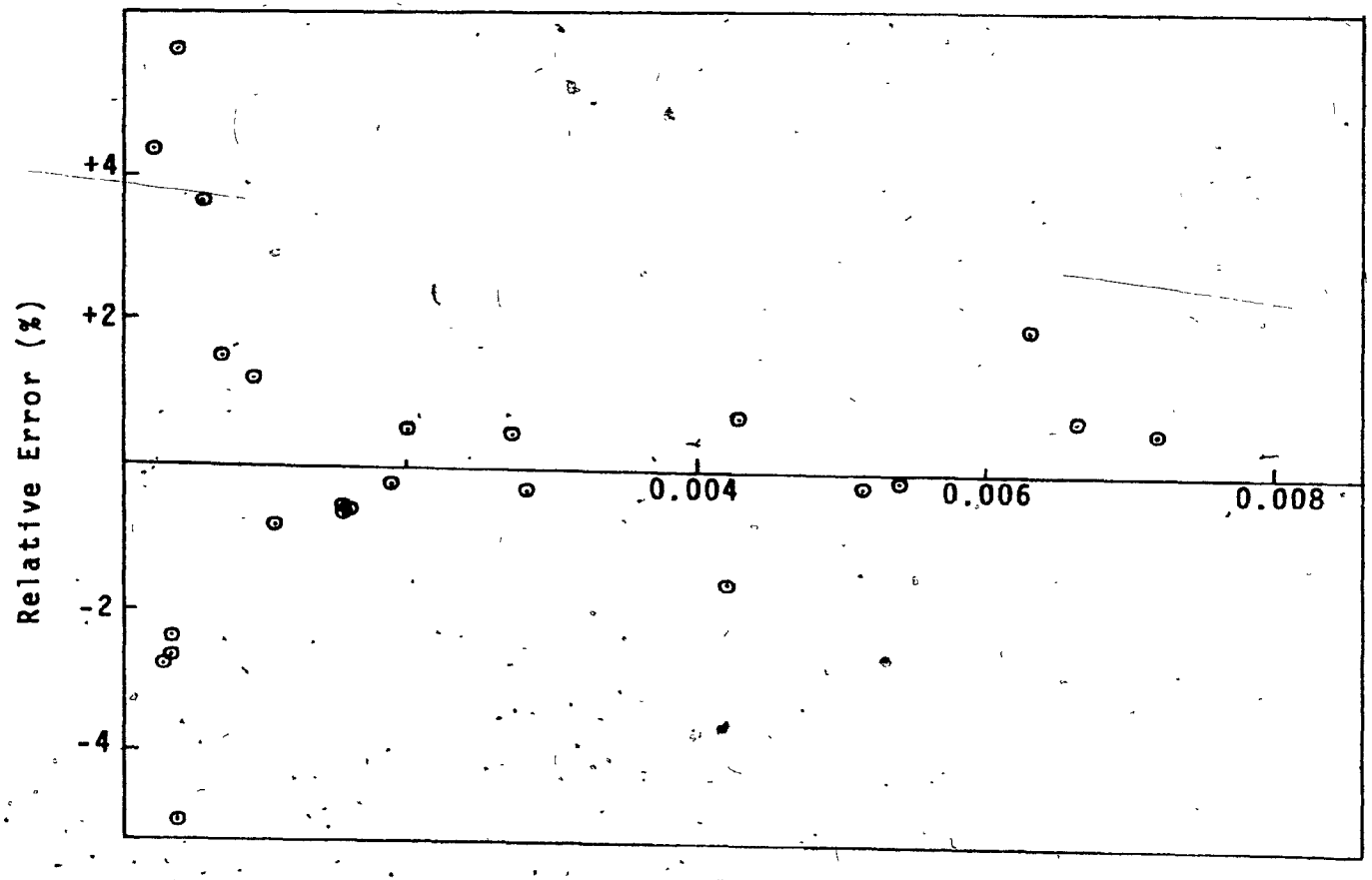

TABLE A.3.2.6 IRON ANALYSIS - ALUMINUM ALLOYS

SAMPLE	C_{Fe} (std.)	$I_{FeK\alpha}$ (cps)	$I_{FeK\alpha}$ (corrected) (cps)	C_{Fe} (calculated) A	C_{Fe} (calculated) B	Relative Error(%) C	Relative Error(%) D
117-AD	0.00370	3468	1800	0.00366	0.00375	-1.1	1.4
125-AI	0.00320	3029	1577	0.00321	0.00328	0.3	2.5
225-AG	0.00380	3678	1888	0.00383	0.00398	0.8	4.7
226-AC	0.00190	1800	924	0.00188	0.00195	-1.1	2.6
125-AL	0.00190	1822	948	0.00192	0.00197	1.1	3.7
125-AN	0.00200	1978	1031	0.00210	0.00214	5.0	7.0
B143-AA	0.00390	3818	2004	0.00408	0.00413	4.6	5.9
143-AF	0.00350	3336	1744	0.00357	0.00361	2.0	3.1
A143-AT	0.00410	3873	2025	0.00411	0.00419	0.2	2.2
236-AC	0.01210	11605	5996	0.01218	0.01256	0.7	3.8
6165-AA-D	0.00440	4083	2173	0.00441	0.00442	0.2	0.5
24S-AT	0.00280	2706	1382	0.00281	0.00293	0.4	4.6
218-AQ	0.00480	4644	2375	0.00482	0.00503	0.4	4.8
162-AZ	0.00410	3844	2019	0.00414	0.00416	1.0	1.5
38S-AI-D	0.00370	3474	1826	0.00371	0.00376	0.3	1.6
135-AM	0.00150	1413	740	0.00150	0.00153	0.0	2.0
135-AN	0.00190	1801	944	0.00192	0.00195	1.0	2.6
A35-AJ	0.00200	1903	982	0.00197	0.00206	-1.5	3.0
A56S-AB	0.00290	2803	1437	0.00292	0.00303	0.7	4.5
M57S-AC	0.00360	3458	1778	0.00361	0.00374	0.3	3.9
A135-AM	0.00160	1504	770	0.00157	0.00163	-1.9	1.9

TABLE A.3.2.6 cont'd

SAMPLE	C_{Fe}(std.)	$I_{FeK\alpha}$ (cps)	$I_{FeK\alpha}$(corrected) (cps)	C_{Fe}(calculated) A	B	Relative Error(%) C	D
340-AA-D	0.01190	12010	6199	0.01250	0.01300	5.0	9.2
350-AQ	0.00170	1659	839	0.00171	0.00180	0.6	5.9
350-AS	0.00190	1852	940	0.00191	0.00201	0.5	5.8
123-AJ	0.00280	2644	1377	0.00280	0.00286	0.0	2.1
161-AB	0.00990	9227	4889	0.00994	0.00999	0.1	0.9
161-AE	0.00400	3732	1957	0.00402	0.00404	0.5	1.0
B160-AA	0.00830	7732	4105	0.00835	0.00837	0.6	0.8
160-DB	0.00340	3171	1679	0.00341	0.00343	0.3	0.9
F40E-AG	0.00340	3207	1679	0.00341	0.00347	0.3	2.1
6235-AA	0.00160	1544	790	0.00161	0.00167	0.6	4.4
6392-AA	0.00160	1536	790	0.00160	0.00166	0.0	3.8
79S-AD-D	0.00290	2780	1427	0.00290	0.00301	0.0	3.8
79S-AE	0.00290	2783	1433	0.00291	0.00301	0.3	3.8
6448-AA	0.00310	2985	1530	0.00311	0.00323	0.3	4.2
LM24-AA	0.00590	5542	2916	0.00593	0.00600	0.5	1.7
6195-AA-D	0.00650	6102	3210	0.00653	0.00661	0.5	1.7
6195-AC	0.00700	6588	3459	0.00703	0.00713	0.4	1.9
6252-AD	0.00340	3219	1678	0.00343	0.00349	0.9	2.6
6363-AA	0.00250	1891	1241	0.00248	0.00205	0.8	-18.0
B51S-AF-D	0.00250	2364	1223	0.00248	0.00256	0.8	2.4
* 6449-AA-D	0.00250	2309	1230	0.00250	0.00250	0.0	---

FIGURE A.3.2.6 (A) I_{FeK} VS C_{Fe} - ALUMINUM ALLOYS

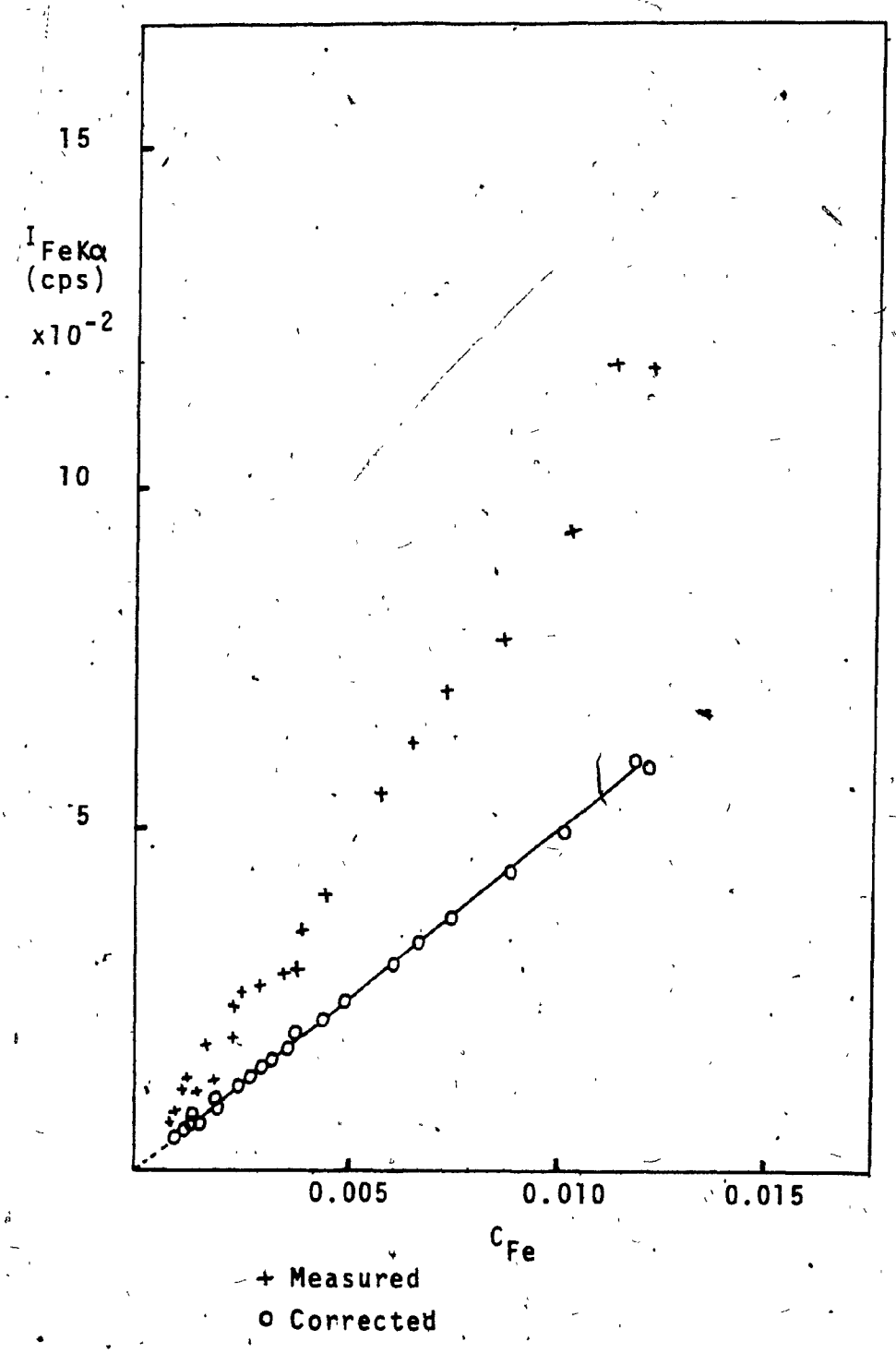

FIGURE A.3.2.6 (B) DISTRIBUTION OF RELATIVE ERROR - C_{Fe}

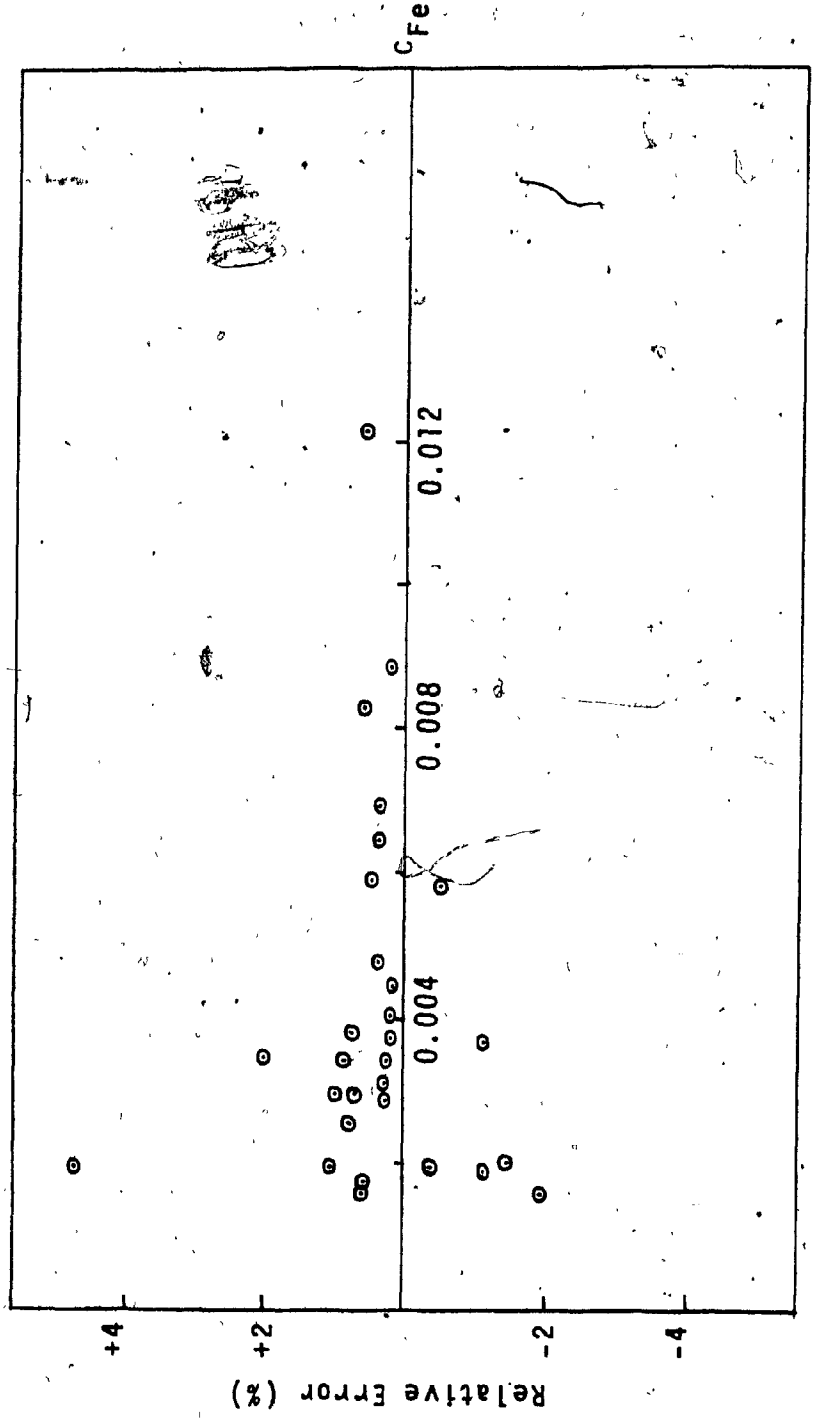

TABLE A.3.2.7 NICKEL ANALYSIS - ALUMINUM ALLOYS

SAMPLE	C_{Ni}(std.)	$I_{NiK\alpha}$ (cps)	$I_{NiK\alpha}$(corrected) (cps)	C_{Ni}(calculated) A	B	Relative Error(%) C	D
117-AD	0.00050	1019	413	0.00049	0.00049	-2.0	-2.0
125-AI	0.00029	609	237	0.00029	0.00029	0.0	0.0
225-AG	0.00110	2310	914	0.00110	0.00111	0.0	0.9
226-AC	0.00050	1053	415	0.00050	0.00050	0.0	0.0
125-AL	0.00030	624	242	0.00029	0.00030	-3.3	0.0
125-AN	0.00042	899	349	0.00042	0.00043	0.0	2.4
B143-AA	0.00050	1032	418	0.00051	0.00049	2.0	-2.0
143-AF	0.00057	1187	477	0.00058	0.00057	1.8	0.0
A143-AT	0.00820	16703	6840	0.00826	0.00799	0.7	-2.6
236-AC	0.00031	611	258	0.00031	0.00029	0.0	-6.5
6165-AA-D	0.01070	21693	8911	0.01076	0.01038	0.6	-3.0
24S-AT	0.00032	662	267	0.00032	0.00032	0.0	0.0
218-AQ	0.02050	41824	17069	0.02063	0.02002	0.6	-2.3
162-AZ	0.02500	50454	20792	0.02533	0.02415	1.3	-3.4
38S-AI-D	0.00840	17443	6997	0.00845	0.00835	0.6	-0.6
135-AM	0.00025	532	205	0.00025	0.00025	0.0	0.0
135-AN	0.00026	547	211	0.00026	0.00026	0.0	0.0
A35-AJ	0.00028	610	232	0.00028	0.00029	0.0	3.6
A56S-AB	0.00028	601	232	0.00028	0.00029	0.0	3.6
M57S-AC	0.00029	623	240	0.00029	0.00030	0.0	3.4
A135-AM	0.00048	1060	400	0.00048	0.00051	0.0	6.3

TABLE A.3.2.7 cont'd

SAMPLE	C_{Ni}(std.)	$I_{NiK\alpha}$ (cps)	$I_{NiK\alpha}$(corrected) (cps)	C_{Ni}(calculated) A	C_{Ni}(calculated) B	Relative Error(%) C	Relative Error(%) D
340-AA-D	0.00035	737	290	0.00033	0.00035	-5.7	0.0
350-AQ	0.00035	784	291	0.00035	0.00038	0.0	8.6
350-AS	0.00036	800	298	0.00036	0.00038	0.0	5.6
123-AJ	0.00020	441	170	0.00021	0.00021	5.0	5.0
161-AB	0.00044	907	369	0.00044	0.00043	0.0	-2.3
161-AE	0.00048	990	399	0.00048	0.00047	0.0	-2.1
B160-AA	0.00037	763	309	0.00037	0.00037	0.0	0.0
160-DB	0.00038	809	320	0.00039	0.00039	2.6	2.6
F40E-AG	0.00036	760	297	0.00036	0.00036	0.0	0.0
6235-AA	0.00010	207	78	0.00009	0.00010	-10.0	0.0
6392-AA	0.00040	867	331	0.00039	0.00041	-2.5	2.5
79S-AD-D	0.00035	755	292	0.00035	0.00036	0.0	2.9
79S-AE	0.00043	924	359	0.00043	0.00044	0.0	2.3
6448-AA	0.00031	661	258	0.00031	0.00032	0.0	3.2
LM24-AA	0.00150	3021	1255	0.00152	0.00145	1.3	-3.3
6195-AA-D	0.00100	2011	831	0.00101	0.00096	1.0	-4.0
6195-AC	0.00046	920	383	0.00046	0.00044	0.0	-4.3
6252-AD	0.00052	1056	432	0.00051	0.00051	-1.9	-1.9
6363-AA	0.01800	29441	15001	0.01769	0.01409	-1.7	-21.7
B51S-AF-D	0.00036	769	299	0.00036	0.00037	0.0	2.7
* 6449-AA-D	0.00037	773	307	0.00037	0.00037	0.0	---

FIGURE A.3.2.7 (A) I_{NiK} VS C_{Ni} - ALUMINUM ALLOYS

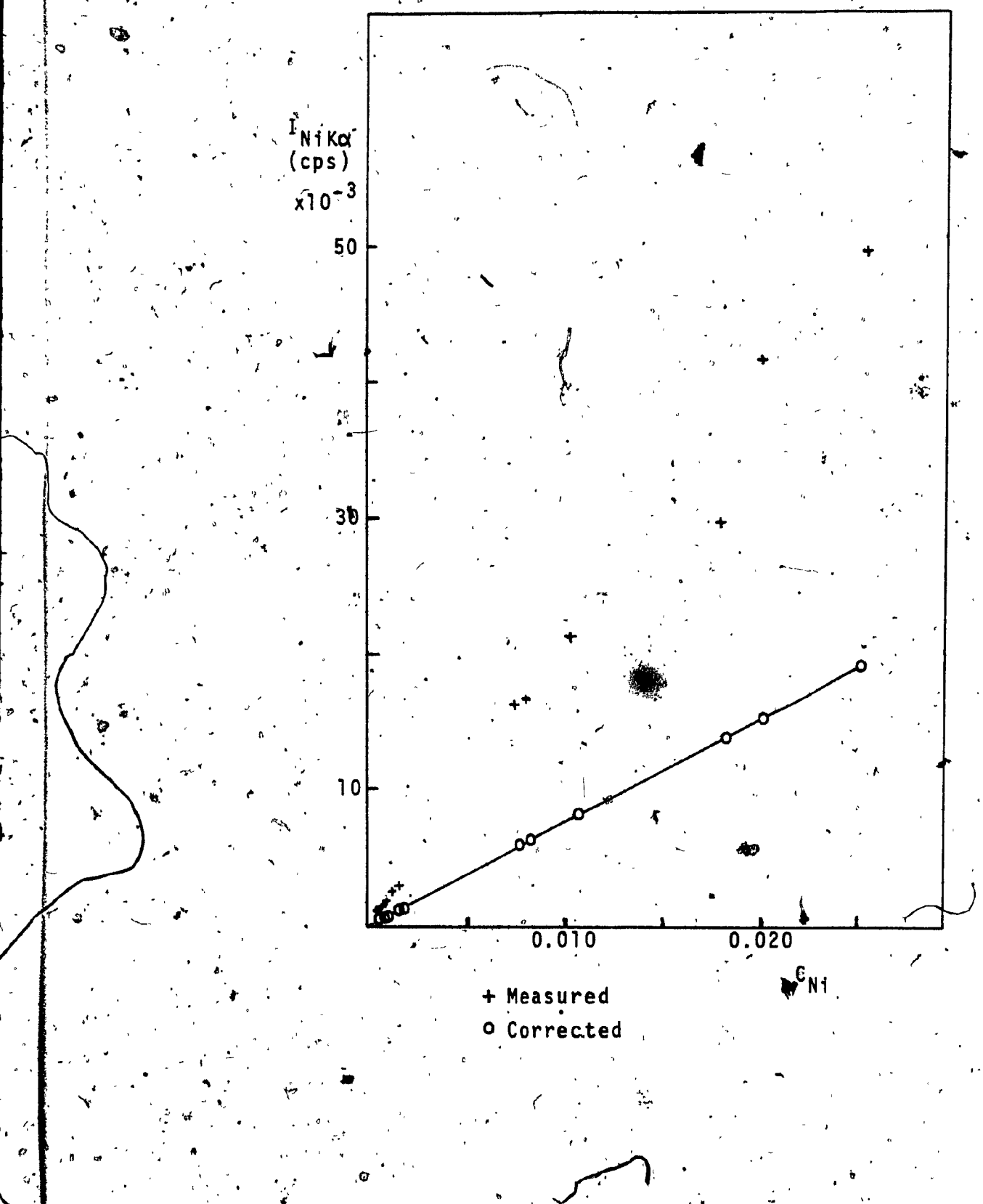

FIGURE A.3.2.7 (B) DISTRIBUTION OF RELATIVE ERROR - C_{Ni}

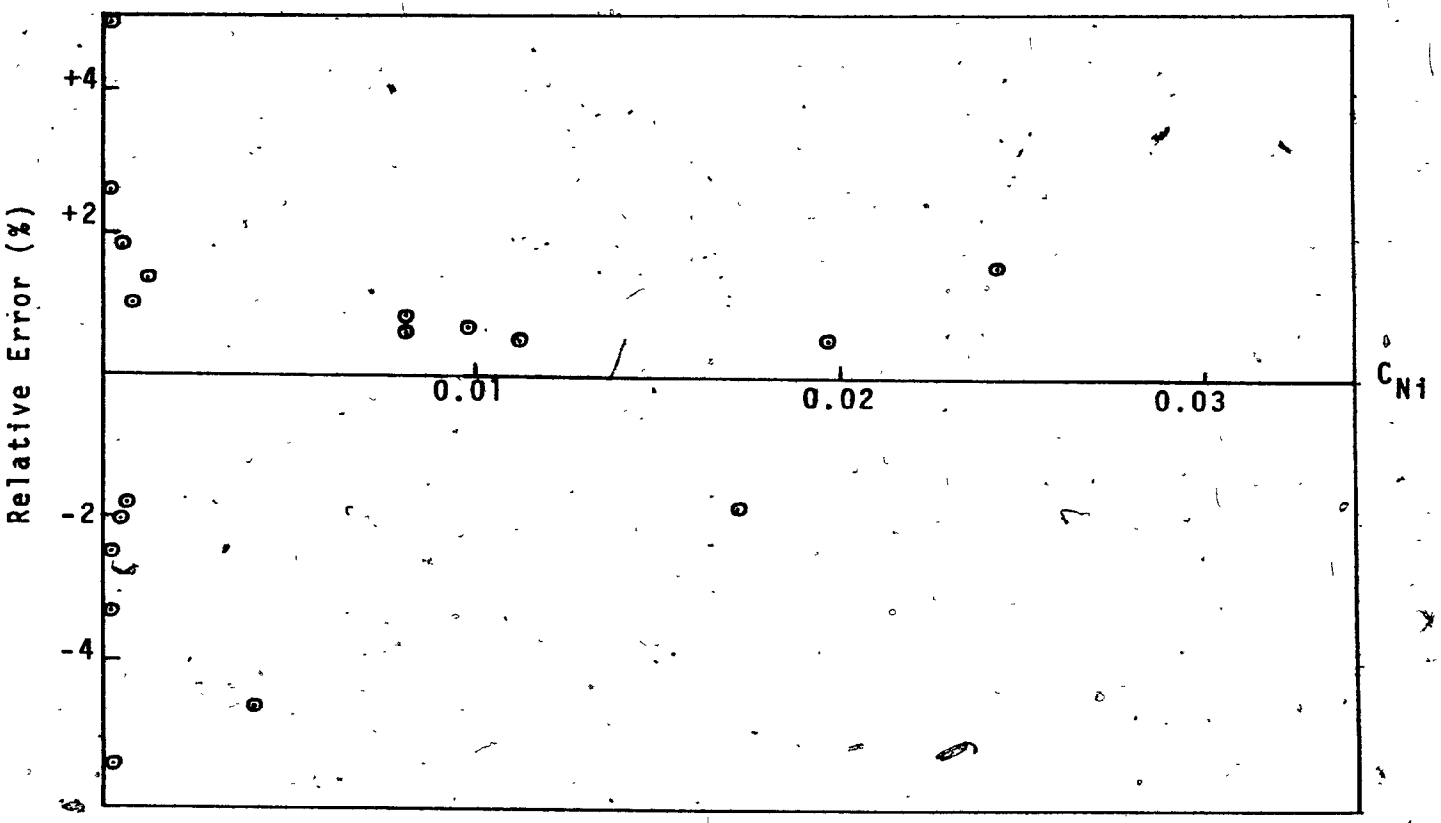

TABLE A.3.2.8 COPPER ANALYSIS - ALUMINUM ALLOYS

SAMPLE	C_{Cu}(std.)	$I_{CuK\alpha}$ (cps)	$I_{CuK\alpha}$(corrected) (cps)	C_{Cu}(calculated) A	B	Relative Error(%) C	D
117-AD	0.02920	50007	20309	0.02910	0.02782	-0.3	-4.7
125-AI	0.01180	21556	8272	0.01185	0.01199	0.4	1.6
225-AG	0.04200	73444	29426	0.04218	0.04086	0.4	-2.7
226-AC	0.04700	81503	32722	0.04680	0.04534	-0.4	-3.5
125-AL	0.01200	21890	8350	0.01196	0.01218	-0.3	1.5
125-AN	0.01270	23138	8865	0.01271	0.01287	0.1	1.3
B143-AA	0.02920	50301	20389	0.02925	0.02798	0.2	-4.2
143-AF	0.03460	59813	24178	0.03503	0.03328	1.3	-3.8
A143-AT	0.02970	50683	20723	0.02967	0.02820	-0.1	-5.1
236-AC	0.06850	109333	47806	0.06850	0.06083	0.0	-11.2
6165-AA-D	0.01020	17709	7124	0.01021	0.00985	0.1	-3.4
24S-AT	0.04620	78565	32229	0.04618	0.04371	-0.1	-5.4
218-AQ	0.03960	67209	27632	0.03954	0.03739	-0.2	-5.6
162-AZ	0.00790	13724	5528	0.00799	0.00764	1.1	-3.3
38S-AI-D	0.00860	15203	5973	0.00856	0.00846	-0.5	-1.6
135-AM	0.00034	641	241	0.00034	0.00036	0.0	5.9
135-AN	0.00050	925	349	0.00050	0.00051	0.0	2.0
A35-AJ	0.00028	516	192	0.00027	0.00029	-3.6	3.6
A56S-AB	0.00040	740	279	0.00040	0.00041	0.0	2.5
M57S-AC	0.00042	777	292	0.00042	0.00043	0.0	2.4
A135-AM	0.00050	957	352	0.00050	0.00053	0.0	6.0

TABLE A.3.2.8 cont'd

SAMPLE	C_{Cu}(std.)	$I_{CuK\alpha}$ (cps)	$I_{CuK\alpha}$(corrected) (cps)	C_{Cu}(calculated) A	B	Relative Error(%) C	D
340-AA-D	0.00050	908	349	0.00047	0.00051	-6.0	2.0
350-AQ	0.00042	821	296	0.00042	0.00046	0.0	9.5
350-AS	0.00100	1933	700	0.00100	0.00108	0.0	8.0
123-AJ	0.00035	661	248	0.00036	0.00037	2.9	5.7
161-AB	0.00065	1154	457	0.00066	0.00064	1.5	-1.5
161-AE	0.00052	923	326	0.00052	0.00051	0.0	-1.9
B160-AA	0.00060	1076	424	0.00061	0.00060	1.7	0.0
160-DB	0.00040	726	279	0.00040	0.00040	0.0	0.0
F40E-AG	0.00037	633	258	0.00037	0.00035	0.0	-5.4
6235-AA	0.00030	538	213	0.00031	0.00030	3.3	0.0
6392-AA	0.00100	1770	698	0.00100	0.00098	0.0	-2.0
79S-AD-D	0.00620	10821	4339	0.00621	0.00602	0.2	-2.9
79S-AE	0.00650	11241	4538	0.00650	0.00625	0.0	-3.8
6448-AA	0.02050	33691	14278	0.02043	0.01874	-0.3	-8.6
LM24-AA	0.03470	57601	24229	0.03474	0.03204	0.1	-7.7
6195-AA-D	0.03200	53433	22328	0.03201	0.02973	0.0	-7.1
6195-AC	0.03420	56630	23877	0.03422	0.03150	0.1	-7.9
6252-AD	0.03000	48970	20920	0.02870	0.02720	-4.3	-9.3
6363-AA	0.00960	13240	6546	0.00910	0.00737	-5.2	-23.2
B51S-AF-D	0.00045	830	315	0.00045	0.00046	0.0	2.2
* 6449-AA-D	0.00320	5752	2233	0.00320	0.00320	0.0	---

FIGURE A.3.2.8 (A) I_{CuK} VS C_{Cu}(lower) - ALUMINUM ALLOYS

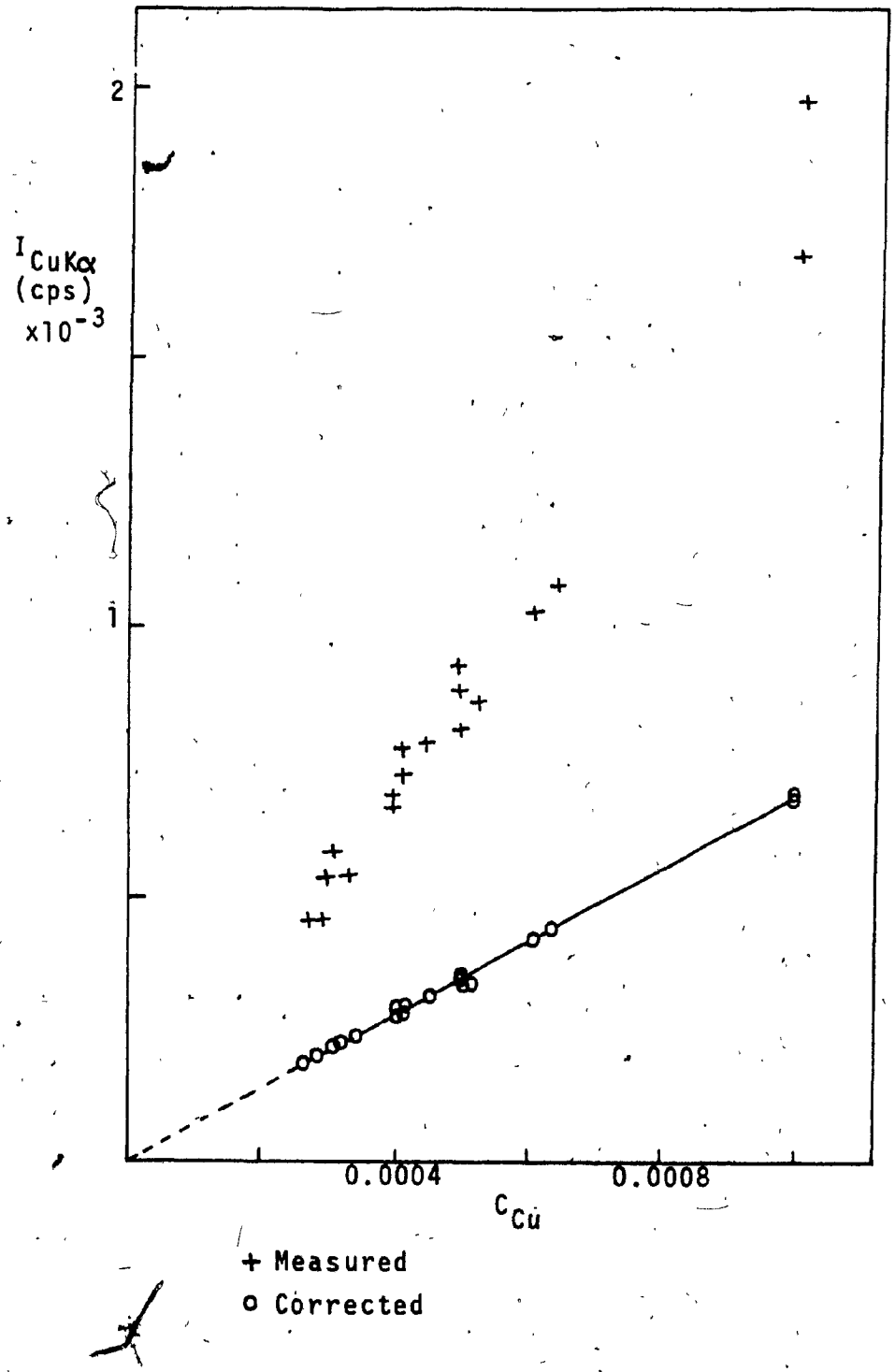

FIGURE A.3.2.8 (B) I_{CuK} VS C_{Cu}(higher) - ALUMINUM ALLOYS

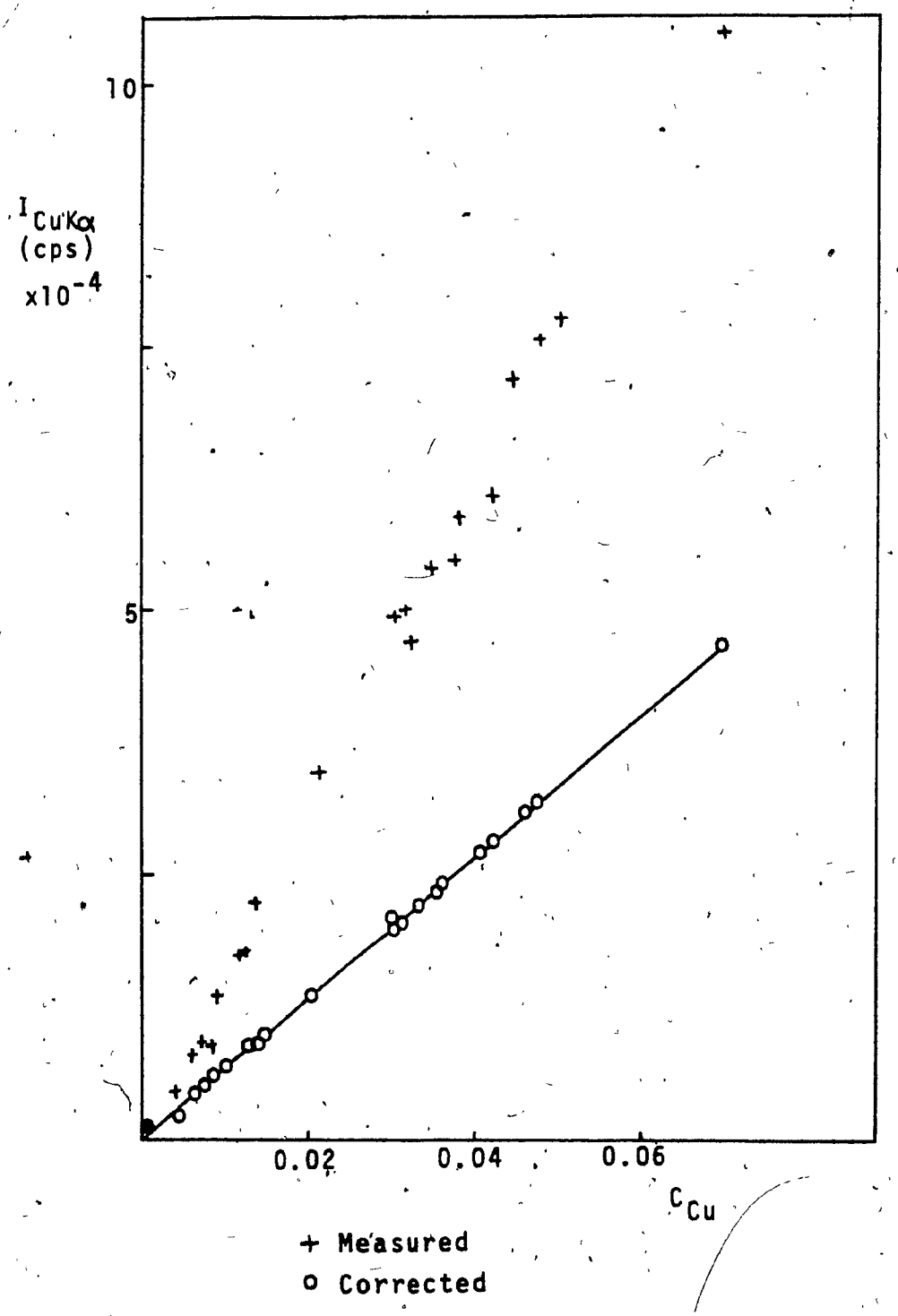

FIGURE A.3.2.8 (C) DISTRIBUTION OF RELATIVE ERROR - C_{Cu}

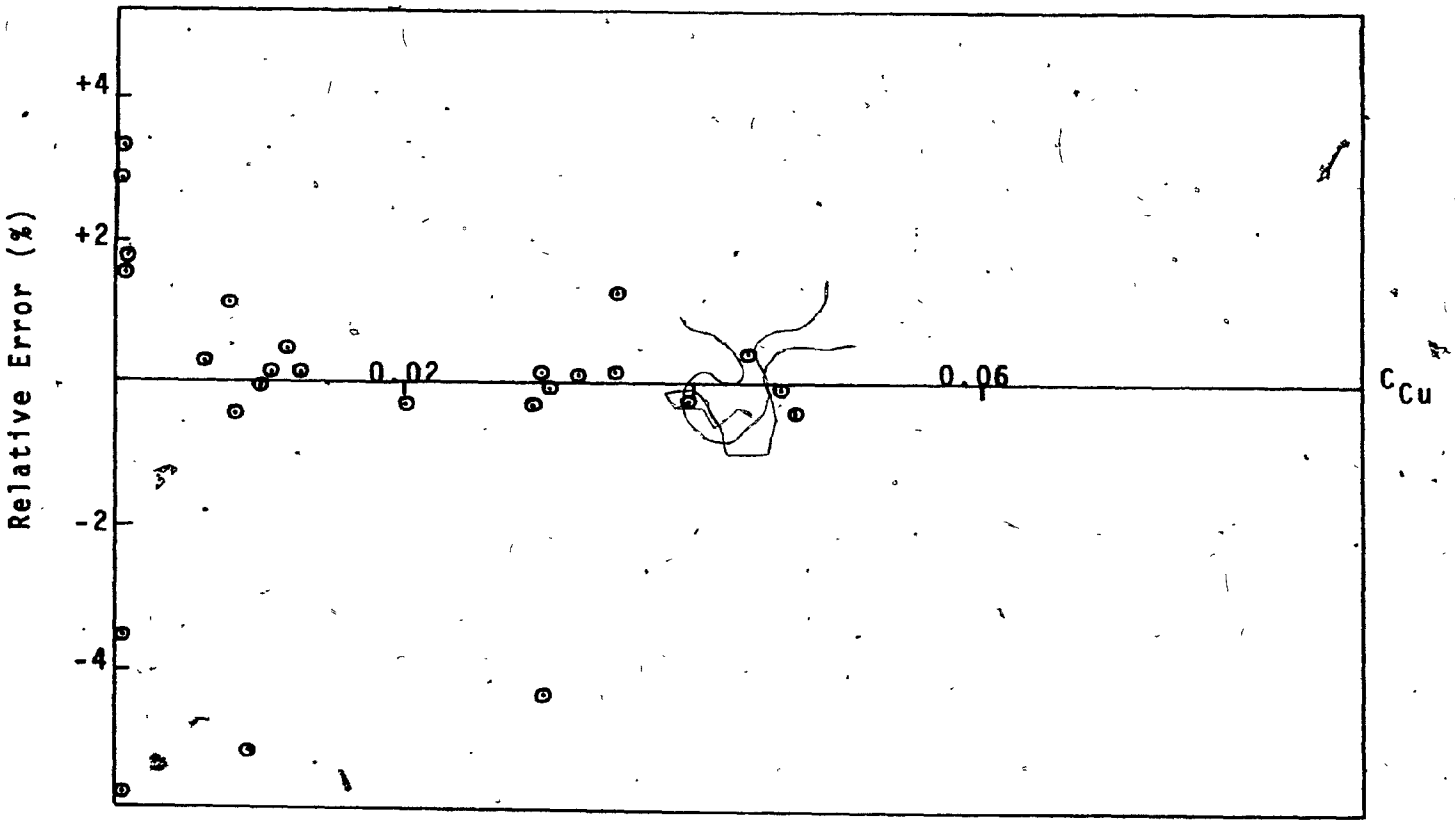

TABLE A.3.2.9 ZINC ANALYSIS - ALUMINUM ALLOYS

SAMPLE	C_{Zn}(std.)	$I_{ZnK\alpha}$ (cps)	$I_{ZnK\alpha}$(corrected) (cps)	C_{Zn}(calculated) A	B	Relative Error(%) C	D
340-AA-D	0.00043	881	280	0.00041	0.00044	-4.7	2.3
350-AQ	0.00033	720	214	0.00033	0.00036	0.0	9.1
350-AS	0.00038	821	246	0.00038	0.00041	0.0	7.9
123-AJ	0.00034	700	219	0.00034	0.00035	0.0	2.9
161-AB	0.00060	1175	389	0.00060	0.00059	0.0	-1.7
161-AE	0.00050	983	322	0.00049	0.00049	-2.0	-2.0
B160-AA	0.00043	844	278	0.00043	0.00042	0.0	-2.3
160-DB	0.00065	1321	425	0.00065	0.00066	0.0	1.5
F40E-AG	0.05450	99870	35351	0.05436	0.04984	-0.3	-8.6
6235-AA	0.05500	104032	35816	0.05510	0.05191	0.2	-5.6
6392-AA	0.04340	82863	28134	0.04327	0.04135	-0.3	-4.7
79S-AD-D	0.04510	84943	29277	0.04503	0.04239	-0.2	-6.0
79S-AE	0.04700	87630	30451	0.04683	0.04373	-0.4	-6.9
6448-AA	0.07190	125862	46638	0.07167	0.06281	-0.3	-12.6
LM24-AA	0.00730	13401	4757	0.00732	0.00669	0.3	-8.4
6195-AA-D	0.00850	15761	5548	0.00854	0.00786	0.5	-7.5
6195-AC	0.00900	16486	5838	0.00898	0.00823	-0.2	-8.6
6252-AD	0.03500	62206	22717	0.03348	0.03104	-4.3	-11.3
6363-AA	0.00040	567	254	0.00038	0.00028	-5.0	-30.0
B51S-AF-D	0.00042	861	272	0.00042	0.00043	0.0	2.3
* 6449-AA-D	0.00050	1002	325	0.00050	0.00050	0.0	---

TABLE A.3.2.9 cont'd

SAMPLE	C_{Zn}(std.)	$I_{ZnK\alpha}$ (cps)	$I_{ZnK\alpha}$(corrected) (cps)	C_{Zn}(calculated) A	C_{Zn}(calculated) B	Relative Error(%) C	Relative Error(%) D
117-AD	0.00060	1148	389.	0.00059	0.00057	-1.6	-5.3
125-AI	0.00030	617	197	0.00030	0.00031	0.0	3.3
225-AG	0.00033	627	210	0.00032	0.00031	-3.0	-6.1
226-AC	0.00048	938	314	0.00048	0.00047	0.0	-2.0
125-AL	0.00030	610	194	0.00030	0.00030	0.0	0.0
125-AN	0.00043	847	271	0.00042	0.00042	-2.3	-2.4
B143-AA	0.00060	1146	388	0.00060	0.00057	0.0	-5.0
143-AF	0.00060	1159	392	0.00061	0.00058	1.7	-3.3
A143-AT	0.00035	641	227	0.00035	0.00032	0.0	-8.6
236-AC	0.00041	723	263	0.00041	0.00036	0.0	-12.2
6165-AA-D	0.00037	657	232	0.00036	0.00033	-2.7	-10.8
24S-AT	0.00041	783	267	0.00041	0.00039	0.0	-4.9
218-AQ	0.00030	521	196	0.00030	0.00026	0.0	-13.3
162-AZ	0.00040	672	254	0.00040	0.00034	0.0	-15.0
38S-AI-D	0.00057	1049	359	0.00055	0.00052	-3.5	-8.7
135-AM	0.00043	892	280	0.00043	0.00045	0.0	4.6
135-AN	0.00050	1080	340	0.00052	0.00054	4.0	8.0
A35-AJ	0.00040	841	259	0.00039	0.00042	-2.5	5.0
A56S-AB	0.00050	1035	324	0.00050	0.00052	0.0	4.0
M57S-AC	0.00033	688	215	0.00033	0.00034	0.0	3.0
A135-AM	0.00053	1130	344	0.00053	0.00056	0.0	5.7

FIGURE A.3.2.9 (A) I_{ZnK} VS C_{Zn}(lower) - ALUMINUM ALLOYS

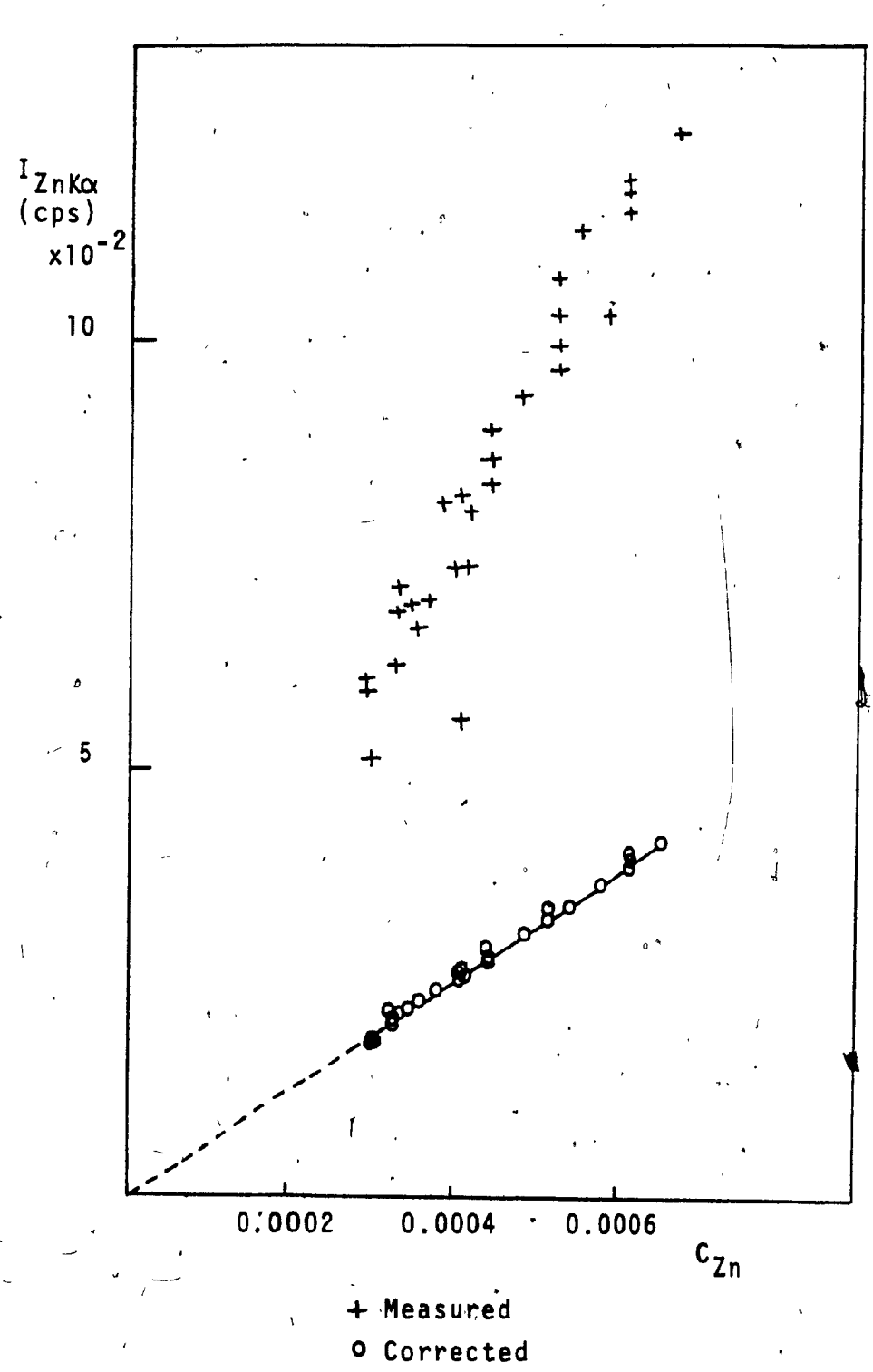

FIGURE A.3.2.9 (B) I'_{ZnK} VS C_{Zn}(higher) - ALUMINUM ALLOYS

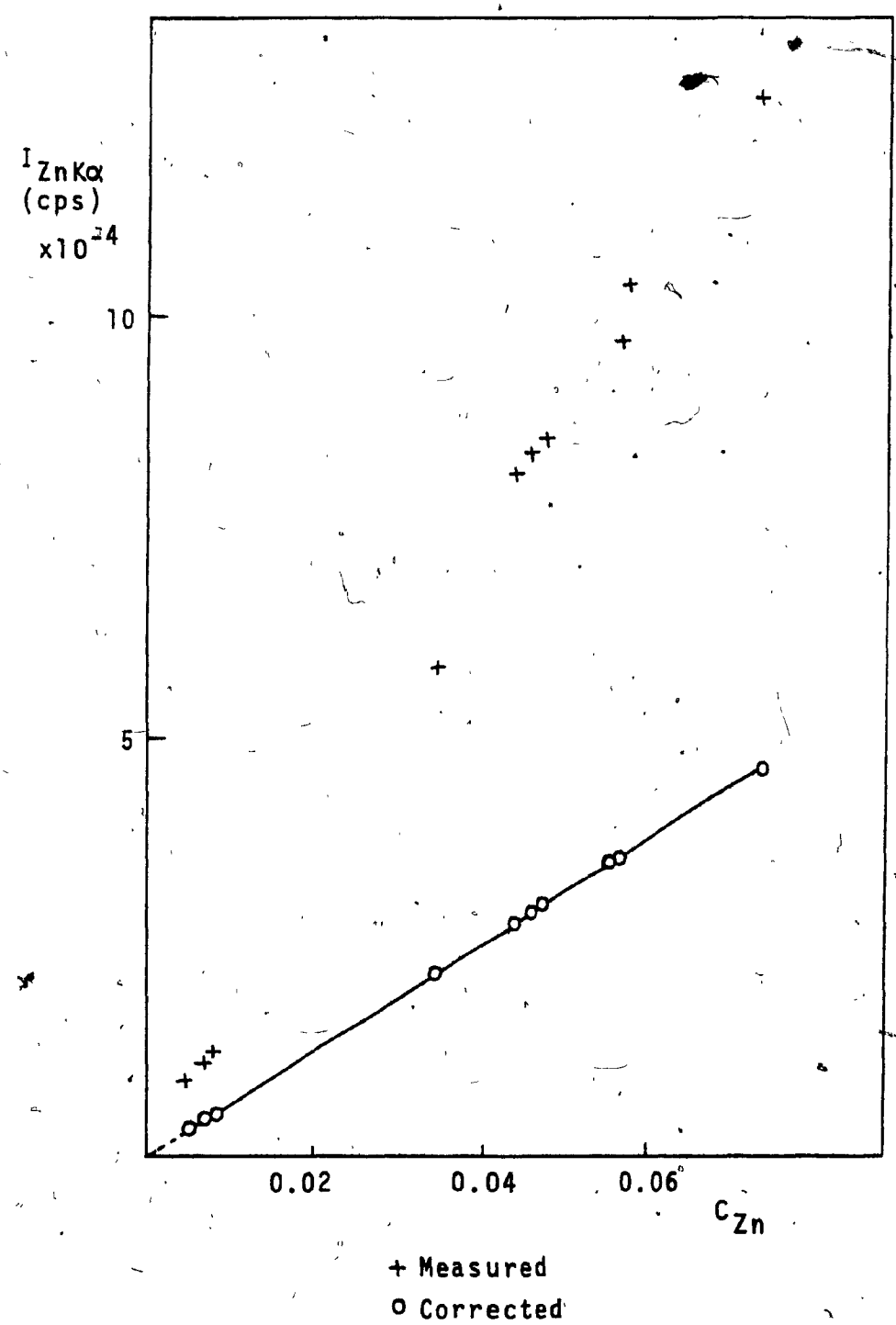

FIGURE A.3.2.9 (C) DISTRIBUTION OF RELATIVE ERROR - C_{Zn}

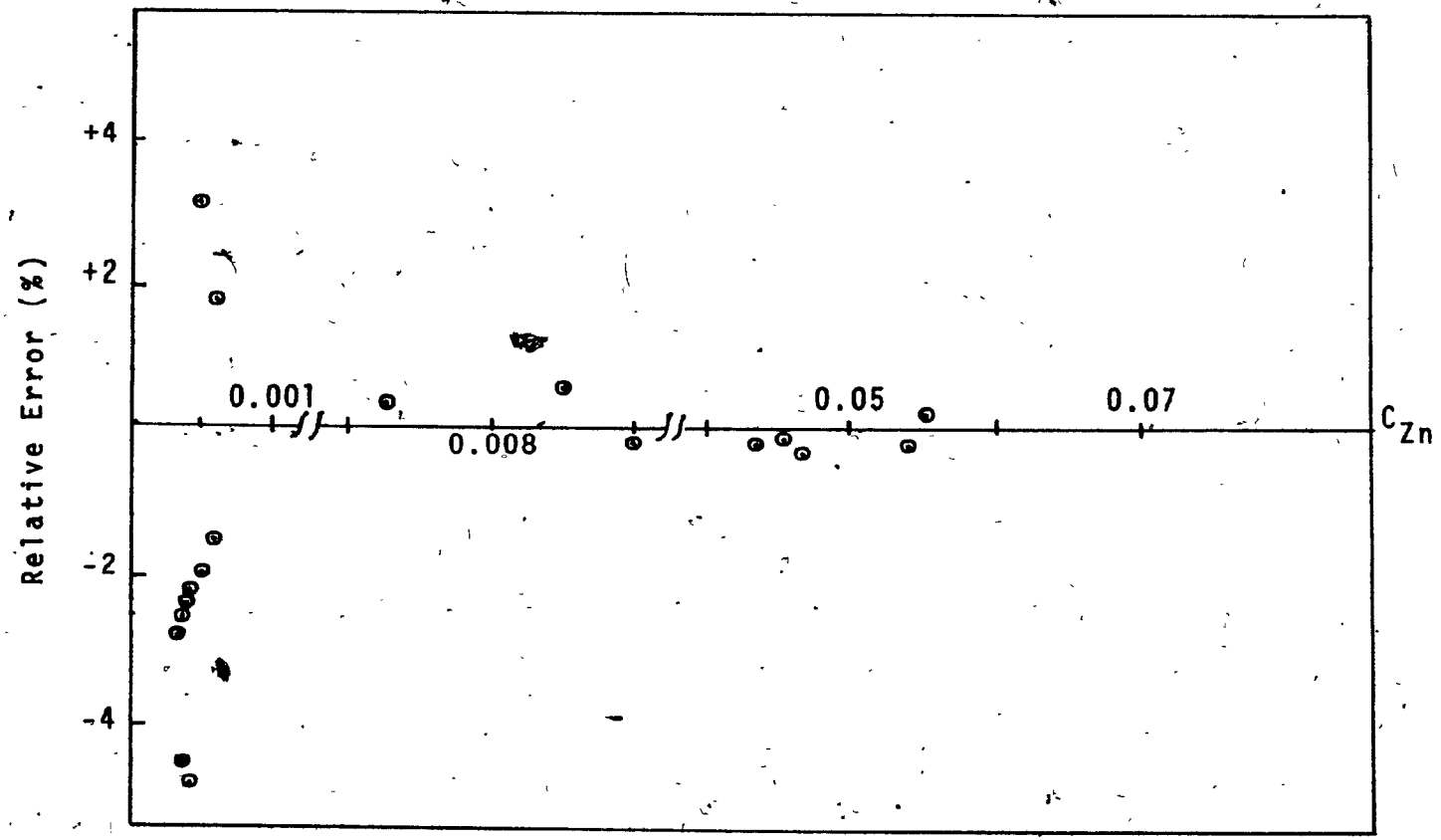

TABLE A.3.2.10 TIN ANALYSIS - ALUMINUM ALLOYS

SAMPLE	C_{Sn}(std.)	$I_{SnK\alpha}$ (cps)	$I_{SnK\alpha}$(corrected) (cps)	C_{Sn}(calculated) A	B	Relative Error(%) C	D
117-AD	0.00034	543	47	0.00033	0.00031	-2.9	-8.8
125-AI	0.00029	548	40	0.00028	0.00031	-3.5	6.9
225-AG	0.00026	382	35	0.00025	0.00022	-3.8	-15.4
226-AC	0.00045	666	64	0.00046	0.00038	2.2	-15.5
125-AL	0.00029	561	41	0.00029	0.00032	0.0	10.3
125-AN	0.00042	804	60	0.00042	0.00046	0.0	9.5
B143-AA	0.00040	655	57	0.00041	0.00037	2.5	-7.5
143-AF	0.00041	637	58	0.00041	0.00036	6.0	-12.2
A143-AT	0.00024	367	33	0.00024	0.00021	0.0	-12.5
236-AC	0.00028	345	39	0.00028	0.00020	0.0	-28.6
6165-AA-D	0.00030	507	41	0.00029	0.00029	-3.3	-3.3
24S-AT	0.00034	482	47	0.00033	0.00027	-2.9	-20.5
218-AQ	0.00030	391	41	0.00029	0.00022	-3.3	-26.6
162-AZ	0.00034	554	48	0.00035	0.00032	2.9	-5.9
38S-AI-D	0.00029	530	41	0.00029	0.00030	0.0	3.4
135-AM	0.00033	707	46	0.00033	0.00040	0.0	21.2
135-AN	0.00032	690	46	0.00032	0.00039	0.0	21.8
A35-AJ	0.00031	640	44	0.00029	0.00036	-6.5	16.1
A56S-AB	0.00034	732	49	0.00035	0.00042	2.9	23.5
M57S-AC	0.00031	666	44	0.00031	0.00038	0.0	22.6
A135-AM	0.00056	1199	78	0.00055	0.00068	-1.8	21.4

TABLE A.3.2.10 cont'd

SAMPLE	C_{Sn}(std.)	$I_{SnK\alpha}$ (cps)	$I_{SnK\alpha}$(corrected) (cps)	C_{Sn}(calculated) A	B	Relative Error(%) C	D
* 340-AA-D	0.00037	761	53	0.00034	0.00043	-8.1	16.2
350-AQ	0.00034	763	48	0.00034	0.00043	0.0	26.5
350-AS	0.00036	801	51	0.00036	0.00046	0.0	27.8
123-AJ	0.00027	581	38	0.00027	0.00033	0.0	22.2
16 -AB	0.00050	989	71	0.00049	0.00056	-2.0	12.0
161-AE	0.00040	809	57	0.00040	0.00046	0.0	15.0
B160-AA	0.00031	631	44	0.00031	0.00036	0.0	-16.1
160-DB	0.00046	967	66	0.00046	0.00055	0.0	19.6
F40E-AG	0.00031	400	44	0.00031	0.00023	0.0	-25.8
6235-AA	0.00030	403	43	0.00030	0.00023	0.0	-23.3
6392-AA	0.00040	570	56	0.00039	0.00032	-2.5	-20.0
79S-AD-D	0.00030	409	43	0.00030	0.00023	0.0	-23.3
79S-AE	0.00042	561	60	0.00042	0.00032	0.0	-23.8
6448-AA	0.00060	631	85	0.00059	0.00036	-1.7	-40.0
LM2[illegible]A	0.00080	1161	116	0.00082	0.00066	2.5	-17.5
6195-AA-D	0.00040	591	57	0.00041	0.00034	2.5	-15.0
6195-AC	0.00051	731	73	0.00051	0.00042	0.0	-17.6
6252-AD	0.00054	661	77	0.00045	0.00038	-16.7	-29.6
6363-AA	0.7190	68402	10204	0.06655	0.03894	-7.4	-45.8
B51S-AF-D	0.00042	881	60	0.00042	0.00050	0.0	-19.0
* 6449-AA-D	0.00044	773	62	0.00044	0.00044	0.0	---

FIGURE A.3.2.10 (A) I_{SnK} VS C_{Sn} - ALUMINUM ALLOYS

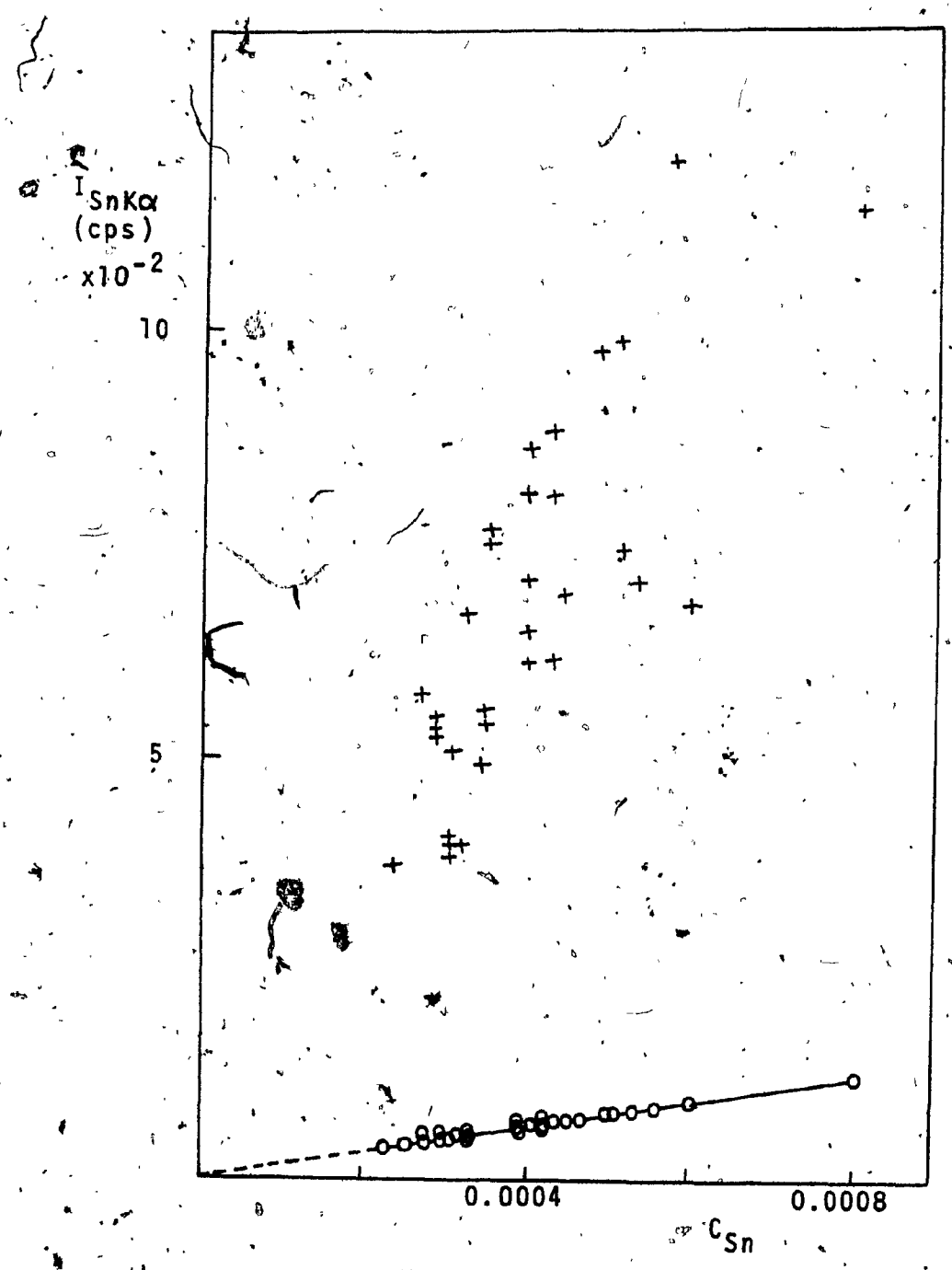

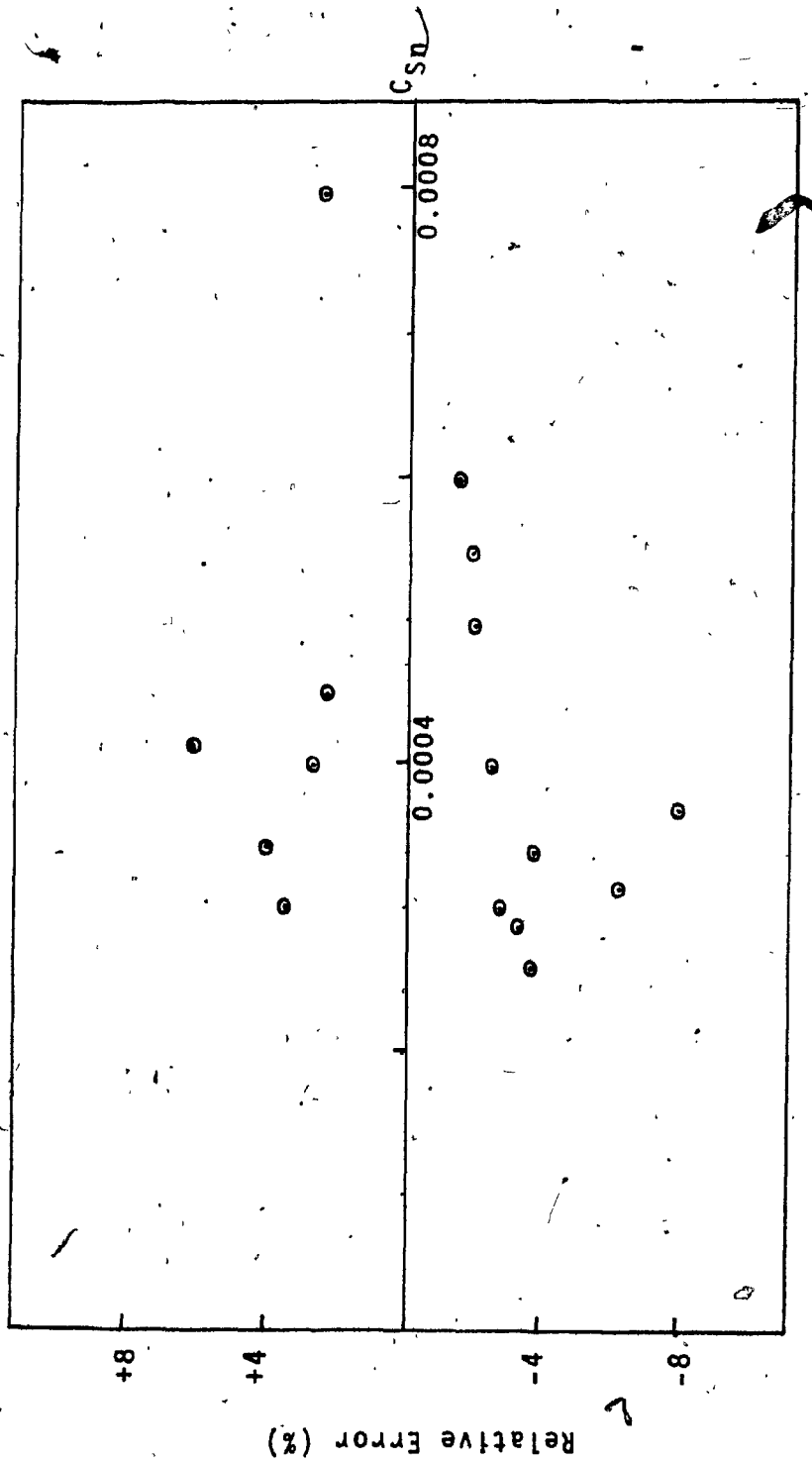

FIGURE A.3.2.10 (B) DISTRIBUTION OF RELATIVE ERROR -C_{Sn}

TABLE A.3.2.11 LEAD ANALYSIS - ALUMINUM ALLOYS

SAMPLE	C_{Pb}(std.)	$I_{PbL\alpha}$ (cps)	$I_{PbL\alpha}$(corrected) (cps)	C_{Pb}(calculated) A	B	Relative Error(%) C	D
117-AD	0.00038	198	33	0.00038	0.00033	0.0	-13.2
125-AI	0.00036	211	31	0.00035	0.00036	-2.8	0.0
225-AG	0.00030	144	25	0.00029	0.00024	-3.3	-20.0
226-AC	0.00060	293	53	0.00061	0.00049	1.7	-18.3
125-AL	0.00031	179	26	0.00030	0.00030	-3.3	-3.2
125-AN	0.00052	300	44	0.00051	0.00051	-1.9	-1.9
B143-AA	0.00048	252	42	0.00049	0.00042	2.1	-12.5
143-AF	0.00060	297	51	0.00059	0.00050	-1.7	-16.7
A143-AT	0.00028	144	25	0.00029	0.00024	3.6	-14.2
236-AC	0.00031	120	25	0.00029	0.00020	-6.5	-36.6
6165-AA-D	0.00025	142	22	0.00026	0.00024	4.0	-4.0
24S-AT	0.00033	163	30	0.00034	0.00027	3.0	-18.2
218-AQ	0.00028	125	24	0.00028	0.00021	0.0	-25.0
162-AZ	0.00030	154	26	0.00030	0.00026	0.0	-13.3
38S-AI-D	0.00030	173	26	0.00030	0.00029	0.0	-3.3
135-AM	0.00032	200	27	0.00031	0.00034	-3.1	6.3
135-AN	0.00033	204	28	0.00032	0.00034	-3.0	3.0
A35-AJ	0.00030	187	25	0.00029	0.00031	-3.3	3.3
A56S-AB	0.00030	188	26	0.00029	0.00032	-3.3	6.7
M57S-AC	0.00030	173	24	0.00027	0.00029	-10.0	-3.3
A135-AM	0.00050	322	43	0.00050	0.00054	0.0	8.0

TABLE A.3.2.11 cont'd

SAMPLE	C_{Pb}(std.)	$I_{PbL\alpha}$ (cps)	$I_{PbL\alpha}$(corrected) (cps)	C_{Pb}(calculated) A	B	Relative Error(%) C	D
340-AA-D	0.00030	185	26	0.00028	0.00031	-6.7	3.3
350-AQ	0.00031	203	27	0.00031	0.00034	0.0	9.7
350-AS	0.00030	199	26	0.00030	0.00034	0.0	13.3
123-AJ	0.00034	217	29	0.00034	0.00037	0.0	8.8
161-AB	0.00050	306	44	0.00050	0.00052	0.0	4.0
161-AE	0.00040	246	35	0.00040	0.00041	0.0	2.5
B160-AA	0.00028	171	24	0.00028	0.00029	0.0	3.6
160-DB	0.00045	281	39	0.00044	0.00047	-2.2	4.4
F40E-AG	0.00028	119	24	0.00027	0.00020	-3.6	-28.6
6235-AA	0.00030	128	25	0.00029	0.00022	-3.3	-26.7
6392-AA	0.00020	93	17	0.00019	0.00016	-5.0	-20.0
79S-AD-D	0.00020	90	17	0.00020	0.00015	0.0	-25.0
79S-AE	0.00041	176	35	0.00039	0.00030	-4.9	-26.8
6448-AA	0.00060	211	53	0.00060	0.00036	0.0	-40.0
LM24-AA	0.00110	504	93	0.00107	0.00085	-2.7	-22.7
6195-AA-D	0.00045	213	39	0.00044	0.00036	-2.2	-20.0
6195-AC	0.00053	251	46	0.00053	0.00042	0.0	-20.7
6252-AD	0.00050	205	43	0.00043	0.00035	-14.0	-30.0
6363-AA	0.00040	188	35	0.00038	0.00032	-5.0	-20.0
B51S-AF-D	0.00040	250	34	0.00040	0.00042	0.0	5.0
* 6449-AA-D	0.00460	2732	398	0.00458	0.00460	-0.4	---

FIGURE A.3.2.11 (A) I_{PbL} VS C_{Pb} - ALUMINUM ALLOYS

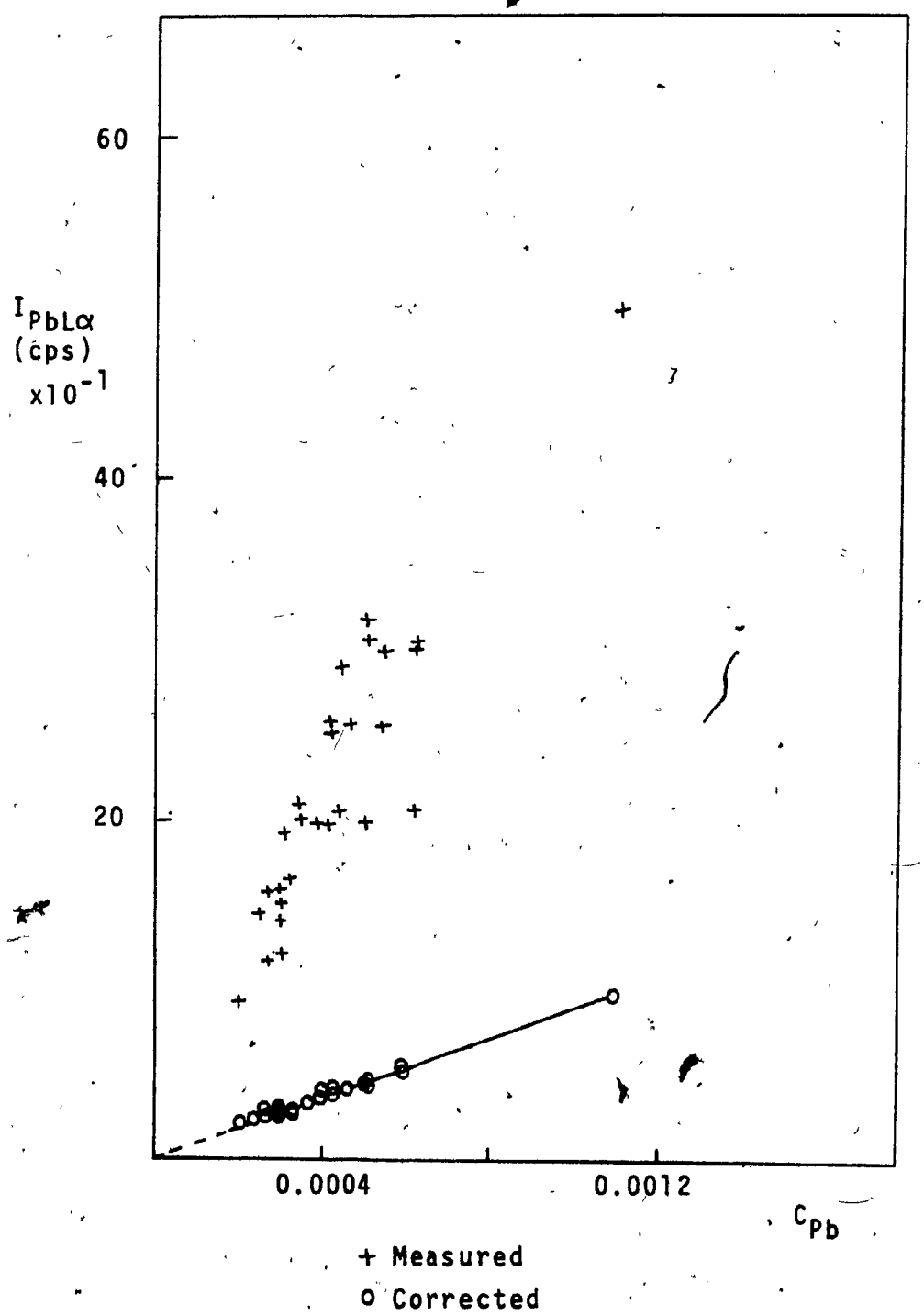

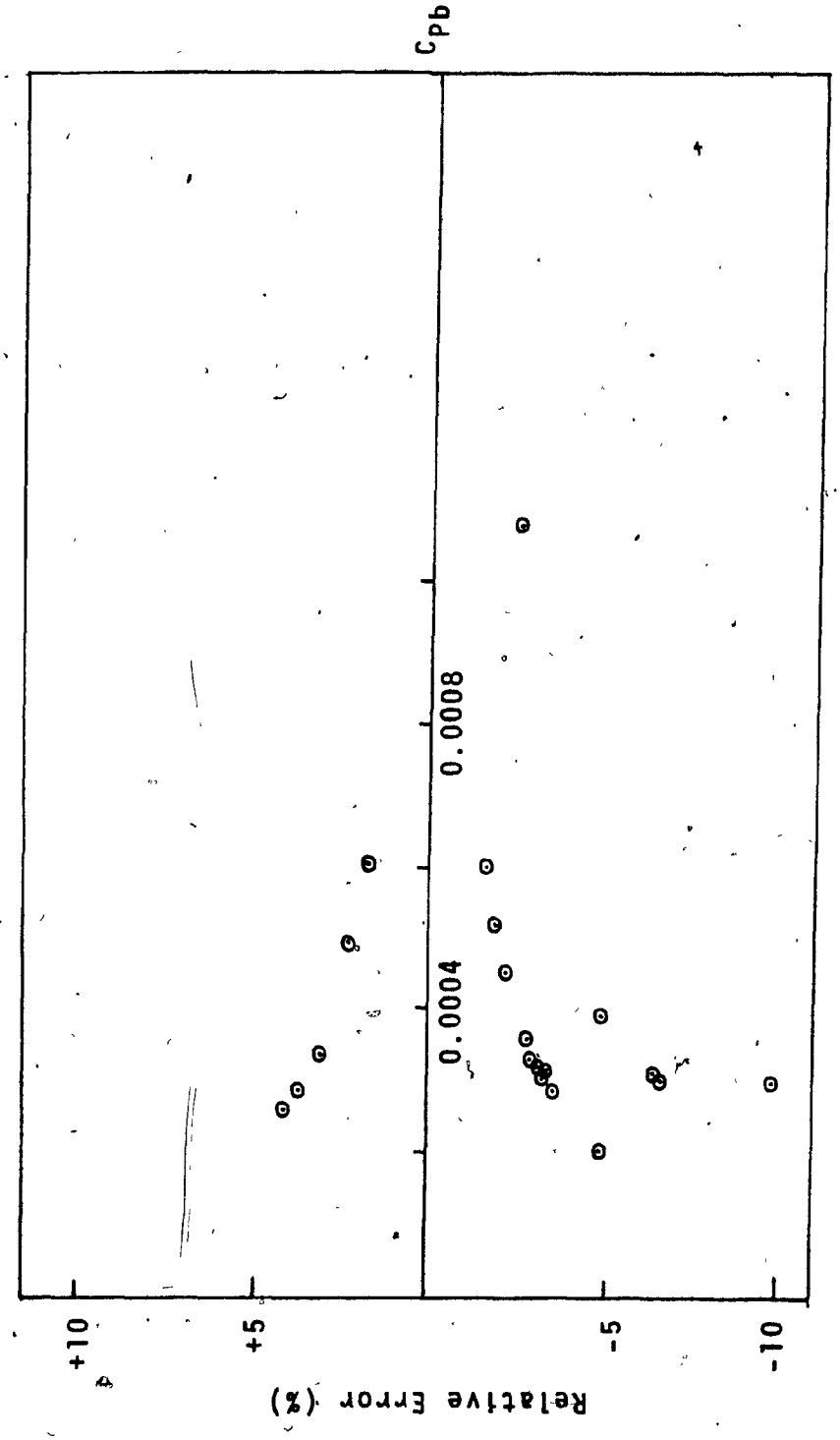

FIGURE A.3.2.11 (B) DISTRIBUTION OF RELATIVE ERROR - C_{Pb}

TABLE A.3.2.12 BISMUTH ANALYSIS - ALUMINUM ALLOYS

SAMPLE	C_{Bi}(std.)	$I_{BiL\alpha}$ (cps)	$I_{BiL\alpha}$(corrected) (cps)	C_{Bi}(calculated) A	C_{Bi}(calculated) B	Relative Error(%) C	Relative Error(%) D
117-AD	0.00030	122	19	0.00028	0.00025	-6.7	-16.7
125-AI	0.00027	130	17	0.00026	0.00027	-3.7	0.0
225-AG	0.00027	109	18	0.00027	0.00022	0.0	-18.6
226-AC	0.00064	246	42	0.00062	0.00051	-3.2	-20.1
125-AL	0.00029	138	19	0.00028	0.00028	-3.5	-3.4
125-AN	0.00038	177	25	0.00037	0.00036	-2.6	-5.3
B143-AA	0.00047	202	32	0.00047	0.00042	0.0	-10.6
143-AF	0.00050	207	33	0.00050	0.00043	0.0	-14.0
A143-AT	0.00030	113	18	0.00028	0.00023	-6.7	-23.3
236-AC	0.00030	98	19	0.00029	0.00020	-3.3	-33.3
6165-AA-D	0.00031	131	19	0.00029	0.00027	-6.5	-12.9
24S-AT	0.00032	123	21	0.00032	0.00025	0.0	-21.8
218-AQ	0.00030	110	20	0.00030	0.00023	0.0	-23.3
162-AZ	0.00020	84	13	0.00019	0.00017	-5.0	-15.0
38S-AI-D	0.00030	147	21	0.00031	0.00030	3.3	0.0
135-AM	0.00031	162	21	0.00031	0.00033	0.0	6.4
135-AN	0.00032	168	21	0.00032	0.00035	0.0	9.3
A35-AJ	0.00028	139	18	0.00026	0.00029	-7.1	3.6
A56S-AB	0.00023	116	15	0.00022	0.00024	-4.3	4.3
M57S-AC	0.00028	145	19	0.00028	0.00030	0.0	-7.1
A135-AM	0.00040	223	28	0.00042	0.00046	5.0	15.0

TABLE A.3.2.12 cont'd

SAMPLE	C_{Bi}(std.)	$I_{BiL\alpha}$ (cps)	$I_{BiL\alpha}$(corrected) (cps)	C_{Bi}(calculated) A	B	Relative Error(%) C	D
340-AA-D	0.00040	203	27	0.00037	0.00042	-7.5	5.0
350-AQ	0.00029	155	19	0.00028	0.00032	-3.4	10.3
350-AS	0.00027	140	17	0.00026	0.00029	-3.7	7.4
123-AJ	0.00032	167	21	0.00032	0.00034	0.0	6.3
161-AB	0.00050	246	33	0.00049	0.00051	-2.0	2.0
161-AE	0.00033	165	22	0.00032	0.00034	-3.0	3.0
B160-AA	0.00043	215	28	0.00043	0.00044	0.0	2.3
160-DB	0.00040	205	27	0.00040	0.00042	0.0	5.0
F40E-AG	0.00035	127	24	0.00035	0.00026	0.0	-25.7
6235-AA	0.00030	101	19	0.00028	0.00021	-6.7	-30.0
6392-AA	0.00040	147	26	0.00038	0.00030	-5.0	-25.0
79S-AD-D	0.00030	111	20	0.00030	0.00023	0.0	-23.3
79S-AE	0.00042	160	29	0.00044	0.00033	4.8	-21.4
6448-AA	0.00021	65	15	0.00021	0.00013	0.0	-38.1
LM24-AA	0.00030	114	20	0.00029	0.00023	-3.3	-23.3
6195-AA-D	0.00030	109	19	0.00027	0.00022	-10.0	-26.7
6195-AC	0.00040	161	28	0.00042	0.00033	5.0	-17.5
6252-AD	0.00048	168	33	0.00043	0.00035	-10.4	-27.0
6363-AA	0.00040	150	27	0.00037	0.00031	-7.5	-22.5
B51S-AF-D	0.00042	221	29	0.00043	0.00046	2.3	9.5
* 6449-AA-D	0.00460	2233	306	0.00457	0.00460	-0.1	---

FIGURE A.3.2.12 (A) I_{BiL} VS C_{Bi} - ALUMINUM ALLOYS